

The Misallocation Channel of Climate Change

Evidence from Global Firm-level Microdata ^{*}

Tianzi Liu [†] Zebang Xu [‡]
Cornell University Cornell University

Preliminary
[Click here for the latest version](#)

Abstract

Extensive literature has documented the negative effect of global warming on TFP, but we know little about the micro origins of this relationship. This paper examines a novel channel: the impact of temperature extremes on capital misallocation. Using global firm-level microdata from 32 countries, we provide causal evidence that a day with extreme heat ($>30^{\circ}\text{C}$) increases the dispersion of marginal revenue products of capital (MRPK) by 0.31 log points, implying a 0.11% annual aggregate TFP loss for an average region-sector. Notably, this effect is more pronounced in hotter and more economically developed regions. Our estimates, while taking future adaptation and development into account, suggest a global aggregate TFP loss of 42.7% from the misallocation channel at the end of the century under the SSP3-7.0 scenario. In light of these findings, we develop a firm dynamics model with time-to-build capital and varying sensitivity to temperature across firms to examine two primary mechanisms behind temperature-induced misallocation. The model reveals that (i) increased firm-level productivity damage volatility from temperature extremes (“level effect”) and (ii) greater temperature forecasting errors (“shock effect”) both exacerbate dispersion in investment mistakes. Applying the model-induced regression to the data, we validate both mechanisms of climate-induced misallocation: in our sample, the level effect leads to a TFP loss of 3%, and the shock effect incurs a loss of 0.81%. Our results uncover the critical role of the misallocation channel and the necessity of considering firm heterogeneity in climate policies.

^{*}We are indebted to Ryan Chahrour, Kristoffer Nimark, Ivan Rudik and Mathieu Taschereau-Dumouchel for guidance throughout developing this paper. We are grateful for the suggestions and comments from Levon Barseghyan, Julieta Caunedo, Luming Chen, Ezra Oberfield, Pablo Ottonello, Jeffrey Shrader, and seminar participants at the Cornell Macro Lunch and SEERE Seminar.

[†]Department of Applied Economics and Management, Cornell University (email:t1567@cornell.edu).

[‡]Department of Economics, Cornell University (email:zx88@cornell.edu).

1 Introduction

How does climate change affect the aggregate economy? The existing literature on climate change economics usually treats aggregate productivity losses from temperature variations as worsening technology. At the micro level, empirical work has shown that extreme temperature conditions can affect firm-level productivity, often interpreted as losses of physical productivity (e.g. [Zhang et al. 2018](#); [Somanathan et al. 2021](#)). At the macro level, a mix of structural and empirical work prioritizes productivity damage as the primary effect of climate change (e.g. [Barrage and Nordhaus 2023](#); [Cruz and Rossi-Hansberg 2023](#)). These works either stay agnostic about the micro origins of the aggregate loss or benchmark their results in efficient economies with little micro-level distortions. However, understanding the sources of the aggregate loss would be essential for the design of climate policies at the micro-level.

Misallocation's role in aggregate productivity has been well-established in the macroeconomic literature since [Restuccia and Rogerson \(2008\)](#) and [Hsieh and Klenow \(2009\)](#), but has been largely overlooked in the context of temperature shocks and climate change. However, the misallocation channel should come as no surprise. While all firms might suffer from climate change and identical heat shocks, the extent of the damage might vary significantly, with heat-loving firms being less affected and more productive than heat-averse firms. As capital is usually considered difficult to adjust in short horizons, a heat shock that all firms face would cause dispersion in capital returns in an economy with varying temperature sensitivity across firms. Therefore, an allocation where more productive and heat-loving firms are allocated with less capital than the more heat-averse firms will induce dispersion in marginal revenue products of capital (MRPK), i.e., misallocation¹, and results in lower aggregate TFP levels compared to an efficient economy.

In this paper, we combine reduced-form causal identification and structural macroeconomic models to first document and project the economic impact of climate change on capital misallocation and aggregate productivity globally, and second to analyze how TFP damage volatility and climate uncertainty govern the induced TFP losses. To estimate the impacts of weather shocks on capital misallocation, we start by building a climate TFP accounting framework in the tradition of [Hsieh and Klenow \(2009\)](#). This framework decomposes region-sector level aggregate TFP into a set of measurable firm-level sufficient statistics, which measure the efficient frontier (i.e., technology) and losses from capital misallocation. Specifically, capital misallocation can be measured with the variance of (log) MRPK across firms in a given year at the region-sector level. We collect a global sample of firm-level microdata from 32 countries. This includes data in 30 European countries extracted from the BvD Orbis dataset, as well as data in China and India obtained from government-conducted surveys. We use the ERA5-Land gridded daily temperature data from the European Centre for Medium-Range Weather Forecasts (ECMWF) to construct historical climate variables and temperature forecasts.

We then empirically estimate the causal elasticities of temperature shocks on capital misallocation using computed region-sector level MRPK dispersion in a pooled regression. Our estimation reveals a U-shaped pattern between capital misallocation and temperature shocks.

1. Throughout the paper, we use MRPK dispersion and capital misallocation interchangeably.

We find significant and robust causal effects of temperature on capital misallocation in both developed and developing economies. Specifically, an extra day with a temperature above 30°C relative to a day in 5-10°C in a year will increase MRPK dispersion by about 0.31 log points, which translates to 0.11% annual TFP loss from temperature-induced capital misallocation. Relatedly, we explore the heterogeneous effects of temperature-induced misallocation across regional climates and income levels. Our results show that the effect of heat shocks on capital misallocation is worse in hotter and more economically developed regions, suggesting limited potential for firm-level adaptation to mitigate the misallocation loss over the long run.

What do our estimates imply for the misallocation cost of future climate change? Using our estimates of the heterogeneous temperature-misallocation elasticities, along with the climate projections from the CMIP6 model and income projections from the OECD Env-Growth model under the SSP3-7.0 scenario, we project the impact of global warming on misallocation-induced TFP loss by the end of the century. Our projection indicates that, compared to the current levels, the global cost of climate-induced misallocation will amount to 42.69% of aggregate TFP. Empirically, the projected loss can be decomposed into three channels: a 4.99% contribution from the shock effect due to shifted daily temperature distribution, 17.7% from the income effect of projected development, and most significantly, 20.0% from the level effect of the average temperature increase. Remarkably, the magnitude of these estimates is comparable to the overall projected impact reported by [Burke, Hsiang, and Miguel \(2015\)](#).

To better understand the drivers of climate-induced misallocation, particularly how both temperature shocks and temperature levels can create dispersion in capital returns, we develop a firm dynamics model featuring time-to-build capital and temperature-productivity interactions. Specifically, we allow firms' productivity to be heterogeneous in their persistent and idiosyncratic sensitivities to temperature. The persistent sensitivity reflects a firm's specific characteristics and whether a firm is heat-loving or heat-averse by nature. It is assumed to be known by the firm and affects its capital investment decisions differentially. For example, a heat-averse firm will invest less than an average firm due to its relatively more negative productivity effect from higher expected heat. The idiosyncratic sensitivity, on the other hand, is unknown to the firm and randomly assigned to each firm at each period. It reflects the heightened likelihood of extreme firm-level events, such as plant-level fire hazards, associated with temperature extremes. Since the idiosyncratic sensitivity is unknown to the firm, it does not influence the firm's capital investment decisions (to the first order). However, it does contribute to productivity shocks and, consequently, affects the marginal revenue product upon realization, particularly in cases of temperature extremes.

Both the level and unexpected shocks of temperature can influence a firm's relative MRPKs through their heterogeneous sensitivities. Given the time-to-build nature of capital, any unexpected shocks in productivity (and thus sales) immediately translate into changes in MRPK. First of all, the persistent sensitivity determines how unexpected temperature shocks differentially impact the relative MRPK of heat-loving and heat-averse firms. For example, an unexpected heat shock decreases the MRPK for heat-averse firms while increasing it for heat-loving firms. From an ex-post perspective, heat-averse firms, anticipating higher productivity than realized, over-invest in capital, resulting in their invested capital being less effectively uti-

lized compared to that of heat-loving firms or firms experiencing less damage than expected. Secondly, the idiosyncratic sensitivity influences how the level of temperature affects firms' relative MRPKs. Some firms might experience unforeseen temperature-related operational challenges, such as machinery malfunctions, while other firms of similar type may be less affected. This discrepancy creates notable differences in MRPKs, and these differences would be larger if the temperature of a region is too hot or too cold.

Therefore, the presence of the large heterogeneity of firm-level sensitivity naturally implies that such temperature variations contribute to MRPK dispersion and, consequently, to capital misallocation across firms. This dispersion arises from two key mechanisms. Firstly, the "level effect" of temperature, operating through idiosyncratic sensitivity, amplifies damage volatility in productivity shocks among firms, leading to greater dispersion in capital returns. As the temperature increasingly deviates from the optimal level, the economy experiences heightened misallocation. Secondly, the 'shock effect' of temperature, driven by heterogeneous persistent sensitivities, variably impacts investment returns across firms: heat shocks decrease returns for heat-averse firms while benefiting heat-loving ones, and cold shocks have the inverse effect. Overall, higher climate uncertainty, associated with larger unexpected temperature shocks, exacerbates capital misallocation across firms. These mechanisms closely explain our reduced-form results: the level effect due to damage volatility explains why a region-sector's geographical location and long-run climates matter for capital misallocation. The shock effect, stemming from climate uncertainty, explains why more severe weather shocks lead to increased misallocation.

We then empirically test the mechanisms of our model by exploiting variations at both the firm and the region-sector levels. We first examine the link between heterogeneous sensitivities and differential MRPK response to temperature shocks using firm-level panel data. As the firm-specific sensitivities are hard to measure directly, we use firm size and AC installation as proxies. This approach allows us to test how firms' MRPKs respond heterogeneously to identical heat shocks within a region-sector. Our estimates reveal that heat shocks significantly lower the MRPK for smaller firms and firms without AC, but have minimal impact on the MRPK for larger firms and AC-installed firms, as they are less sensitive to temperature. Additionally, the role of firm size as a determinant of heterogeneous sensitivities helps rationalize the income effect identified in our reduced-form regression. We find that regions with higher levels of economic development exhibit a greater dispersion of firm sizes, which leads to greater differences in the ability (and resources) to adapt to shocks for firms. This, in turn, results in a higher dispersion of persistent sensitivity across firms, and thus, an increased susceptibility to misallocation due to temperature shocks at the aggregate level.

Next, we estimate and evaluate the quantitative implications of the level and shock effects using model-implied regressions. We empirically test the level effect by estimating how temperature levels non-linearly affect TFP volatility and MRPK dispersion across firms at the region-sector level. Our findings confirm the model's predictions that temperature extremes increase damage volatility: TFP volatility exhibits a U-shaped relationship with temperature. We identify an optimal temperature of around 13°C, at which point TFP volatility reaches the lowest level, thereby imposing the least burden on allocative efficiency and aggregate TFP

through the misallocation channel. We also provide direct evidence of the shock effect using forecast data from the monthly long-range temperature forecasts released by ECMWF ([Copernicus Climate Change Service and Climate Data Store 2018](#)). By aggregating these monthly gridded long-run temperature forecasts at the region-year level, the model-induced regression shows that conditional on the realized temperature, a 1°C error in temperature forecast for all months would lead to at least a 1.6 log point increase in MRPK dispersion. Such an increase in capital misallocation is equivalent to an approximate 0.58% annual aggregate TFP loss when compared to the perfect information counterfactual. Our findings suggest that temperature forecast errors are costly: unexpected temperature shocks lead to dispersion in investment mistakes among firms due to their varying sensitivity to heat. Therefore, in our context, the aggregate importance of temperature forecasts is highlighted through a new channel: accurate forecasting increases the allocative efficiency of capital.

Lastly, using the model parameters identified in the model-induced regression, we quantitatively examine the contributions of the level and shock effects of temperature to misallocation in our sample. We find that, on average, the level effect of temperature accounts for 8.4 log points of MRPK dispersion, equivalent to a TFP loss of 3%. On the other hand, the shock effect contributes approximately 0.023 log points to MRPK dispersion, implying a TFP loss of 0.81%. The magnitude of the level effect exceeds that of the shock effect by more than three times. Broadly consistent with our reduced-form projections, these estimates suggest that the level effect of global warming might play a more significant role in the misallocation channel, as rising temperatures are likely to lead to increased damage volatility in firms' productivity and make efficient investment more difficult.

We conclude that capital misallocation is a quantitatively important channel for how climate change affects the aggregate economy. Climate-induced misallocation stems from substantial cross-sectional firm-level heterogeneity in temperature sensitivity. The estimated loss due to misallocation across firms is considerable, indicating that the average effect of firm-level productivity loss alone is insufficient to capture the aggregate cost of climate change in the economy. Our results suggest that climate policies that solely target the average effect, while overlooking firm heterogeneity, may have limited efficacy.

Contributions to the Literature. Our study contributes to several strands of literature. Firstly, we contribute to the empirical climate econometrics literature ([Dell, Jones, and Olken 2012; Hsiang 2016; Deryugina and Hsiang 2017; Mérel and Gammans 2021; Carleton et al. 2022; Lemoine 2018](#)). These studies have used econometric techniques to estimate the impacts of climate change on various economic outcomes. We extend this literature by introducing a novel methodology for a measurable decomposition of climate damage on aggregate TFP, achieved by integrating results from reduced-form identification with structural modeling. This allows us to isolate the specific channels through which climate change affects the economy. Our approach provides an empirical framework to link the climate-induced micro-level distortions with the aggregate outcomes.

Secondly, we contribute to the literature on the macroeconomic modeling of climate change ([Nath 2023; Nath, Ramey, and Klenow 2023; Cruz and Rossi-Hansberg 2023; Bakkensen and](#)

Barrage 2021; Casey, Fried, and Gibson 2022; Rudik et al. 2021). The existing models have incorporated climate change into workhorse macro and trade models of efficient economies. Naturally, these models would be silent on the causes and effects of how climate change would drive distortions and misallocation of productive factors in the economy. This paper provides a static general equilibrium framework to measure the costs of the temperature-induced misallocation channel via an easy-to-implement sufficient statistics approach. The study that is most closely related to our work is by Caggese et al. (2023), which investigates how temperature shocks impact labor, capital, and material productivity in Italy and uses firm-level estimates to project the potential effects of temperature on Italy's aggregate productivity under various global warming scenarios. In contrast, our work directly identifies the effect of temperature shocks on capital misallocation across firms in a causal manner from historical data encompassing a broad range of geographies (EU, China, and India)². Additionally, we build a novel firm dynamics model to provide insights into the endogenous mechanisms behind climate-induced misallocation that stem from firm-level heterogeneity. We also relate to the literature on the effect of climate on capital stocks, including Hsiang and Jina (2015) and the recent contribution by Bilal and Rossi-Hansberg (2023); our work analyzes how climate change affects capital productivity at the firm level and its aggregate consequences.

Thirdly, our research contributes to the burgeoning literature on the economic value and impacts of weather forecasts. We build on the work of Schlenker and Taylor (2021) on the market internalization of weather forecasts and the work of Shrader (2023) and Shrader, Bakkensen, and Lemoine (2023) on the direct impacts of weather forecasting in production and health. Our study aims to empirically and theoretically demonstrate the overall importance of accurate weather forecasting. We focus on how forecast errors can increase aggregate productivity losses, especially in summer. Firms with greater temperature sensitivity are most affected, as inaccuracies in forecasts can lead to more frequent investment errors. Thus, our research complements micro-level findings at the macro level but also emphasizes the vital role of precise weather forecasting in reducing economic disruptions and boosting productivity.

Finally, we contribute to the literature on misallocation. Since the recent contributions by Restuccia and Rogerson (2008) and Hsieh and Klenow (2009), a large body of work has been studying the aggregate (Gopinath et al. 2017, David and Zeke 2021, among others) and firm-level (Asker, Collard-Wexler, and Loecker 2014, David and Venkateswaran 2019, Baqaee and Farhi 2019, among others) causes of misallocation. This paper contributes to this literature by showing that environmental factors, such as temperature variations and climate change, are also sources of misallocation and might become increasingly important in the future. We also relate to a small but burgeoning literature that studies the causal identification of the drivers of misallocation using (quasi-)natural experiments (Sraer and Thesmar 2023, Bau and Matray 2023, among others). These studies have used exogenous shocks to explore the causes and consequences of misallocation. We extend this literature by using exogenous temperature

2. Our works depart from other dimensions as well. The projection exercise in Caggese et al. (2023) relies on the assumption of the homogeneous effect of temperature across firms and geographical grids, while our empirical identification requires no such assumptions and allows for explicit heterogeneity to matter. Rather than allowing capital to be substitutable and reallocatable across regions and sectors, we identify rising misallocation with temperature extremes within a narrowly defined region-sector pair, which should be interpreted as a lower bound for climate-induced misallocation.

variations to study the effects of climate change. Using large-scale global firm-level data with highly disaggregated measurements (region-sector level), we causally identify the effect of temperature variations on misallocation using a sufficient statistics approach.

The structure of the paper is organized as follows. In Section 2, we develop our climate growth accounting framework. Our data sources and methodology for constructing variables are detailed in Section 3. Section 4 outlines our empirical identification strategy and reduced-form results. Section 5 presents the firm dynamics model to explain the underlying mechanisms. Evidence at the firm level, which tests the proposed channels, is provided in Section 6, and Section 7 offers evidence at the aggregate level. We conclude with Section 8.

2 A Framework for Climate TFP Accounting

In this section, we develop a framework for TFP accounting in the presence of climate conditions. The economic structure follows the seminal work by Hsieh and Klenow (2009), a closed economy model with heterogeneous firms and firm-level distortions on output price and input allocations. We allow firm-level productivity, demand shifter, and distortions to respond endogenously to climate conditions in a flexible manner. We show how climate conditions affect aggregate productivity through two distinct channels in a distorted economy: micro-level productivity (technology) and input and output distortions (misallocation). We also derive measurable sufficient statistics of the misallocation channel that will guide our empirical strategy in Section 4.

2.1 Model Preliminaries

The economy is comprised of regions $r \in \mathcal{R}$ and sectors $s \in \mathcal{S}$. We use $n = (r, s)$ to denote a region-sector pair; there are $N = |\mathcal{R}| \cdot |\mathcal{S}|$ region-sector pairs. We focus on the aggregation of firm-level economic activities within a region-sector pair. We allow a rich set of firm-level economic fundamentals to be arbitrary functions of present and past climate and economic conditions which are listed below.

Climate Conditions \mathbf{T}_{rt} . Every year, each region r experiences its own climate conditions \mathbf{T}_{rt} , a $1 \times N_T$ vector summarized by the climate sufficient statistics including the realizations of daily temperature, precipitation, and other types of extreme weather events. The history of climate conditions up to year t is denoted as $\tilde{\mathbf{T}}_{rt} = (\mathbf{T}_{rt}, \tilde{\mathbf{T}}_{rt-1})$, which combines current year's climate conditions and the past history³.

Economic Conditions. We also consider a general representation of aggregate and idiosyncratic economic conditions that shape the fundamentals of the economy. The aggregate state of the region-sector pair is summarized by the vector \mathbf{X}_{nt} , and the idiosyncratic state of the firm i is summarized by \mathbf{Z}_{nit} , with their histories of realization represented as $\tilde{\mathbf{X}}_{nt} = (\mathbf{X}_{nt}, \tilde{\mathbf{X}}_{nt-1})$ and $\tilde{\mathbf{Z}}_{nit} = (\mathbf{Z}_{nit}, \tilde{\mathbf{Z}}_{nit-1})$. Both $\tilde{\mathbf{X}}_{nt}$ and $\tilde{\mathbf{Z}}_{nit}$ are assumed to be exogenous to the contemporaneous temperature \mathbf{T}_{rt} , yet they may be influenced by the historical climate history $\tilde{\mathbf{T}}_{rt-1}$.

3. Our empirical analysis focuses on realizations of daily temperature and long-run climate.

2.2 Aggregation Model with Micro Effects of Climate Conditions

We now describe the aggregation model and how we incorporate the micro effects of climate conditions into the model.

Industry Production. The industrial output Y_{nt} for each region-sector pair is given by a constant elasticity of substitution (CES) production function of differentiated products of measure J_n ⁴:

$$Y_{nt} = \left(\int_0^{J_n} B_{nit}^{\frac{1}{\sigma_n}} Y_{nit}^{\frac{\sigma_n-1}{\sigma_n}} di \right)^{\frac{\sigma_n}{\sigma_n-1}}, \quad (1)$$

where B_{nit} is a good-specific preference shifter, Y_{nit} denotes the output of firm i and $\sigma_n > 1$ is the elasticity of substitution between products within region-sector n . It is assumed that each product is produced by a unique firm. Profit maximization of industrial output producers leads to the inverse demand function for the output of each firm, Y_{nit} :

$$Y_{nit} = B_{nit} Y_{nt} \left[\frac{P_{nit}}{P_{nt}} \right]^{-\sigma_n}, \quad (2)$$

where $P_{nt} = \left(\int_0^{J_n} B_{nit} P_{nit}^{1-\sigma_n} di \right)^{\frac{1}{1-\sigma_n}}$ is the price index of the region-sector. The demand shifter $B_{nit} := B_{ni}(\tilde{T}_{rt}, \tilde{X}_{nt}, \tilde{Z}_{nit})$ is a firm-specific function of climate and economic conditions to capture the possibility that some goods or services might be less preferable in hotter climates compared to cooler ones, even in the same region and sector. The demand-side effects emerge in developed economies in which leisure and recreational activities are important in the consumption basket.⁵.

Firm-level Production. Firms produce their products with Cobb-Douglas technology and their output is given by:

$$Y_{nit} = A_{nit} K_{nit}^{\alpha_{Kn}} L_{nit}^{\alpha_{Ln}}, \quad (3)$$

where A_{nit} is physical productivity⁶, K_{nit} is capital stock and L_{nit} is labor input employed by firm i . α_{Kn}, α_{Ln} are the factor elasticities that satisfy constant returns to scale in production such that $\alpha_{Kn} + \alpha_{Ln} = 1$. We allow A_{nit} to be a firm-specific function of climate conditions \tilde{T}_{rt} , recognizing the highly heterogeneous sensitivity to heat or cold among different types of firms within and across various sectors and regions. The heterogeneity is potentially attributed to the distinct nature of production processes and varying levels of adaptability to climate conditions as documented in [Nath \(2023\)](#).⁷ Of course, climate conditions are not the only

4. In theory, we could allow J_n to be time-varying as well to account for potential entry-exit. However, almost all firm-level data we use have some changes in sampling methodologies such that it is hard to measure the entry-exit dynamics accurately within a granular region-sector pair.

5. This is evident in industries where climate variations directly affect consumer behavior. For instance, in the service industry, [Zivin and Neidell \(2014\)](#) found that Americans are more likely to shift to indoor recreational activities from outdoor ones (such as recreational fishing ([Dundas and Haefen 2020](#))) when exposed to heat shocks.

6. It is a measure of quantity-based total factor productivity (TFPQ), reflecting the overall efficiency with which the firm uses its inputs to produce units of physical output ([Bils, Klenow, and Ruane 2021](#)). TFPQ cannot be directly measured in the absence of price or quantity data, barring any additional structural assumptions. In a Cobb-Douglas framework, the notion of physical productivity (TFPQ) nests the effect of factor-specific productivity.

7. Such heterogeneity is present even within the same region-sector. For example, in manufacturing, the pro-

factors determining the fundamentals of the economy. We also allow a general set of aggregate and firm-specific economic states, denoted as $(\tilde{\mathbf{X}}_{nt}, \tilde{\mathbf{Z}}_{nit})$ to affect A_{nit} . Therefore, we can write each firm's productivity as $A_{nit} := A_{ni}(\tilde{\mathbf{T}}_{rt}, \tilde{\mathbf{X}}_{nt}, \tilde{\mathbf{Z}}_{nit})$.

Distortions. Each firm faces a variety of distortions, represented as an output wedge on revenue τ^Y and a set of wedges on all inputs τ^F . Subject to the inverse demand and wedges, each firm i engages in monopolistic competition and optimally chooses its quantity of inputs and price to maximize profits:

$$\begin{aligned} & \max_{P_{nit}, K_{nit}, L_{nit}} (1 - \tau_{nit}^Y) P_{nit} \underbrace{A_{nit} K_{nit}^{\alpha_K s} L_{nit}^{\alpha_L n}}_{Y_{nit}} - (1 + \tau_{nit}^K) R_{nt} K_{nit} \\ & \quad - (1 + \tau_{nit}^L) W_{nt} L_{nit} \\ & \text{subject to : } Y_{nit} = B_{nit} Y_{nt} \left[\frac{P_{nit}}{P_{nt}} \right]^{-\sigma_n}, \end{aligned} \tag{4}$$

where R_{nt} is the user cost of capital, W_{nt} denotes the wage and P_{nt}^M denotes the price for the intermediate input bundles. τ_{nit}^Y is the firm-specific wedge that distorts output, and τ_{nit}^F denote the input-specific wedge on factor $F \in \{K, L\}$. For example, τ_{nit}^K denotes capital distortion that raises the marginal cost of capital relative to the market rental rate R_{nt} . We assume all firms take these wedges as exogenous for now and model the endogenous nature of these frictions and their relationship with climate change in Section 5.

These wedges are reduced-form representations of all the frictions in the economy that prevent the optimal allocation of inputs in our static ex-post accounting exercise⁸, including climate-related frictions. Thus, similar to demand shifters and productivity, we assume them to be firm-specific functions of climate as well as the states of the region-sector and the firm itself.

Specifically, the output wedge $\tau_{nit}^Y := \tau_{ni}^Y(\tilde{\mathbf{T}}_{rt}, \tilde{\mathbf{X}}_{nt}, \tilde{\mathbf{Z}}_{nit})$ captures the distortions (or exogenous markups) the firm faces on prices or quantities relative to the Dixit-Stiglitz benchmark⁹. These distortions can arise from policy interventions or market imperfections. For example, some firms might have relatively higher markups as temperature shocks increase the local industry concentration Ponticelli, Xu, and Zeume (2023), which is not captured by the Dixit-Stiglitz markup. Similarly, input wedges denoted as $\tau_{nit}^F = \tau_{ni}^F(\tilde{\mathbf{T}}_{rt}, \tilde{\mathbf{X}}_{nt}, \tilde{\mathbf{Z}}_{nit})$, disincentivize firms from using input $F \in \{K, L\}$ as if they were effectively paying a higher factor price¹⁰. Any channels through which climate conditions prevent the optimal allocation of inputs would be captured by the function τ_{ni}^F , such as weather-induced capital depreciation (Hsiang and Jina 2015; Bilal and Rossi-Hansberg 2023). Importantly, in the context of dynamic input choices such as capital, the wedge function $\tau_{ni}^K(\tilde{\mathbf{T}}_{rt}, \cdot)$ would capture the different degree

ductivity of a firm with AC installation is less susceptible to heat shocks than those without ACs (Somanathan et al. 2021). In agriculture, rainfed farms often suffer more than irrigated farms when facing heat (Piao et al. 2010).

8. "Ex-post" is in a sense that we use the set of wedges to rationalize the firm's behavior in the static accounting framework after the input and production has taken place

9. τ_{nit}^Y also represent price distortions that reflect potential heterogeneity in revenue taxes, markups, or prices across firms not captured by the constant Dixit-Stiglitz markup.

10. For a firm to be (boundedly) productive, it is necessary that all prices are positive, which requires $1 - \tau_{nit}^Y > 0$ and $1 + \tau_{nit}^F > 0$.

of investment mistakes induced by unexpected temperature shocks (e.g. when a heat-averse firm invested too much capital before a heat shock hits).

Factor Supply. The total productive factors in the region-sector n follows that $K_{nt} = \sum_{i=1}^{J_n} K_{nit}$, $L_{nt} = \sum_{i=1}^{J_n} L_{nit}$. The total factor supply is treated as exogenously given every period.

Equilibrium. The equilibrium allocations in a region-sector depend on the set of fundamentals $(B_{nit}, A_{nit}, \tau_{nit}^Y, \tau_{nit}^F)$, $\forall i$ and $\forall F \in \{K, L\}$. Given preference shifter B_{nit} , physical productivity A_{nit} , output distortions $\tau_{nit}^Y < 1$, factor distortions $\tau_{nit}^F > -1$ for all firms i , and total factor supply of K_{nt} and L_{nt} , a general equilibrium consisting of goods prices P_{nit} , factor prices, and equilibrium factor allocation F_{nit} is defined where all markets clear. We call the equilibrium defined by $(B_{nit}, A_{nit}, \tau_{nit}^Y, \tau_{nit}^F)$ the *distorted equilibrium* and the equilibrium defined by $(B_{nit}, A_{nit}, 0, 0)$ the *efficient equilibrium*¹¹ to denote the first best outcome in this economy without distortions.

Distortions and Misallocation. We now examine how climate-related input frictions could shape the differences in marginal products in the cross-section of firms. For any input $F \in \{K, L\}$, the firm's optimality condition with respect to F_{it} will yield that the marginal revenue product of factor F (MRPF) equals to the factor price P_{nit}^F times the weather-affected wedges $\frac{1+\tau_{ni}^F(\tilde{\mathbf{T}}_{rt}, \cdot)}{1-\tau_{ni}^Y(\tilde{\mathbf{T}}_{rt}, \cdot)}$:

$$MRPF_{nit} = \alpha_{F_n} \frac{\sigma_n - 1}{\sigma_n} \frac{P_{nit} Y_{nit}}{F_{nit}} = \frac{1 + \tau_{ni}^F(\tilde{\mathbf{T}}_{rt}, \cdot)}{1 - \tau_{ni}^Y(\tilde{\mathbf{T}}_{rt}, \cdot)} P_{nit}^F. \quad (5)$$

Equation 5 states that any shift in climate conditions would affect the input (and output) wedges and thus MRPF. Moreover, any heterogeneity in the way wedges respond to temperature would result in unequal marginal revenue return to factors among firms in the cross-section. Such dispersion of marginal revenue return to factors is often referred to as "mislocation", indicating there are potential gains from reallocating the factor from firms with a low marginal product to the ones with a high marginal product. We can explicitly link these distortions to equilibrium (mis-)allocation of factors as follows.

Proposition 1 Equilibrium (Mis-)allocation. *The distorted equilibrium allocation of capital, labor, and material inputs must satisfy that for any factor $F \in \{K, L\}$,*

$$\begin{aligned} \log\left(\frac{F_{nit}}{F_{nit}^*}\right) = & -\log(1 + \tau_{nit}^F) + \sigma_n \log(1 - \tau_{nit}^Y) - \\ & (\sigma_n - 1) \sum_{F'=\{K,L\}} \alpha_{F'_n} \log(1 + \tau_{ni}^{F'}) + \log(C_{Fnt}), \end{aligned} \quad (6)$$

where C_{Fnt} is a region-sector-year specific constant and F_{nit}^* is the efficient equilibrium allocation of factors that are entirely determined by preference shifter and physical productivity within the region-

11. In the accounting framework, efficiency is defined in a static and unconstrained sense (similar to Carrillo et al. 2023).

sector:

$$F_{nit}^* = \frac{B_{ni}(\tilde{\mathbf{T}}_{rt}, \cdot) A_{ni}(\tilde{\mathbf{T}}_{rt}, \cdot)^{\sigma_n - 1}}{\sum_j B_{nj}(\tilde{\mathbf{T}}_{rt}, \cdot) A_{sj}(\tilde{\mathbf{T}}_{rt}, \cdot)^{\sigma_n - 1}} F_{nt} \quad (7)$$

Proof. See Appendix C.1. ■

The relative gap $\log(F_{nit}) - \log(F_{nit}^*)$ decreases with factor-specific wedges $\log(1 + \tau_{ni}^F(\tilde{\mathbf{T}}_{rt}, \cdot))$ due to increased effective cost of the factor, increases with output wedge due to greater price incentives, and decreases with the distortions of all other factors (i.e., "mixed" distortions), $\sum_{F'=\{K,L\}} \alpha_{F'_n} \log(1 + \tau_{ni}^{F'}(\tilde{\mathbf{T}}_{rt}, \cdot))$, as higher costs of one factor would lead to reduced usage of other factors (as $\sigma_n > 1$).

Equation 7 reveals that in an efficient economy free of distortions, climate only affects preferences and physical productivity, leading to a resource allocation favoring firms whose products are preferred by customers and those with higher physical productivity. On the other hand, in a distorted equilibrium with temperature-sensitive wedges, more factors are allocated to firms with lower output distortion (e.g. higher markups) and lower input distortions (e.g. lower price of factors). This results in a state of misallocation of F_{nit} compared to its efficient counterpart F_{nit}^* .

In the context of temperature effects, if firm A's capital wedge increases with the current temperature (a variable in $\tilde{\mathbf{T}}_{rt}$), while firm B's decreases, a temperature shock would raise the effective price of capital for firm A. As a result, firm A would allocate less capital than is efficient for its production compared to firm B, thereby creating a misallocation of resources. We will remain agnostic on the endogenous mechanism for now and leave the detailed discussion and identification of mechanisms driving these climate-induced distortions in Section 5, 6, and 7.

A Remark on Climate Conditions and Firm-level Fundamentals. Recall that we have assumed that all firm-level fundamentals $\{B_{nit}, A_{nit}, \tau_{nit}^Y, \tau_{nit}^F\}$ to be firm-specific and smooth functions based on the realized histories of three key factors, including climate conditions ($\tilde{\mathbf{T}}_{rt}$), aggregate economic conditions ($\tilde{\mathbf{X}}_{nt}$), and firm-level states ($\tilde{\mathbf{Z}}_{nit}$):

$$\begin{aligned} A_{nit} &= A_{ni}(\tilde{\mathbf{T}}_{rt}, \tilde{\mathbf{X}}_{nt}, \tilde{\mathbf{Z}}_{nit}), & B_{nit} &= B_{ni}(\tilde{\mathbf{T}}_{rt}, \tilde{\mathbf{X}}_{nt}, \tilde{\mathbf{Z}}_{nit}), \\ \tau_{nit}^Y &= \tau_{ni}^Y(\tilde{\mathbf{T}}_{rt}, \tilde{\mathbf{X}}_{nt}, \tilde{\mathbf{Z}}_{nit}), & \tau_{nit}^F &= \tau_{ni}^F(\tilde{\mathbf{T}}_{rt}, \tilde{\mathbf{X}}_{nt}, \tilde{\mathbf{Z}}_{nit}), \quad \forall F \in \{K, L\}. \end{aligned}$$

Allowing these relationships to be firm-specific is essential as it implies that the same regional climate conditions $\tilde{\mathbf{T}}_{rt}$ could have heterogeneous effect on physical productivity A_{nit} , demand B_{nit} , and input distortions τ_{nit}^Y and τ_{nit}^F , across different firms. This heterogeneous impact leaves room for differential response of marginal products to climate variations, which will be the key mechanisms to be inspected in this paper.

2.3 Aggregation, TFP Decomposition and Misallocation

We proceed to perform aggregation in this accounting framework. We adopt a widely-used assumption in the misallocation literature (see Hsieh and Klenow (2009) and Sraer and Thesmar (2023)) that productivity and all associated wedges follow a joint log-normal distribution

across firms in any region-sector-year pair, which holds very well in the data. More formally, we assume that for any given set of arguments $(\tilde{\mathbf{T}}_{rt}, \tilde{\mathbf{X}}_{nt}, \{\tilde{\mathbf{Z}}_{nit}\}_i)$, the joint distribution of the realized values of the sets of functions, $\mathbf{S}_{nit} = (B_{nit}, A_{nit}, 1 + \tau_{nit}^Y, 1 + \tau_{nit}^K, 1 + \tau_{nit}^L)$, can be characterized as follows:

$$\log(\mathbf{S}_{nit}(\tilde{\mathbf{T}}_{rt}, \tilde{\mathbf{X}}_{nt}, \tilde{\mathbf{Z}}_{nit})) \sim \mathcal{N}\left(\mu_s^{(n)}(\tilde{\mathbf{T}}_{rt}, \tilde{\mathbf{X}}_{nt}), \Sigma_{ss}^{(n)}(\tilde{\mathbf{T}}_{rt}, \tilde{\mathbf{X}}_{nt})\right). \quad (8)$$

Here, $\mu_s^{(n)}$ represents the mean vector of firm-level fundamentals, while $\Sigma_{ss}^{(n)}$ is the covariance matrix of these fundamentals across firms. Each element of these are smooth functions of their respective arguments¹². For tractability, we adopt the aggregation notation of [Krusell and Smith \(1998\)](#) that the distribution of firm-level fundamentals $\tilde{\mathbf{Z}}_{nit}$ (over i) can be summarized by a finite set of moments and stacked into the aggregate states of the economy $\tilde{\mathbf{X}}_{nt}$. The log-normality assumption allows us to transparently show how micro-level wedges are translated into losses in aggregate productivity:

Proposition 2 Aggregation and TFP Decomposition. *Under the log-normality assumption, each region-sector n admits an aggregate production function of the form*

$$Y_{nt} = TFP_{nt} K_{nt}^{\alpha_K n} L_{nt}^{\alpha_L n}, \quad (9)$$

where the region-sectoral aggregate Total Factor Productivity $TFP_{nt} := TFP_n(\tilde{\mathbf{T}}_{rt}, \tilde{\mathbf{X}}_{nt})$ can be decomposed as follows:

$$\begin{aligned} \log TFP_n(\tilde{\mathbf{T}}_{rt}, \cdot) &= \underbrace{\frac{1}{\sigma_n - 1} \log \left[J_n \mathbb{E}_i \left[B_{ni}(\tilde{\mathbf{T}}_{rt}, \cdot) \left(A_{ni}(\tilde{\mathbf{T}}_{rt}, \cdot) \right)^{\sigma_n - 1} \right] \right]}_{\text{Technology}(\log TFP_n^E)} - \underbrace{\frac{\sigma_n}{2} \text{var}_{\log(1 - \tau_{ni}^Y)}(\tilde{\mathbf{T}}_{rt}, \cdot)}_{\text{Output Wedge Dispersion}} \\ &\quad - \underbrace{\sum_{F \in \{K, L\}} \frac{\alpha_{Fn} + \alpha_{Fn}^2 (\sigma_n - 1)}{2} \text{var}_{\log(1 + \tau_{ni}^F)}(\tilde{\mathbf{T}}_{rt}, \cdot)}_{\text{Factor Wedge Dispersion}} \\ &\quad + \underbrace{\sigma_n \sum_{F \in \{K, L\}} \alpha_{Fn} \text{cov}_{\log(1 - \tau_{ni}^Y), \log(1 + \tau_{ni}^F)}(\tilde{\mathbf{T}}_{rt}, \cdot)}_{\text{Output-Factor Mixed Distortion}} \\ &\quad - \underbrace{(\sigma_n - 1) \alpha_{Kn} \alpha_{Ln} \text{cov}_{\log(1 + \tau_{ni}^K), \log(1 + \tau_{ni}^L)}(\tilde{\mathbf{T}}_{rt}, \cdot)}_{\text{Factor Mixed Distortion}} \end{aligned} \quad (10)$$

Proof. See Appendix C.2. ■

All the variance and covariance terms are elements in the variance matrix $\Sigma_{ss}^{(n)}(\tilde{\mathbf{T}}_{rt}, \tilde{\mathbf{X}}_{nt})$ in Equation 8. Each of them is a region-sector-specific function of weather conditions and other economic fundamentals. They describe how these conditions would alter the distribution of wedges over the cross-section of firms.

12. This smoothness follows the principle that population moments are smooth functions of the variables \mathbf{S}_{nit} .

The efficient TFP level is given by $\log \text{TFP}_n^E = \frac{1}{\sigma_n - 1} \log \left[J_n \mathbb{E}_i \left[B_{ni}(\tilde{\mathbf{T}}_{rt}, \cdot) \left(A_{ni}(\tilde{\mathbf{T}}_{rt}, \cdot) \right)^{\sigma_n - 1} \right] \right]$ in the absence of distortions, which is determined by the variety, preference shifter and love-for-variety-adjusted physical productivity of the firm. This represents the production possibility frontier of the economy. We call this **technology** in the spirit of Basu and Fernald (2002) and Baqaee and Farhi (2019). The rest of the terms represent the costs of distortions in the economy, referred to as **misallocation loss**. Dispersion in output wedges $\text{var}_{\log(1-\tau_{ni}^Y)}$ and factor input wedges $\text{var}_{\log(1+\tau_{ni}^F)}$ will both lead to dispersion in the marginal revenue product of factors, creating more misallocation of factors and lowering sectoral TFP.

The impact of factor wedge dispersion on TFP is determined by two key parameters: σ_n and α_{F_n} . A greater σ_n implies higher product substitutability and, consequently, larger gains from reallocation. α_{F_n} indicates the factor's importance in production. For a factor F , a higher α_{F_n} renders the dispersion of factor wedges more costly. Furthermore, the interactions of wedges also impact productivity. All else being equal, greater productivity losses occur when firms with lower markups are also likely to endure higher input distortions ($\text{cov}_{\log(1-\tau_{ni}^Y), \log(1+\tau_{ni}^F)} < 0$). Similarly, misallocation costs tend to be higher in cases where firms experiencing capital distortions are also more likely to face higher labor distortions ($\text{cov}_{\log(1+\tau_{ni}^F), \log(1+\tau_{ni}^{F'})} > 0$). These interactions are often referred to as "mixed" distortions.

2.4 Decomposing the Impact of Climate Change on TFP

Our decomposition framework shows that aggregate TFP depends on moments concerning technology and misallocation, which are endogenous to climate conditions. Since we have assumed that all moments are smooth functions of climate conditions $\tilde{\mathbf{T}}_{rt}$, we can decompose the first-order impact of climate change on TFP via a set of causal elasticities for each relevant moment. We formalize this in a case when only capital wedges are present.

Special Case: only capital wedges are present. This is the benchmark case in David and Venkateswaran (2019), Sraer and Thesmar (2023), and Asker, Collard-Wexler, and Loecker (2014), with a view that capital is more of a dynamic input than labor or material. The dispersion of capital distortions is also measured to be larger than that of labor (Gorodnichenko et al. 2018) as they cannot be adjusted easily after the realization of shocks. Therefore, how capital misallocation is affected by climate conditions will be the main focus of empirical analysis throughout the paper. We will revisit the general case featuring various channels of misallocation in the Appendix C.

When the capital wedge is the only source of distortions in the economy within region-sector n , the MRPK of each firm i satisfies that:

$$\text{MRPK}_{nit} = \alpha_{Kn} \frac{P_{it} Y_{it}}{K_{it}} \propto (1 + \tau_{nit}^K) R_{nt}.$$

The dispersion of capital is therefore given by the variance of log(MRPK) across firms

$$\text{var}(\log(1 + \tau_{nit})) = \text{var}(mrpk_{nit}) = \text{var} \left(\log \left(\frac{P_{it} Y_{it}}{K_{it}} \right) \right), \quad (11)$$

where we define $mrpk = \log(MRPK)$. Equation 11 shows that the cross-sectional variance of (log) capital distortions across firms is identical to the dispersion of (log) MRPK, which can be computed via the variance of log sales over capital stock given the Cobb-Douglas technologies. Now, the effect of climate conditions on aggregate TFP can be written as:

$$\begin{aligned} \frac{\partial \log TFP_n(\tilde{\mathbf{T}}_{rt}, \cdot)}{\partial \tilde{\mathbf{T}}_{rt}} &= \frac{\partial \text{Technology}_{nt}}{\partial \tilde{\mathbf{T}}_{rt}} - \frac{\partial \text{Misallocation Loss}_{nt}}{\partial \tilde{\mathbf{T}}_{rt}} \\ &= \frac{1}{\sigma_n - 1} \frac{\partial \log \mathbb{E}_i \left[B_{ni}(\tilde{\mathbf{T}}_{rt}, \cdot) (A_{ni}(\tilde{\mathbf{T}}_{rt}, \cdot))^{\sigma_n - 1} \right]}{\partial \tilde{\mathbf{T}}_{rt}} \\ &\quad - \frac{\alpha_{Kn} + \alpha_{Kn}^2 (\sigma_n - 1)}{2} \frac{\partial \text{var}_{mrpk,n}(\tilde{\mathbf{T}}_{rt}, \cdot)}{\partial \tilde{\mathbf{T}}_{rt}}, \end{aligned} \quad (12)$$

such that the (first-order) cost of climate-induced misallocation would be reduced to the estimation of elasticity $\frac{\partial \text{var}_{mrpk,n}(\tilde{\mathbf{T}}_{rt}, \cdot)}{\partial \tilde{\mathbf{T}}_{rt}}$. The decomposition shows that the first-order effect of climate conditions on aggregate TFP can be captured entirely through the effect on technology and the effect on inefficiency losses through capital misallocation. This proposition provides theoretical foundations to understand the different channels through which climate conditions may result in aggregate losses and a practical framework for quantitatively measuring these changes.

In theory, the derivatives of our structural objects with respect to climate conditions are globally well-defined and could vary with various histories of climate and economic conditions. However, in practice, it is preferable to think of them as "reduced form," which means that they can only be well estimated with respect to observed equilibrium allocations and are not necessarily invariant to the evolving climate conditions in the long run. For example, these first-order effects could increase with worsening global warming or decrease with gradual adaptation. We will address this explicitly in Section 4.3 to capture the effect of long-run climate conditions and economic development.

3 Data

3.1 Global Firm-level Microdata

We compile a global sample of firm-level microdata from both developed and developing economies that include 30 European countries, China and India, which covers 38.6% of world GDP. The firm-level panels for the 30 European countries were from Bureau van Dijk's (BvD) Orbis database, and the data for China and India were obtained from government-conducted surveys, China National Bureau of Statistics (NBS), and India ASI. The datasets contain financial accounting information such as revenue, fixed assets, wage bills, and employment. The three datasets have been widely employed in the literature and could be regarded as nationally representative.

Table A.1 provides a comprehensive list of countries, year coverage, and data sources for the three datasets. For all datasets, we harmonize the sectoral classifications of all firms into

eight major divisions according to the U.S. Standard Industrial Classification (USSIC) code¹³. Regions are defined to be the NUTS3 regions in Europe, prefectures in China, and districts in India. The sizes of these regions are close to a U.S. county.

Our key economic variables of interest are the sufficient statistics of firm-level activities that map directly into aggregate TFP at the region-sector-year level, in particular, the variance of marginal revenue product of capital across firms. Thus, for all datasets we use, we restrict ourselves to work with firm-year observations that report data on both revenue and capital stock. We measure revenue $P_i Y_i$ with the reported operating revenue in both Orbis and China NBS data, and the reported total sales in India ASI. We use the book value of gross fixed assets as a measure of firm-level capital stock K_i ¹⁴. For each country, we trim the observations of extreme values of MRPK and TFPR at 0.1%.

For all reduced-form analysis using region-sector-year level sufficient statistics, we restrict our sample to the region-sector-year pairs with more than 30 firm-year observations of revenue and capital stock data, to minimize the noises in the variance measures and preserve log-normality in the data. To make sure variations in these sufficient statistics are not due to changes in data collection patterns and measurement errors, we also drop the observations after which there are sudden jumps in the number of firms and aggregate sales in the region-sector. The final region-sector sample is an unbalanced sample consisting 124,567 of region-sector-year observations, covering 76,826,956 firm-year observations. For the firm-level analysis in section 6, we include all firm-year observations in the raw data after trimming the 0.1% extreme values of all firm-level dependent variables and covariates. Below, we provide a brief overview of each of the datasets.

BvD Orbis. The firm-level data for the 30 European countries are drawn from Orbis, a database maintained by Bureau van Dijk (BvD). Orbis originates from administrative records collected at the firm level, primarily by each country's local Chambers of Commerce. A significant advantage of focusing on European countries with Orbis is that company reporting is regulatory, even for small private firms. It covers firms from all sectors and approximately 99 percent of the companies included are private entities.

To organize and clean the Orbis dataset, we follow the approach in [Kalemli-Ozcan et al. \(2015\)](#), [Gopinath et al. \(2017\)](#), and [Nath \(2023\)](#). A notable departure from the papers cited earlier lies in our method for expanding MRPK's coverage. We include firms that have complete data on revenue and capital (fixed assets) while allowing for variability in the extent of coverage for other variables such as material costs, wage bills, and employee numbers.¹⁵ Each firm in the Orbis data has its associated USSIC sector code, and its various address information can be matched with a NUTS3 region in Europe. Different countries in Orbis have different years of data coverage, detailed in Table A.1. We use the sample period of 1998-2018.

13. The industries included are agriculture, mining, construction, manufacturing, transportation & utilities, wholesale trade, retail trade, finance, insurance, and real estate(FIRE) and Services.

14. Only exception is India ASI, which reports the book value of net fixed assets in a much more consistent manner while the gross values are reported with a major amount of missing values

15. [Nath \(2023\)](#) keeps the firms with complete revenue and labor data, while [Gopinath et al. \(2017\)](#) use a more restrictive sample that only preserves observations having all production-related information in south European countries.

China NBS. The annual firm-level data for China is derived from surveys conducted by the National Bureau of Statistics (NBS) in China. These surveys encompass all industrial firms with annual sales exceeding nominal CNY 5 million (approximately USD 0.61 million) from 1998 to 2007. Such firms are commonly referred to as “above-scale” industrial firms¹⁶. The NBS data includes sectors such as mining, manufacturing, and utilities, with manufacturing constituting more than 90% of the total observations in the dataset. In processing the NBS data, we follow the methodology outlined in [Zhang et al. \(2018\)](#). Each firm in the dataset is categorized using a four-digit Chinese Industry Classification (CIC) code and is harmonized to the USSIC division level. Each firm’s reported location can be mapped into a prefecture-level division. We only use the sample period of 1998-2007 due to inconsistent reporting after 2008 as discussed in [Brandt, Van Bieseboeck, and Zhang \(2014\)](#) and [Nath \(2023\)](#).

India ASI. Our data for India are drawn from India’s Annual Survey of Industries (ASI). ASI is a census of large plants employing more than 100 workers and a random sample of about one-fifth of smaller plants that are registered under the Indian Factories Act.¹⁷ The sampling procedure assures representativeness at the state and industry levels. Almost all plants included in the ASI data are in the manufacturing sector. We match the plants to the Indian districts following the approach of [Somanathan et al. \(2021\)](#). From 2001 to 2014, ASI also collects whether the plant is AC equipped which we will utilize as a proxy variable for a firm’s adaptability. We use the sample period of 1998 to 2018.

3.2 Weather and Forecast Data

Climate. For climate data, we use the land component of the European ReAnalysis, known as ERA5-Land ([Sabater 2019](#)), produced by the European Centre for Medium-Range Weather Forecasts (ECMWF). ERA5-Land is a reanalysis dataset that combines historical observations with models to create a consistent time series of various climate variables. A main advantage of ERA5-Land is its enhanced temporal and horizontal resolution. It provides hourly data on surface variables at a spatial resolution of $0.1^\circ\text{longitude} \times 0.1^\circ\text{latitude}$ (approximately 9 km), covering the entire world. Such high resolution allows for a clearer depiction of the spatial patterns of surface temperature between neighboring locations.

Our analysis uses variables of air temperature at 2 meters above the land surface. We aggregate daily average temperatures¹⁸ up to the annual level. Specifically, in our main specification, we bin daily temperature every 5°C from -5°C to 30°C . Each temperature bin counts the number of days in a year when the daily average temperature falls within specific temperature ranges. This is calculated for every region in each year.

16. [Brandt, Van Bieseboeck, and Zhang \(2014\)](#) shows that when comparing to the 2004 NBS census of industrial firms that covers all industrial plants in China, these above-scale firms in the sample account for over 90.7% of the total output.

17. As noted by [Allcott, Collard-Wexler, and O’Connell \(2016\)](#), large plants in the census scheme are defined as factories with 100 or more workers in all years except 1997-2003 when it included only factories with 200 or more workers. The sampling scheme for smaller registered plants included one-third of factories until 2004 and one-fifth since then.

18. The daily average temperature is the simple geometric average of the maximum and minimum temperatures. The daily maximum temperature is identified by the highest value among the hourly temperatures, and the daily minimum temperature is the lowest recorded value.

Figure 1a plots the difference of the number of hot days above 25°C in a year between periods of our sample firm coverage, 1999-2008 and 2009-2018, and the baseline periods, from 1951 to 1980. The dark red color represents an increase of more than 13.2 days in a year with temperatures above 25°C. Figure 1b depicts the daily temperature distributions in baseline periods, sample periods, and the projection year of 2100. The global warming trend reveals that the number of days above 25 has increased, and the number of days below 10 has reduced in each country in the past decades. The temperature distribution shifts rightward when we compare across and within countries, as climates grow warmer.

The use of temperature bins in our analysis better conceptualizes climate. Because climate change represents a long-term shift in weather patterns, the year-to-year variation in the whole temperature distribution offers a more accurate depiction of climate change than merely examining year-to-year variations in mean temperature. A key feature of climate change is the increased frequency of extreme heat events (Oudin Åström et al. 2013; Christidis, Mitchell, and Stott 2023), therefore the increase in the number of extreme hot bins, indicative of a rightward shift in the tail of the weather distribution, captures the idea of global warming more accurately.

Projection and Forecast. We collect global projection data computed by the sixth phase of the Coupled Model Intercomparison Project (CMIP6). We use the SSP3-7.0 experiment that is based on SSP3 where climate change mitigation challenges dominate, and RCP7.0, a future pathway with a radiative forcing of 7.0 W/m² in the year 2100¹⁹. The SSP3-7.0 scenario represents the high end of plausible future pathways and is comparable to the CMIP5 experiment RCP7.0²⁰. We use SSP3-7.0 projection in the main analysis and present results from other scenarios in the Appendix.

For weather forecast data, we collect the long-range (seasonal) forecast from ECMWF (Copernicus Climate Change Service and Climate Data Store 2018), which provides information about atmospheric and oceanic conditions up to seven months into the future. The forecast data have a spatial resolution of 1-degree longitude by 1-degree latitude²¹. We collect forecast daily maximum and minimum 2m temperature from the first day of each month from January to December with forecasts up to 30 days measured in 724 lead-hours.

19. According to Hausfather et al. (2022) and Shiogama et al. (2023), the SSP-RCPs, successors to the RCPs, were developed by Integrated Assessment Model (IAM) researchers. These include four primary scenarios: SSP1–2.6, SSP2–4.5, SSP3–7.0, and SSP5–8.5, with the numbers after the dash indicating radiative forcing levels. Notably, SSP3–7.0, introduced in CMIP6, represents a mid-range outcome among baseline projections from energy system models. This scenario assumes moderate air quality policies leading to stable or increased aerosol emissions and significant forest area reductions, unlike other SSP-RCPs. Its global mean precipitation changes are comparable to those in SSP2–4.5. During CMIP6 and AR6’s research period, significant shifts in global mitigation policies occurred, particularly after the 2015 Paris Agreement. These developments have cast doubt on the likelihood of the high-end SSP5–8.5 scenario, which is now often considered an unlikely worst-case scenario for impact assessments. Consequently, SSP3–7.0 has gained prominence as an alternative high-end scenario for Impacts, Adaptation, and Vulnerability (IAV) studies.

20. We use the GFDL-ESM4 model with a 1-degree nominal horizontal resolution produced by the National Oceanic and Atmospheric Administration, Geophysical Fluid Dynamics Laboratory (NOAA-GFDL).

21. From 1981 to 2016, the forecast values were hindcasts generated with a 25-member ensemble. Starting in 2017, they are forecasts produced monthly with a 51-member ensemble. These ensembles are run on the first day of each month, providing forecasts for up to seven months ahead.

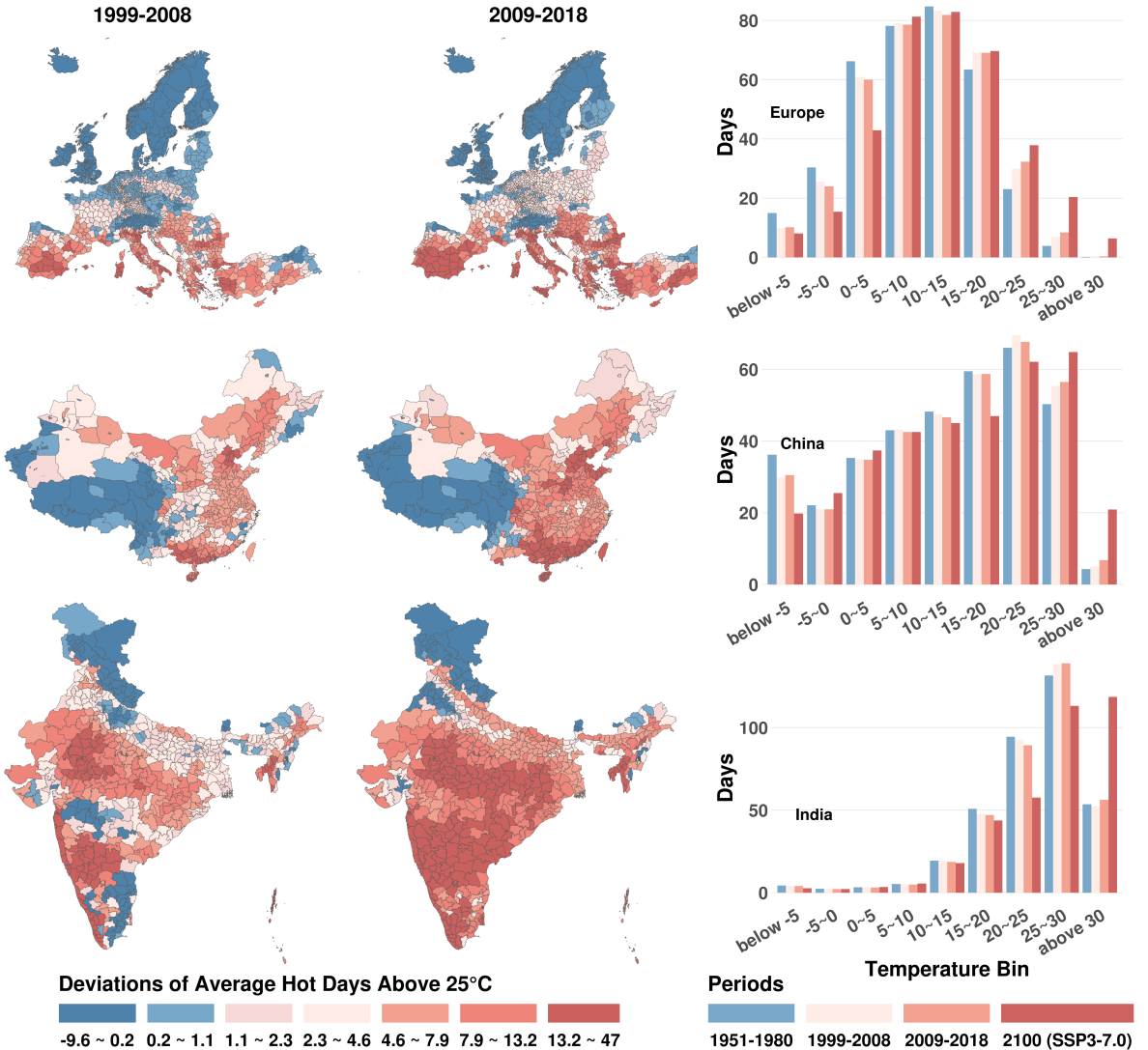
3.3 Other Data

Regional GDP. We collect regional-level global GDP data from DOSE (Wenz et al. 2023). We then clean and map global GDP data to our firm and weather datasets using spatial coordinates. This involves aligning different geographical units with administrative divisions like NUTS, prefectures, and districts.

Income Projection Projections of national income per capita are collected from the SSP Database, using the OECD EnvGrowth model (Dellink et al. 2017) hosted by the International Institute for Applied Systems Analysis.

Figure 1: Climates of our sample regions

(a) Number of Hot Days Deviation Relative to 1951-1980 (b) Average Daily Temperature Distribution



Notes: Figure 1a plots the difference of average number of days above 25°C between sample periods and baseline periods. The baseline period is from 1950 to 1980. The sample periods consist of two parts, 1999 to 2008, and 2009 to 2018. We calculate the 10-year average number of days above 25°C and deduct the 30-year baseline average number of days to obtain the difference. Figure 1b plots the average daily temperature distributions for baseline periods 1950-1980, two sample periods, and the projection year of 2100 under the SSP3-7.0 scenario.

4 Estimating the Misallocation Effect of Climate Change

4.1 Identification of the Causal Elasticities on Misallocation

We now estimate the first-order causal elasticities on capital misallocation $\frac{\partial \text{var}_{mfpk_{ni}}(\tilde{\mathbf{T}}_{rt}, \cdot)}{\partial \tilde{\mathbf{T}}_{rt}}$. Note that for each region-sector $n = (r, s)$, a Taylor expansion around the observed steady-state $(\overline{\text{var}_{mfpk_{(s,r)i}}}, \tilde{\mathbf{T}}_r, \tilde{\mathbf{X}}_{s,r})$ can be written as

$$\begin{aligned} \text{var}_{mfpk_{(s,r)i}}(\tilde{\mathbf{T}}_{r,t}, \tilde{\mathbf{X}}_{s,r,t}) &= \overline{\text{var}_{mfpk_{(s,r)i}}} + \boldsymbol{\lambda}_{\sigma^2_{mfpk}}^{s,r} \cdot (\tilde{\mathbf{T}}_{r,t} - \overline{\tilde{\mathbf{T}}_r}) + \boldsymbol{\delta}_{\sigma^2_{mfpk}}^{s,r} \cdot (\tilde{\mathbf{X}}_{s,r,t} - \overline{\tilde{\mathbf{X}}_{s,r}}) + H.O.T. \\ &\approx \boldsymbol{\lambda}_{\sigma^2_{mfpk}}^{s,r} \cdot \tilde{\mathbf{T}}_{r,t} + \boldsymbol{\delta}_{\sigma^2_{mfpk}}^{s,r} \cdot \tilde{\mathbf{X}}_{s,r,t} + \eta_{s,r}, \end{aligned} \quad (13)$$

where $\eta_{s,r}$ is a sector-region specific constant. For our benchmark exercise, we first estimate the average causal elasticity $\boldsymbol{\lambda}_{\sigma^2_{mfpk}} = \mathbb{E}[\boldsymbol{\lambda}_{\sigma^2_{mfpk}}^{s,r}]$ across all climates and sectors. We will revisit the nature of heterogeneity across climates and sectors in Section 4.3 and D.1.

We define current climate conditions, $\mathbf{T}_{r,t}$, in terms of temperature bins, following the approach by Carleton et al. (2022), Deschênes and Greenstone (2011), and Nath (2023). These bins, spanning the vector space $\mathbf{T}_{r,t} = \{\text{Tbin}_{r,t}^{<-5^\circ C}, \text{Tbin}_{r,t}^{-5 \sim 0^\circ C}, \text{Tbin}_{r,t}^{0 \sim 5^\circ C}, \text{Tbin}_{r,t}^{5 \sim 10^\circ C}, \text{Tbin}_{r,t}^{10 \sim 15^\circ C}, \text{Tbin}_{r,t}^{15 \sim 20^\circ C}, \text{Tbin}_{r,t}^{20 \sim 25^\circ C}, \text{Tbin}_{r,t}^{25 \sim 30^\circ C}, \text{Tbin}_{r,t}^{>30^\circ C}\}$, capture the number of days within specific temperature ranges for region r in year t . Structured in 5-degree Celsius increments, these bins cover a broad spectrum of temperature variations, including extreme heat and cold. Thus, as noted in Deschênes and Greenstone (2011), using daily temperature data enables us to capture weather's nonlinear effects using linear regression models.

To estimate the causal effect of temperature on MRPK dispersion (i.e., misallocation), we follow the standard approach in Deschênes and Greenstone (2011) and Zhang et al. (2018) to exploit the inter-annual variation in the distribution of daily temperatures through the following panel regression:

$$\text{var}_{mfpk_{(s,r),t}} = \sum_{b \in B/(5 \sim 10^\circ C)} \lambda_{\sigma^2_{mfpk}}^b \times \text{Tbin}_{r,t}^b + \boldsymbol{\delta}_{\sigma^2_{mfpk}} \mathbf{X}_{s,r,t} + \alpha_{c(r),t} + \eta_{s,r} + \varepsilon_{r,s,t}, \quad (14)$$

where $\eta_{s,r}$ is the region-sector fixed effects, accounting for the unvarying attributes of MRPK dispersion specific to each region-sector pair over time, consistent with the formulation in Equation 13. $\alpha_{c(r),t}$ is the country-by-year fixed effects, capturing the aggregate shocks to the country c that region r resides in. Standard errors are clustered at the region level to account for both serial and spatial correlations between all sectors across all years within each region (NUTS3 in Europe, province in China, first-level administrative divisions in India).

$\lambda_{\sigma^2_{mfpk}}^b$ are coefficients measuring the causal effect of one additional day in temperature bin b on contemporaneous MRPK dispersion. Each $\text{Tbin}_{r,t}^b$ indicates the number of days whose average temperature falls within a specific range $b \in B$, where B is the set of ranges defined in 5-degree Celsius increments. Since the total number of days in a year always equals 365, we employ the temperature bin ranging from $0^\circ C$ to $5^\circ C$ as the reference category, meaning that the coefficient for this category is normalized to zero.

$\mathbf{X}_{s,r,t}$ is a vector of logged control variables at the region-sector-year level, including the to-

tal number of observed firms, average firm-level sales, and average MRPK²². The first two controls for the observed size and region-sector-level business cycle fluctuations. By controlling for the average (log)MRPK across firms at the region-sector-year level, we aim to demonstrate that the observed dispersion in MRPK is not primarily driven by the mechanisms through which temperature influences the average MRPK²³.

4.2 Average Effects of Temperature on Capital Misallocation

The estimates across different specifications of Equation 14 are shown in Table A.2. Figure 2 plots our baseline estimates of the effects of heat exposure on annual MRPK dispersion and the implied TFP loss, as determined from the estimation of equation 14. Specifically, the values on the left Y-axis represent the regression coefficients, denoted as $\hat{\lambda}_{\sigma_{mrpk}^2}^b$, for each bin b . Each $\hat{\lambda}_{\sigma_{mrpk}^2}^b$ quantifies the estimated impact of an additional day in temperature bin b on MRPK dispersion, compared to a day within the 5°C - 10°C range. To facilitate interpretation, we translate the estimates $\hat{\lambda}_{\sigma_{mrpk}^2}^b$ into the marginal effect on aggregate TFP through the misallocation channel using $-\frac{\alpha_{Kn} + \alpha_{Kn}^2(\sigma_n - 1)}{2} \hat{\lambda}_{\sigma_{mrpk}^2}^b$ from Equation 12 under the choice of a well-established conservative choice of $\alpha_{Kn} = 0.35$ and $\sigma_n = 4$ across all n ²⁴. The right Y-axis corresponds to the values of the implied TFP loss.

The estimated coefficients reveal that MRPK dispersion and the inferred TFP loss from temperature-induced misallocation peak at the most extreme temperatures, both coldest and hottest. This observed U-shape pattern between MRPK dispersion and temperature can also be translated into an inverted U-shape pattern between TFP and temperature, which is well known in the climate econometrics literature (Burke, Hsiang, and Miguel 2015; Nath 2023).

For temperatures above 25°C and below -5°C, the effects on MRPK dispersion are both economically and statistically significant at 1% level. Specifically, the point estimates indicate that substituting a day in the 5-10°C range with a day exceeding 30°C results in an increase of 0.31 log points in MRPK dispersion, translating to a decrease of 0.11% in annual aggregate TFP due to capital misallocation. On the cold end, we find that an additional day colder than -5°C in a year leads to an approximate 0.26 log points increase in annual MRPK dispersion and 0.09% loss in annual TFP.

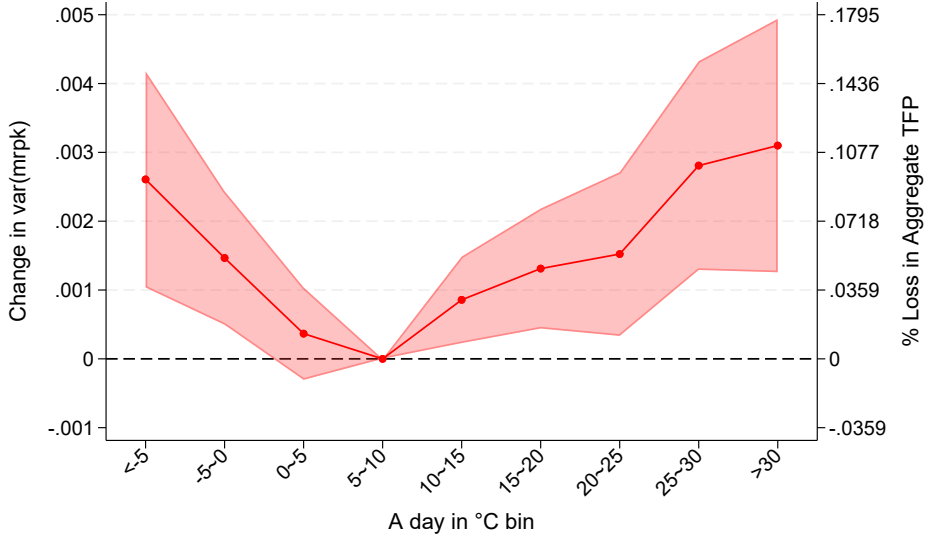
Robustness. Table A.2 presents results of estimates of equation 14 with different specifications of fixed effects, inclusions of control variables, and various weighting methods. Columns 1 and 6 report the baseline estimates and inferred TFP loss that was used to create Figure 2. Columns 2 - 4 provide robustness checks. We introduce country-sector-year fixed effects instead of country-year fixed effects in column 2, absorbing all unobserved country and year-specific, region-invariant factors affecting MRPK dispersion in each sector. Column 3 adds

22. We exclude these controls in our preferred specification as they may block a potential pathway for affecting dispersion, although adding these controls have very little effect on our estimates.

23. This control allows us to isolate the specific impact of temperature on MRPK dispersion, independent of its effects on the average level of MRPK. Controlling for average MRPK also reflects the average financial constraints across firms.

24. For the elasticity of substitution, we choose $\sigma_n = 4$ as in Bils, Klenow, and Ruane (2021). For capital share, we pick a common value of $\alpha_{Kn} = 0.35$.

Figure 2: Estimated impact of daily temperature shocks on annual MRPK dispersion and implied TFP loss



Notes: This figure shows the aggregate impact linking annual MRPK dispersion and TFP loss to average daily temperatures. This is derived by applying equation 14 to the variance in MRPK and the calculated TFP loss due to misallocation. The formula for computing TFP loss from misallocation is $-\frac{\alpha_{Kn} + \alpha_{Kn}^2(\sigma_n - 1)}{2} \hat{\lambda}_{\sigma_{mrpk}}^b$. The estimation is normalized by setting the range of 5°C - 10°C as the reference category. Therefore, each $\hat{\lambda}_{\sigma_{mrpk}}^b$ represents the estimated effect of an additional day in temperature bin b on annual MRPK dispersion or TFP loss, relative to a day with temperatures between 5°C - 10°C. The figure also includes the 90% confidence interval for these estimates where standard errors are clustered at the region level.

control variables, including total number of observed firms, average firm-level sales, and average level of MRPK across firms in a region-sector-year, all in logarithmic form. Column 4 reports the results of the weighted OLS using the 1995 region-sector value-added as the regression weight. The objective is to assess whether assigning greater influence to region-sector observations with a larger size would affect our analysis. Our results, in particular the “U-shaped” pattern, remain robust under various specifications.

4.3 Heterogeneous Effect by Climate and Development

Our benchmark specification in Equation 14 captures the average effect of temperature on capital misallocation $\mathbb{E}[\lambda_{\sigma_{mrpk}}^{s,r}]$. We now try to estimate the heterogeneous impact of temperature shocks across regions with different long-run climate and development levels.

It is not immediately clear if a hot day would consistently cause more or less misallocation in regions that are already warm or economically thriving. The ambiguity arises from two potentially counteracting factors. For simplicity, consider a case where the mass of firms can be divided into two groups: heat-tolerant and heat-sensitive. On the one hand, heat-sensitive firms in warmer climates might already adapt to high temperatures and thus experience less damage. However, it's also possible that in warmer regions, heat-sensitive businesses might still face greater damages with any additional heat shocks due to the limitation of adaptability (e.g., Moscona and Sastry 2023) and the damage convexity due to cumulative exposure of heat, as found by the observed non-linear effects in Burke, Hsiang, and Miguel (2015). Similarly, in

regions with higher income levels, while firms may possess greater resources for adaptation to heat shocks, these economies often have highly specialized productions and exhibit larger dispersion in firm sizes (e.g., Chen (2022) and Poschke (2018)), which leads to more heterogeneous responses to climate conditions, as later shown in Section 6a that differences in firm sizes contributes to the MRPK divergence when facing heat shocks.

Therefore, to more precisely account for the heterogeneous impact stemming from different long-run climate and development levels across regions, we follow the approach of Carleton et al. (2022) and Nath (2023) by interacting a time-invariant measure of climate (i.e., long-run average temperature) and GDP per capita with each temperature bin. This approach allows us to capture how climate and income jointly influence the effects of temperature variations on capital misallocation. The modified regression model is formulated as follows:

$$\begin{aligned} \sigma_{mrpk_{s,r,t}}^2 = & \sum_{b \in B/(5 \sim 10^\circ C)} \lambda^b \times \text{Tbin}_{r,t}^b + \sum_{b \in B/(5 \sim 10^\circ C)} \lambda_T^b \times \text{Tbin}_{r,t}^b \times \bar{T}_r \\ & + \sum_{b \in B/(5 \sim 10^\circ C)} \lambda_{\text{GDP}_{pc}}^b \times \text{Tbin}_{r,t}^b \times \ln \overline{\text{GDP}_{pc,r}} + \delta \tilde{\mathbf{X}}_{s,r,t} + \alpha_{c,t} + \eta_{s,r} + \varepsilon_{s,r,t}, \end{aligned} \quad (15)$$

where \bar{T}_r represents the long-run annual average temperature for region r and $\ln \overline{\text{GDP}_{pc,r}}$ is the log of long-run average GDP per capita in region r ²⁵. Both long-run temperature and GDP per capita are computed as sample averages from 1997-2018. The coefficients λ_T^b and $\lambda_{\text{GDP}_{pc}}^b$ quantify how the impact of daily temperature shocks on MRPK dispersion varies across regions with different income levels and climates²⁶.

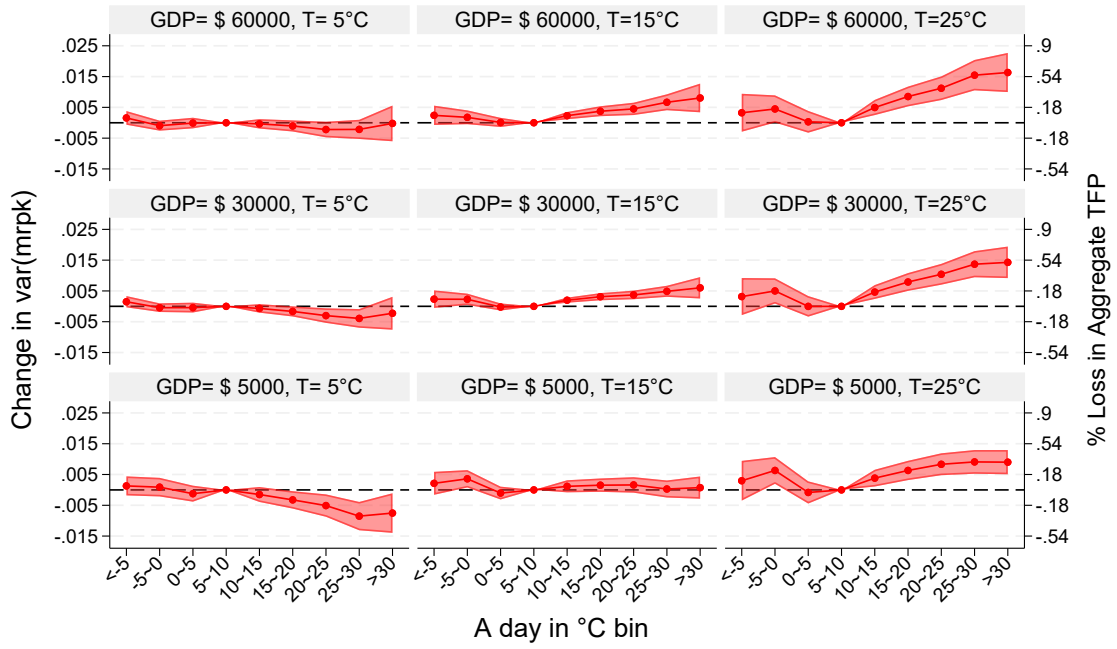
Figure 3 presents the results from estimating Equation 15. Under the assumption that regions with similar climates and income would respond similarly to the same set of daily temperature shocks, we predict the impact of temperature shocks on MRPK dispersion and its equivalent TFP loss across three levels of income and four levels of long-run climate, which are broadly representative of the 32 countries in our regression sample. The left Y-axis indicates the projected effects of temperature shocks on MRPK dispersion, while the right Y-axis shows the implied TFP loss suggested by the estimates.

Level Effect: Hotter regions suffer more from the misallocation channel. Figure 3 shows that an extremely hot day (above 30°C) would result in greater MRPK dispersion in regions with a hotter average level of temperature. In regions of comparable wealth, the adverse effects of extreme heat on misallocation intensify as the regional climate becomes warmer, as observed when moving from the left column to the right for each income level. For regions with a high average temperature of 25°C, experiencing an additional day over 30°C leads to a notable TFP loss (ranging from 0.3% to 0.58%) due to misallocation, regardless of income levels. In contrast, in colder climates (e.g., where $\bar{T}_r \approx 5^\circ C$), heat shocks appear to have negligible

25. The sub-national level (PPP-adjusted) GDP per capita data is from DOSE. It is important to use sub-national level data as countries like India and China admit large income heterogeneity across the districts or prefectures. The GDP per capita data is in 2017 International Dollars

26. Interacting temperature bins with the region's long-term average temperature allows us to analyze how an additional hot day has differential effects across areas with varying baseline climates. Similarly, by interacting temperature bins with a country's annual per capita income, we evaluate how the same heat shock impacts developed and developing economies differently.

Figure 3: MRPK Dispersion and TFP Loss Across Climates and Income



Notes: The graphs plot the predicted effect of exposure to daily mean temperature bins on MRPK dispersion and TFP loss at varying levels of income and climates. These predicted effects are derived from the interacted panel regression specified in Equation 15. The graphs include 90% confidence intervals, and standard errors are clustered at the regional level. The left y-axis indicates changes in MRPK dispersion, and the right y-axis shows the calculated TFP loss. The reference temperature is at 5~10°C.

or even reducing effects on MRPK dispersion, thereby decreasing TFP loss. Interestingly, even a cold shock, such as an additional day below 0°C, tends to increase misallocation more significantly in hotter regions than colder ones. In general, compared to the reference level, the effect of a cold shock ($<0^\circ\text{C}$) is always economically less significant than a heat shock ($>30^\circ\text{C}$), with the notable exception being hot and low-income regions like India (GDP=\$ 5000, $\bar{T} = 25^\circ\text{C}$).

The quantitative implications can be best understood by comparing two regions with the same income level but different climates. For example, Arizona (US) and Norway have similar average per capita income across the sample period, around 60000\$, while their annual average temperature largely differs: 14.84°C in Arizona but only 1.97°C in Norway. Extrapolating using our estimates, an additional day with a temperature above 30°C compared to a 5-10°C day in Norway will lead to a 0.29 log points decrease in MRPK dispersion, which translates to a 0.1% increase in TFP, whereas in Arizona, the same heat shock leads to 0.8 increase in MRPK dispersion and a 0.3% decrease in TFP. In Section 5, we will explore how the divergent results across climates in our reduced-form regressions can be explained by regions' deviations from the optimal "bliss-point" temperature for production, estimated to be around 13°C.

Income Effect: Richer economies suffer more from the misallocation Channel. A second key finding is that wealthier economies are more adversely affected by the misallocation channel due to extreme heat; we call this the *Income Effect*. This can be better understood by comparing countries across different income levels within similar climates. As presented in Figure 3, in each column with fixed long-run temperature, moving from the bottom (low income)

to the top (high income) would increase the misallocation effect of the same heat shocks and make the response function more and more U-shaped. As a more concrete example, France and Turkey have similar average temperatures of around 10.5°C, while the income per capita of France (\$45922) is over 1.5 times higher than that of Turkey (\$28150). Our estimates suggest that the effect of an additional hot day $>30^{\circ}\text{C}$ would lead to a 0.08% TFP loss for Turkey and a 0.14% TFP loss for France. To explain the income effect, in Section 6, we will show that firm size dispersion increases with the region's economic development, resulting in greater MRPK divergence in response to the same heat shocks.

To sum up, the heterogeneous effect shows that the nature of the misallocation channel of climate change might be significantly different from other channels, such as labor productivity (Nath 2023) and mortality risk (Carleton et al. 2022). Previous empirical analysis showed that richer economies and hotter regions suffer much less from heat shocks regarding labor productivity and mortality, suggesting that some effects of climate change are somewhat adaptable²⁷. However, the cost of climate shocks through the misallocation channel reveals an opposite pattern²⁸ by incurring a larger loss in hotter and richer countries, suggesting that market-based adaptation might have limited effect. As an economy develops to be more sophisticated in its techniques of production among firms (along with rising incomes), it might become more vulnerable in the sense that achieving efficient resource allocations becomes more challenging.

4.4 End-of-the-century Projection of the Misallocation Channel

In this subsection, we utilize the empirical estimates from 4.3 to project the effect of climate-induced misallocation on aggregate TFP loss by the end of the 21st century (2081-2100) for 4,881 regions in 172 countries around the world²⁹.

Such projections require detailed region-level daily temperature projections, average levels of temperature, and GDP per capita at the end of the century. We use near-surface air temperature projection in SSP3-7.0 from the sixth phase of the Coupled Model Intercomparison Project (CMIP6) (Copernicus Climate Change Service 2021). To project the daily temperature distribution, we calculate the average number of days in each temperature bin as defined in 4.1 and average temperature from 2081-2100. We use the 20-year average for all variables to avoid inaccurate representations due to year-to-year fluctuations in climate model predictions. We follow Carleton et al. (2022) and use projections of national income per capita derived from the SSP 3 scenarios, using the OECD EnvGrowth model (Dellink et al. 2017) projections. For

27. For example, the estimates in Nath (2023) show that as a region becomes consistently hotter, workers are more adapted to the hotter climate and would not find a heat shock damaging to its productivity. Secondly, as an economy grows richer, workers suffer less from the temperature extremes. Both channels suggest that the cost of climate change might be lower in developed economies.

28. In Section 6, we identify some potential mechanisms that could help explain why hotter and richer regions suffer more from heat shocks. Specifically, we find that a positive temperature shock in hotter regions would increase TFP volatility, making firms more prone to input mistakes, while a hot temperature shock in cold regions might enjoy a slight decrease in TFP volatility. Moreover, a firm's adaptability to heat and cold shocks depends heavily on size. On the firm level, we show that smaller firms' MRPK is more sensitive to extreme temperatures than larger firms. Across region-sector pairs, we find that economies with larger size dispersion suffer more misallocation, which is consistent with the firm-level evidence. We find those region-sectors with large size dispersion are also those with higher incomes (i.e., more developed), consistent with Poschke (2018).

29. Regions in our 32-country sample is defined as in Section 3, while the regions in all other countries are defined as GADM1-level region from the GADM dataset.

an average region in the sample, the average annual temperature is projected to increase by about 2.7°C , and the average GDP per capita is projected to increase by about 20814\$ (in 2017 International Dollar). A detailed illustration of the current and projected evolution of income and average temperature can be found in Figure B.1.

Our goal is to compute the following: compared to current (2019) climate conditions, how much more will global warming contribute to aggregate TFP loss through misallocation by the end of the 21st century (EOC)? To make transparent the forces at play here, we decompose the total effect of climate-induced misallocation into three components:

$$\underbrace{\Delta \text{Loss ln TFP}_r}_{\text{Total Effect}_r} = \frac{\alpha_{Kn} + \alpha_{Kn}^2(\sigma_n - 1)}{2} \left[\underbrace{\sum_b \left(\lambda^b + \lambda_{\text{GDP}_{pc}}^b \ln \text{GDP}_{pc,r,2019} + \lambda_{\bar{T}}^b \bar{T}_{r,2019} \right) \times \Delta \text{Tbin}_r^b}_{\text{Shock Effect}_r} \right. \\ + \underbrace{\sum_b \lambda_{b,\bar{T}} \text{Tbin}_{r,EOC}^b \times \Delta T_r}_{\text{Level Effect}_r} \\ \left. + \underbrace{\sum_b \lambda_{\text{GDP}_{pc}}^b \text{Tbin}_{r,EOC}^b \times \Delta \ln \text{GDP}_{pc,r}}_{\text{Income Effect}_r} \right], \quad (16)$$

where we use Δ to denote the change in a variable between its end-of-century (EOC) value and its current value (measured in 2019). The *shock effect* refers to the change in TFP Loss due to shifts in daily temperature distributions ΔTbin_r^b , conditional on the baseline income and long-run temperature computed in 2019; the *level effect* refers to the change in TFP Loss due to the change in long-run temperature ΔT_r ; and the *income effect* reflects the cost of the region's increasing misallocation due to the shift in economic development, measured by the change in (log) GDP per capita, $\Delta \ln \text{GDP}_{pc,r}$. To make the quantitative results more interpretable, we aggregate all measures of regional TFP loss to the country level by performing a weighted sum using the projected regional GDP share in each country under SSP-3³⁰.

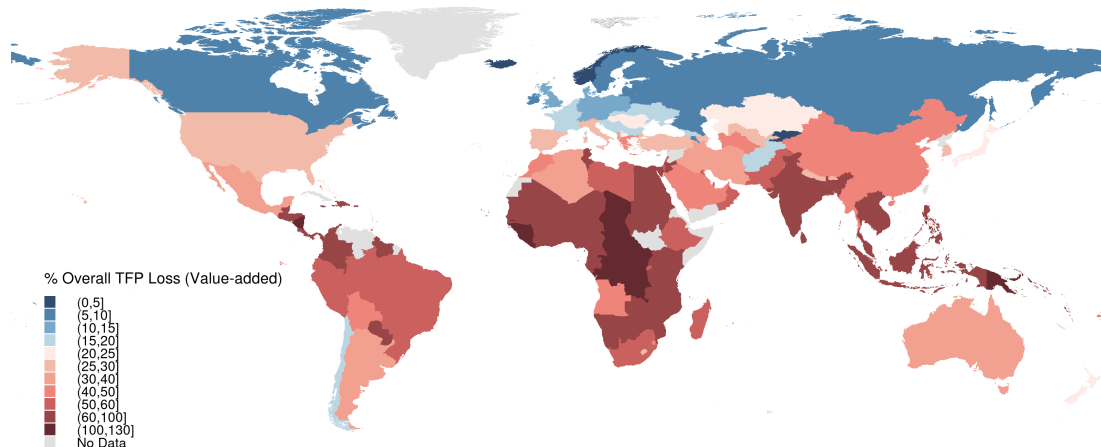
Figure 4 plots each country's projected TFP loss from the capital misallocation channel in percentage terms. While the overwhelming majority of countries will experience significant TFP losses, the projected TFP loss exhibits large heterogeneity across countries. The country-level TFP loss projections from other emission scenarios are presented in Figure B.3 and B.4.

In countries most severely affected, such as Guinea, the Republic of Congo, Malaysia, and India, TFP losses are as high as above 60% compared to today. India, for instance, with a current average temperature of 23.29°C and an income per capita of \$6608, the number of days above 25°C is projected to rise from 176 to 227 by the end of the century together with a large rise in average temperature to 25.97°C and income to \$14615. Together, these forces result in a TFP loss of about 61.88%. These projections stem from the results that for countries like India that are already warm (tropical/subtropical) but relatively under-developed, the effect of extreme heat becomes more severe as they get hotter and more developed, as implied by the third column in Figure 3, showing the country moving from the bottom cell to the top right.

³⁰ We use the grid-level projected SSP-3 GDP are from Wang and Sun (2022) to obtain the projected GDP share.

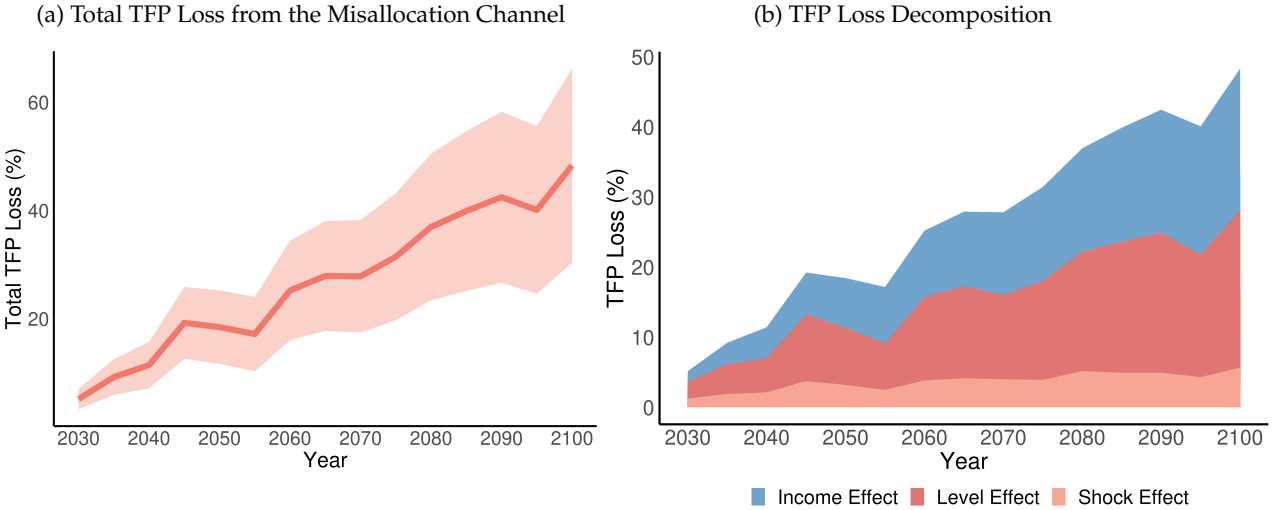
Less affected countries, such as the United States, Turkey, and Spain, will see TFP losses between 25% and 30%. For example, in the United States, the projected change in TFP loss due to global warming is about 28.8% at the end of the century. On average, in the US, income per capita is expected to rise from \$62478 to \$95800, while the annual temperature is expected to rise from 9.9°C to 13.5°C with the number of days above 25°C is projected to increase from 29 to 64. Countries with more mild damage, like Norway, Finland, Canada, and Germany, will see TFP losses below 15%. For example, in Finland, the national average temperature is predicted to rise from 2.92°C to 5.59°C, the number of days above 25°C is expected to increase from 0 to 1.55 days, and income per capita is projected to rise from \$48583 to \$97820. Together, these result in the TFP loss in Finland is projected to be 13.46% due to misallocation. For developed countries in temperate and maritime climates, climate change might shift up the average temperature, but the extreme heat exposure is still quite limited. Therefore, while large in terms of absolute value, the increase in climate-induced misallocation is still more moderate compared to tropical countries.

Figure 4: End-of-century Projected TFP Loss Due to the Misallocation Channel



Notes: Figure shows the projected TFP loss from capital misallocation under SSP3-7.0 scenarios. The estimation follows Equation 16 where we estimate the total effect in MRPK dispersion and compute the equivalent value of TFP loss.

Figure 5: Projected Global TFP Loss and Its Decomposition: 2030-2100



Notes: Figure 5a plots the total TFP loss across years. The dark red line plots the estimates and the shaded area is 90% confidence intervals from the parameter uncertainty. Figure 5b plots the three effects contributing to total TFP loss. All computations are under the SSP3-7.0 scenario and the percentage loss is compared to the 2019 level.

Finally, using each country's projected GDP share³¹, we compute the global average TFP loss due to climate-induced misallocation can be computed as:

$$\frac{\Delta \text{Loss}_{\ln \text{TFP}}}{\text{Total Effect}=42.69\%} = \underbrace{\text{Shock Effect}}_{4.99\%} + \underbrace{\text{Level Effect}}_{20.0\%} + \underbrace{\text{Income Effect}}_{17.7\%},$$

where we projected that relative to today, the global cost of climate-induced misallocation to be 42.7% of aggregate TFP (GDP), with the shock effect from daily temperature distribution contributing to 4.99%, income effect contributing to 17.7% and, most significantly, the level effect of average temperature increase takes 20.0%. We present the evolution of TFP loss from the misallocation channel in Figure 5a, along with the 90% confidence intervals that account for parameter uncertainty. This graph shows a projected increase in TFP loss from 5.16% in 2030 to 48.32% by 2100. Additionally, Figure 5b breaks down the projected TFP loss into three components over time and indicates that the income effect and the level effect are the primary drivers of the increasing TFP loss from the misallocation channel over the years.

The size of these estimates is large and is comparable to the overall projected impact of Burke, Hsiang, and Miguel (2015). Much of the projected total effect comes from the sharp rise in the semi-elasticities of daily temperature shocks due to the projected rise in temperature and income. These, of course, are subject to a range of caveats, including out-of-sample extrapolation, as the income and temperature levels by the end of the century are unprecedentedly high compared to the records in the past. However, even if we only account for the projected daily temperature variations and keep the first-order semi-elasticities of temperature shocks constant as the ones estimated today, we still project a global aggregate TFP loss

31. The TFP loss of this weighting approach would exactly correspond to a model-implied aggregate TFP loss where the total Global Output is defined as a Cobb-Douglas aggregator of country-level value-added output and can be viewed as a first-order approximation for the TFP loss under any other constant returns to scale aggregator for global output.

of 4.99% coming from the misallocation channel, which should serve as a lower bound for our estimate.³² Country-level misallocation loss projections under other climate change scenarios are provided in . The results are quantitatively similar.

5 A Firm Dynamics Model of Temperature Shocks and MRPK Dispersion

In the previous section, we empirically demonstrated how temperature shocks lead to increased misallocation, particularly in countries with hotter long-term climates. We now explore why both temperature shocks and their levels can generate dispersion in capital returns within a standard dynamic investment model. Given the time-to-build nature of capital inputs, a natural explanation is that temperature influences the dispersion of expectation errors in capital returns across firms. We present two mechanisms in the model: (i) firms do not have perfect foresight of the future temperature and are heterogeneous in temperature sensitivity, and (ii) firms do not have perfect foresight of their sensitivity to temperature so that temperature extremes could lead to unexpected extreme losses in the firm level. These two mechanisms imply that misallocation depends on both the “level” and the “shock” of temperature. We will generate regression equations with model interpretations to test them empirically in Section 6 and Section 7.

5.1 Setup

Similar to the accounting framework in Section 2, our model describes the action of firms and the aggregate economy within a region-sector $n = (r, s)$. We suppress the region-sector label to avoid notation burdens. Our model follows a partial equilibrium set-up similar to that of David and Zeke (2021).

Production and Demand. We begin by describing the production side of the economy. Each firm i produces differentiated products of quantity Y_{it} with Cobb-Douglas technology:

$$Y_{it} = \tilde{A}_{it} K_{it}^{\tilde{\alpha}_K} N_{it}^{\tilde{\alpha}_N}, \quad \tilde{\alpha}_K + \tilde{\alpha}_N = 1, \quad (17)$$

where \tilde{A}_{it} is the physical productivity, K_{it} is the capital input (which is dynamic) and N_{it} represents labor. The firm’s product faces a constant elasticity downward-sloping demand curve with demand shifter B_{it} :

$$Y_{it} = B_{it} P_{it}^{-\sigma}.$$

Combining production and demand functions, we obtain the equilibrium revenue function of the form:

$$P_{it} Y_{it} = \hat{A}_{it} K_{it}^{\alpha_K} N_{it}^{\alpha_N} \quad (18)$$

32. A detailed breakdown of each effect on the country level is presented in Figure B.2.

where $\alpha_F = (1 - \frac{1}{\sigma})\tilde{\alpha}_F$, $\forall F \in \{K, N\}$ and $\hat{A}_{it} = B_{it}^{\frac{1}{\sigma}} (\tilde{A}_{it})^{(1-\frac{1}{\sigma})}$ is the revenue-based productivity (TFPR). We will be referring to this simply as productivity.

Productivity and Heterogeneity in Temperature Sensitivity. We now introduce how firms' productivity is heterogeneously impacted by temperature. For parsimony, we allow the annual temperature to be a sufficient statistic for climate conditions in the structural model (as in Dell, Jones, and Olken (2012) and Cruz and Rossi-Hansberg (2023)). We assume that firms' productivity is determined by:

$$\hat{A}_{it} = \exp(\hat{\beta}_{it}(T_t - T^*))\hat{Z}_{it}, \quad (19)$$

where T_t is the realized temperature at year t , and T^* is the optimal temperature for firms' production (in the sense that at T^* , the temperature would be irrelevant for all firms' production). We assume that each firm i 's productivity changes linearly with temperature's deviation from optimum, $T_t - T^*$, subject to the sensitivity $\hat{\beta}_{it}$. \hat{Z}_{it} denotes the firm-specific idiosyncratic productivity, which captures all the variations apart from the effect of temperature.

We allow a firm i 's temperature sensitivity $\hat{\beta}_{it}$, to be firm-specific and time-varying. There are two sources of heterogeneity in a firm's sensitivity to temperature:

$$\hat{\beta}_{it} = \underbrace{\hat{\beta}_i}_{\text{Persistent sensitivity to temperature}} + \underbrace{\hat{\xi}_{it}}_{\text{Idiosyncratic sensitivity to temperature}} + \underbrace{c(T_t - T^*)}_{\text{common state-dependent sensitivity}}$$

(1) The persistent sensitivity to temperature, $\hat{\beta}_i$, is assumed to be observable and known to firms (e.g., a ski resort's $\hat{\beta}_i$ is negative, and the owner knows about it). We assume that $\hat{\beta}_i$ is distributed as $\hat{\beta}_i \sim \mathcal{N}(\bar{\beta}, \sigma_{\hat{\beta}}^2)$ across firms, where $\sigma_{\hat{\beta}}^2$ measures the dispersion of persistent sensitivity within a region-sector.

(2) The idiosyncratic sensitivity, $\hat{\xi}_{it}$, is i.i.d. across firm and time and cannot be predicted. It follows a normal distribution, $\hat{\xi}_{it} \sim \mathcal{N}(0, \sigma_{\hat{\xi}}^2)$, where $\sigma_{\hat{\xi}}^2$ measures the damage uncertainty within a region-sector. The impact of idiosyncratic sensitivity on TFP scales with $T_t - T^*$ to capture the increased damage uncertainty associated with extreme temperature (e.g. plant-level fire hazards are more likely in extreme heat).

(3) The state-dependent sensitivity $c(T_t - T^*)$ captures the potential non-linear trend in temperature's effect on a firm's productivity. We assume the nonlinear term to be common across firms.³³ This term will play no role in our analysis of misallocation.

Jointly, we model $\hat{\beta}_{it}$ in such ways to capture the idea that a firm would react to (realized and expected) temperature conditions according to their known knowledge of the firm's characteristics. However, with the presence of dynamic inputs that take time to build, firms could not act optimally as there is always some unknown damage sensitivity to temperature every period.

33. We will also discuss how the constant c can be parameterized flexibly to counteract the mechanical beneficial

Law of Motion for Productivity and Temperature. We assume (agents perceive that) temperature and (log) idiosyncratic productivity $\hat{z}_{it} = \log \hat{Z}_{it}$ ³⁴ follow an AR(p) process, with persistence ρ_T and ρ_z , respectively:

$$(T_{t+1} - \bar{T}) = \sum_{h=1}^p \rho_{T,h} (T_{t+1-h} - \bar{T}) + \eta_{t+1}^T, \quad (20)$$

$$\hat{z}_{it+1} = \rho_z \hat{z}_{it} + \hat{\varepsilon}_{it+1},$$

where we assume that temperature oscillates around a local average \bar{T} . $\eta_{t+1}^T \sim \mathcal{N}(0, \sigma_\eta^2)$ is the temperature shock and the idiosyncratic productivity shocks $\hat{\varepsilon}_{it+1} \sim \mathcal{N}(0, \sigma_\varepsilon^2)$ are independent across firms and time.

At the firm level, uncertainty arises from three sources: 1) idiosyncratic damage sensitivity $\hat{\xi}_{it}$, normally distributed with variance σ_ξ^2 ; 2) aggregate temperature uncertainty with variance σ_η^2 ; and 3) idiosyncratic uncertainty, with variance σ_ε^2 . We assume firms have full information regarding all realized shocks and hold rational expectations regarding the future states of the economy. We refer to the cross-sectional variance of unexpected firm-level TFP shocks as *TFP Volatility*, following [Asker, Collard-Wexler, and Loecker \(2014\)](#)³⁵. TFP volatility in the model depends endogenously on temperature levels T_t and the temperature shocks η_t^T :

Lemma 1 *TFP Volatility*, $\text{Var}(\hat{a}_{it} - \mathbb{E}_{t-1}[\hat{a}_{it}])$, and can be written as:

$$\text{Var}(\hat{a}_{it} - \mathbb{E}_{t-1}[\hat{a}_{it}]) = (T_t - T^*)^2 \sigma_\xi^2 + \hat{\eta}_t^{T2} \sigma_\beta^2 + \sigma_\varepsilon^2 \quad (21)$$

TFP Volatility reaches its minimum when the temperature reaches its optimum $T_t = T^$, and there is no unexpected change in temperature, $\eta_t^T = 0$.*

This lemma illustrates that TFP volatility is dependent on the regional climate. Suppose a region is too hot or cold compared to T^* . In that case, firm-level productivity is too volatile due to the damage uncertainty σ_ξ^2 . We will test this empirically in Section 7.1.

Temperature and wages. Firms hire a composite of flexible inputs, “labor”, on a period-by-period basis at a competitive wage, W_t . For simplicity in modeling the temperature-related supply- and demand-side frictions in the labor market (e.g., temperature-related disutility of work or temperature-induced loss of labor productivity), we assume the equilibrium wage is given by:

$$W_t = \bar{W} \exp(\chi(T_t - T^*)),$$

where the wage is a function of temperature (deviation from T^*) with constant elasticity χ , indicating the sensitivity of which wages respond to temperature³⁶.

effect of climate-induced productivity dispersion induced by the CES aggregator in the Appendix.

34. We use lower case to denote variables in logs, except for temperature T_t .

35. This can also be viewed as a theoretical counterpart to the cross-sectional measures of uncertainty as in [Bloom \(2009\)](#).

36. This assumption is commonly used in business cycle analysis. See [Blanchard and Galí \(2010\)](#), [Alves et al. \(2020\)](#), and [Flynn and Sastry \(2023\)](#).

Flexible Input Choice and Profits. Optimal choice of flexible inputs is made after capital inputs are allocated, and all shocks are realized. The static input choice solves

$$\max_{N_{it}} \exp\left(\hat{\beta}_{it}(T_t - T^*)\right) \hat{Z}_{it} K_{it}^{\alpha_K} N_{it}^{\alpha_N} - W_t N_{it},$$

and results in the operating profits Π_{it} , calculated as revenue minus labor costs, expressed as

$$\Pi_{it} = G A_{it} K_{it}^\alpha := G \exp(\beta_{it}(T_t - T^*) + z_{it}) K_{it}^\alpha, \quad (22)$$

where $G := \overline{W}^{-\frac{\alpha_N}{1-\alpha_N}} \alpha_N^{\frac{\alpha_N}{1-\alpha_N}} (1 - \alpha_N)$, $z_{it} = \frac{1}{1-\alpha_N} \hat{z}_{it}$, and $\alpha = \frac{\alpha_K}{1-\alpha_N}$. We define capital profitability as $A_{it} := \exp(\beta_{it}(T_t - T^*) + z_{it})$, where $\beta_{it} = \frac{\hat{\beta}_{it} - \chi \alpha_N}{1-\alpha_N}$ is the sensitivity of capital profitability to temperature, transformed from the firm's productivity's temperature sensitivity, $\hat{\beta}_{it}$, and the wage's temperature sensitivity, χ . α is the curvature of the profit function.

Dynamic Capital Investment. Capital is a dynamic input that takes time to build. It needs to be invested one period ahead before all shocks (including temperature) are realized. Naturally, the investment problem of a firm i can be formulated into the Bellman equation of the form:

$$V(T_t, Z_{it}, K_{it}) = \max_{K_{it+1}} G \exp(\beta_{it}(T_t - T^*) + z_{it}) K_{it}^\alpha - K_{it+1} + (1 - \delta) K_{it} \\ + \frac{1}{1+r} \mathbb{E}_t [V(T_{t+1}, Z_{it+1}, K_{it+1})],$$

where $\frac{1}{1+r}$ is the discount factor. Firms are risk-neutral and face no adjustment costs in the model³⁷. The optimal investment K_{it+1} solves the Euler equation:

$$1 = \underbrace{\frac{1}{1+r}}_{\text{Discount Factor}} \left(\underbrace{\alpha G K_{it+1}^{\alpha-1} \mathbb{E}_t [\exp(z_{it+1} + \beta_{it+1}(T_{t+1} - T^*))]}_{\text{Expected Value of Marginal Profits of Capital}} + \underbrace{(1-\delta)}_{\text{Value of Undepreciated Capital}} \right). \quad (23)$$

Equation (23) shows that capital investment is increasing in the forecast of capital profitability, which in turn depends on the expectation of profitability-based idiosyncratic productivity z_{it+1} and temperature sensitivity β_{it+1} , as well as temperature T_{t+1} .

Solving the Euler Equation yields the firm's optimal investment policy as a function of expectations in logs (while suppressing some higher-order "risk-adjusted" terms):

$$k_{it+1} \approx \frac{1}{1-\alpha} \mathbb{E}_t[a_{it+1}] + k_0 \\ = \frac{1}{1-\alpha} \left(\frac{1}{1-\alpha_N} \mathbb{E}_t[\hat{a}_{it+1}] - \frac{\alpha_N}{1-\alpha_N} \mathbb{E}_t[w_{t+1} - \bar{w}] \right) + k_0 \\ = \frac{1}{1-\alpha} \left(\frac{1}{1-\alpha_N} (\mathbb{E}_t[\hat{z}_{it+1}] + \mathbb{E}_t[\hat{\beta}_{it+1}(T_{t+1} - T^*)]) - \frac{\alpha_N \chi}{1-\alpha_N} \mathbb{E}_t[T_{t+1} - T^*] \right) + k_0, \quad (24)$$

where $k_0 = \frac{1}{1-\alpha} \left(\log \left[\frac{\alpha G}{r+\delta} \right] \right)$ and lowercase denotes logs. The derivations illustrate the follow-

37. Our benchmark model abstracts from the presence of adjustment costs in capital investment. If we introduce

ing logic: investment is proportional to the expected profitability of capital, which is increasing in expected (revenue) productivity and decreasing in expected wages. These are, in turn, dependent on the firm's expectation of future temperature sensitivity and future temperature.

The size of persistent temperature sensitivity $\hat{\beta}_i$ will determine how a firm's investment decision responds to expected temperature. Firm i 's investment, relative to the average firm in the economy at date t , would be:

$$k_{it+1} - \bar{k}_{it+1} = \frac{1}{1-\alpha} \left(\mathbb{E}_t[\hat{z}_{it+1}] + \frac{(\hat{\beta}_i - \bar{\hat{\beta}}_i)}{1-\alpha_N} \mathbb{E}_t[(T_{t+1} - T^*)] \right).$$

Specifically, for a *heat-averse firm* with $\hat{\beta}_i < \bar{\hat{\beta}}_i$ (say, a ski resort), a higher temperature forecast $\mathbb{E}_t[T_{t+1}]$ will lead to a relatively lower level of expected productivity and consequently lower investment compared to an average firm with $\hat{\beta}_i$. In contrast, a *heat-loving firm* with $\hat{\beta}_i > \bar{\hat{\beta}}_i$ (say, a water park), would invest more than an average firm due to the relatively positive productivity effect from higher expected heat.

MRPK. Upon the realization of idiosyncratic productivity and temperature conditions, firms' labor choice is made and production takes place. From equation (22), realized marginal revenue product of capital ($MPRK_{it} := \alpha_K \frac{P_{it} Y_{it}}{K_{it}}$)³⁸ of firm i can be derived as (in logs):

$$mrpk_{it} = a_{it} + (\alpha - 1)k_{it} + \log(\alpha_K \bar{G})^{39} \quad (25)$$

Plugging in the policy function k_{it} as a function of past expectation, we write down find how $mrpk_{it}$ depends on the realization of shocks in the next proposition:

Proposition 3 *Relative to the average level, MRPK is higher in the firms with higher unexpected change in productivity:*

$$mrpk_{it} - \bar{mrpk}_{it} = \frac{1}{1-\alpha_N} \left\{ \underbrace{(\hat{\beta}_i - \bar{\hat{\beta}}_i)\eta_t^T}_{\substack{\text{Unexpected} \\ \text{Temperature Shock} \\ \text{on Productivity}}} + \underbrace{\hat{\xi}_{it}(T_t - T^*)}_{\substack{\text{Unexpected} \\ \text{Damage} \\ \text{Sensitivity}}} + \hat{\varepsilon}_{it} \right\}, \quad (26)$$

where the relative MRPK of heat-averse firms with $\hat{\beta}_i < \bar{\hat{\beta}}_i$ will decrease with a positive temperature shock η_t^T ; while the relative MRPK of heat-loving firms $\hat{\beta}_i > \bar{\hat{\beta}}_i$ will increase with a positive temperature

an adjustment cost of the form $-\frac{\kappa}{2} \left(\frac{I_{it}}{K_{it}} - \delta \right)^2$ at the time of investment, then the MRPK dispersion in the economy would take the form:

$$\sigma_{mrpk,(r,s),t}^2 = \left(\frac{1}{1-\alpha_N} \right)^2 \left[(T_{r,t} - T^*)^2 \sigma_{\xi,(r,s)}^2 + \eta_{r,t}^T \sigma_{\beta,(r,s)}^2 + \sigma_{\varepsilon,(r,s)}^2 \right] + (\alpha - 1)^2 \phi_3^2 \sigma_{k,t-1}^2 + \text{Adj. Cost Channel}_{(r,s),t},$$

for some constant ϕ_3 . The Adj. Cost Channel_{(r,s),t} captures how adjustment costs interact with past and present climate conditions. It includes terms that are linear in $\eta_{r,t}^T$ as well as the interactions of past temperature conditions with $\eta_{r,t}^T$. The interaction between adjustment costs and climate conditions operates separately from our main mechanisms. It is unlikely to affect the identification of the damage uncertainty channel and climate uncertainty channel in the data when additional controls are added.

38. Note that the marginal revenue product of capital and the marginal profitability of capital are the same up to

shock.

Proof. See Appendix. ■

First, notice that equation (26) suggests that $mrpk_{it}$ would be the same across all firms when productivity is perfectly known at the time of investment. Otherwise, the MRPK would increase with forecast error of (revenue) productivity in the cross-section.

This reveals the key mechanism in the model. All firm's MRPK would change with (1) the unexpected temperature shock η_t^T due to their temperature sensitivity $\hat{\beta}_i$ and (2) with the level of temperature $T_t - T^*$ since part of their damage sensitivity $\hat{\xi}_{it}$ was unknown to them at the time of investment. In a region-sector with an unexpected heat shock, $\eta_t^T > 0$, the firms with relatively low MRPKs in the cross-section are those that are (1) heat-averse ($\hat{\beta}_i < \bar{\beta}_i$) such that the productivity suffers unexpectedly more than an average firm; (2) unexpectedly damaged with heat sensitivity $\hat{\xi}_{it}(T_t - T^*) < 0$. Judging from the ex-post, these firms invested too much capital due to their erroneous expectation of higher-than-realized productivity, and the capital in those firms cannot be used as productively as those firms that are heat-loving ($\hat{\beta}_i > \bar{\beta}_i$) or those experiencing an unexpectedly less damage $\hat{\xi}_{it}(T_t - T^*) > 0$.

The large heterogeneity of firm-level sensitivity implies that temperature conditions could change the dispersion in capital return and thus capital misallocation across firms, summarized by the following proposition, where we add back the notation for a region-sector pair $n = (r, s)$:

Proposition 4 *Within a region-sector pair $n = (r, s)$, the mrpk dispersion across firms is increasing in TFP Volatility, $\text{Var}(\hat{a}_{nit} - \mathbb{E}_{t-1}[\hat{a}_{nit}])$, and can be decomposed into:*

$$\begin{aligned}\sigma_{mrpk,(r,s),t}^2 &= \left(\frac{1}{1-\alpha_N}\right)^2 \text{Var}(\hat{a}_{nit} - \mathbb{E}_{t-1}[\hat{a}_{nit}]) \\ &= \left(\frac{1}{1-\alpha_N}\right)^2 \left[\underbrace{(T_{r,t} - T^*)^2 \sigma_{\xi,(r,s)}^2}_{\substack{\text{Damage Volatility} \\ (\text{Level Effect})}} + \underbrace{\eta_{r,t}^T \sigma_{\beta,(r,s)}^2}_{\substack{\text{Climate Uncertainty} \\ (\text{Shock Effect})}} + \sigma_{\varepsilon,(r,s)}^2 \right] \end{aligned} \quad (27)$$

Within $n = (r, s)$, mrpk dispersion is increasing in:

- (1) squared deviation from optimal temperature, $(T_{r,t+1} - T^*)^2$,
- (2) squared (unexpected) temperature shocks $\eta_{r,t}^T$.

As the cross-sectional MRPK differences depend solely on the unexpected shocks on productivity in the model, it follows naturally that MRPK dispersion scales with the dispersion in the unexpected shocks on productivity among firms. The higher the TFP volatility, the larger the dispersion of the input mistakes that would take place. Using our decomposition of TFP Volatility in equation (21), we find temperature variations contribute to misallocation through two channels: level effect (due to damage volatility) and shock effect (due to climate uncertainty).

(1) Level Effect. The level of temperature affects misallocation through the change in damage volatility. As the temperature deviates more from the “bliss point” T^* , firms who receive extreme realizations of the idiosyncratic damage sensitivity $\hat{\xi}_{it}$ will get larger unexpected damage (e.g., a larger fraction of firms will experience severe factory fire). Therefore, the productivity becomes harder to forecast, and more investment mistakes are made. The economy will thus suffer from more misallocation as $(T_{r,t+1} - T^*)^2$ rises.

(2) Shock Effect. The magnitude of the climate uncertainty channel relies on the size of unexpected temperature shocks. As different firms have heterogeneous sensitivity to these shocks, larger unexpected temperature shocks, either heat or cold, will make the return to investment of heat-averse firms unexpectedly low and the heat-loving firms unexpectedly high. Therefore, we will see an increasing level of capital misallocation with a more considerable unexpected temperature shock $\eta_{r,t}^{T^2}$.

These two effects help explain how a region-sector’s geographical locations and long-run climate might matter for capital misallocation, as we have identified in Figure 3 in Section 4. Regions experiencing extreme temperatures - either too hot or too cold - or those subject to uncertain temperature conditions are prone to higher levels of capital misallocation. In Section 7, we will try to gauge the quantitative importance of how the level effect and the shock effect contribute to climate-induced capital misallocation through the lens of model-induced regressions.

Equation (27) also has predictions across region-sectors on how the average degree of misallocation in the region-sector depends on the average climate conditions and the distribution of the firm’s weather-related characteristics. For example, when given the same climate conditions, a region-sector with higher dispersion in persistent sensitivity $\sigma_{\beta,(s,r)}^2$ or larger damage uncertainty $\sigma_{\xi,(s,r)}^2$ will suffer more climate-induced misallocation.

Paired with the model’s implication that the average level of temperature sensitivity $\bar{\hat{\beta}}_{(s,r)}$ in a region-sector does not matter for the degree of misallocation, we can try to rationalize why developed countries suffer more from temperature shocks via the misallocation channel. Although developed countries might feature a higher level of “heat preparedness” $\bar{\hat{\beta}}_{(s,r)}$, but might have a larger dispersion $\sigma_{\beta,(s,r)}^2$ due to the larger scope of specialized production and more extensive variety. More developed countries also have a larger dispersion of firm sizes (Poschke 2018), which would naturally matter for dispersion of temperature sensitivity as larger firms have more resources and working capital to defend against sudden climate shocks. Although we do not model this explicitly in the benchmark model, we will empirically test how firm sizes might proxy for temperature sensitivity in Section 6.

TFP Loss from Misallocation. Finally, we formalize how temperature-induced misallocation affects region-sector aggregate TFP in the model. In the Appendix, we show that under a CES a transformation, which implies that their cross-sectional log dispersion should be the same.

aggregator⁴⁰, the economy admits an aggregate production function of the form:

$$y_{nt} = a_{nt} + \tilde{\alpha}_K k_{nt} + \tilde{\alpha}_N n_{nt},$$

where the cost of misallocation can be expressed as the deviation from the level of TFP, a_{nt}^* when MRPks are equalized across firms:

$$a_{nt} - a_{nt}^* = -\frac{\tilde{\alpha}_K + \tilde{\alpha}_K^2(\sigma - 1)}{2} \sigma_{mrpk,nt}^2 \quad (28)$$

This formula is reminiscent of equation (8) in the accounting framework and shows that the intuitions behind the cost of misallocation are similar in the firm dynamics model.

6 Firm-level Evidence: Heterogeneous Sensitivity, Temperature Shocks, and MRPk Divergence

We now provide direct evidence from firm-level data on how temperature shocks could lead to heterogeneous responses in the MRPk among firms with differing levels of persistent temperature sensitivity⁴¹, $\hat{\beta}_i$. Since directly measuring $\hat{\beta}_i$ for each firm is challenging, we instead explore two possible major factors contributing to this heterogeneity: firm size and adaptability, particularly regarding the installation of air conditioning (AC) facilities. We investigate whether firms of different sizes and levels of adaptability (those equipped with AC versus those without) exhibit distinct responses to identical temperature shocks in their MRPks.

The choice to use firm size and AC installation as proxies for temperature sensitivity is grounded in the empirical literature. Regarding size, studies have shown that larger firms are less sensitive to temperature shocks and better equipped to cope with extreme heat compared to smaller firms (Ponticelli, Xu, and Zeume 2023), leading to a higher level of $\hat{\beta}_i$ in the model. As for the importance of AC, Somanathan et al. (2021) demonstrates that hot days significantly suppress output for plants without climate control, whereas plants with climate control facilities are unaffected.

We test the key prediction by the model from Equation 26 (reproduced below). In the same region-sector pair, a more heat-averse firm (i.e. lower $\hat{\beta}_i$) would have a lower MRPk from an unexpected positive temperature shock compared to the average. As the temperature shock was not expected at the time of investment decisions, a more heat-averse firm would be seen to have made a bigger “investment mistake” as the return on the capital can be lower.

$$mrpk_{it} - \overline{mrpk_{it}} = \frac{1}{1 - \alpha_N} \left\{ \underbrace{(\hat{\beta}_i - \bar{\beta}_i)\eta_t^T}_{\substack{\text{Unexpected} \\ \text{Temperature Shock} \\ \text{on Productivity}}} + \underbrace{\hat{\xi}_{it}(T_t - T^*)}_{\substack{\text{Unexpected} \\ \text{Damage} \\ \text{Sensitivity}}} + \hat{\varepsilon}_{it} \right\},$$

40. Following Midrigan and Xu (2014), in a partial equilibrium context, one can define aggregate production and misallocation by considering the problem of a planner with a CES aggregator and faces no restrictions on how to reallocate inputs across firms.

41. This also serves to identify climate-induced misallocation directly using firm-level microdata without the log-normality assumption.

$\hat{\beta}_i$ and MRPK: Empirical Approach We run the following regression as the empirical counterpart of the equation (26) to explore whether the two heat-sensitivity proxy variables: firm sizes and AC installation, lead to different responses of MRPK to temperature shocks:

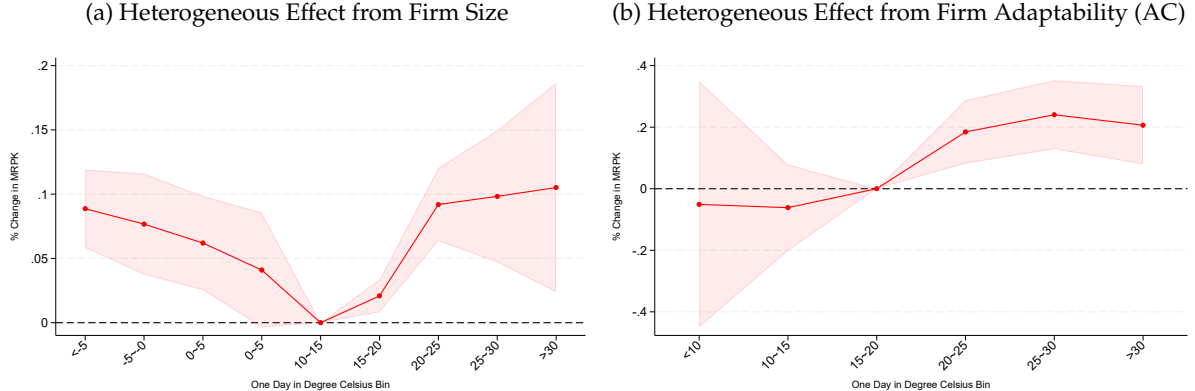
$$\begin{aligned} \log(MRPK_{r,s,i,t}) = & \sum_{b \in B / \{5-10^\circ C\}} \lambda_b \times Tbin_{r,t}^b \\ & + \sum_{b \in B / \{5-10^\circ C\}} \lambda_{b,\hat{\beta}\text{-proxy}} \times Tbin_{r,t} \times \hat{\beta}\text{-proxy}_{it}^{r,s} + \delta \mathbf{X}_{i,t} \\ & + \delta_i + \alpha_{s,c(r),t} + \varepsilon_{s,c(r),i,t}, \quad \hat{\beta}\text{-proxy} \in \{\text{Relative Size, AC}\}. \end{aligned} \quad (29)$$

In this model, r represents the region, s the sector, i the firm, and t the year. $\hat{\beta}\text{-proxy}_{it}^{s,r}$ is a firm-level proxy for $\hat{\beta}_i$, defined either as Relative Size $_{it}^{sr}$ or AC $_{it}^{sr}$ in our two settings. η_i indicates firm fixed effects, which remove time-invariant, unobserved firm-level heterogeneity that could otherwise bias the estimates. $\alpha_{s,c(r),t}$ are country-sector-year fixed effects that control for unobserved characteristics specific to each region-sector pair annually, such as country-sector level business cycle fluctuations. Standard errors are clustered at the region level to address serial and spatial correlation within all firm-year observations in a region. The coefficients of interest, $\lambda_{b,\hat{\beta}\text{-proxy}}$, are identified by comparing firms within the same country-sector exposed to identical temperature shocks but show differential response in (log) MRPK. A $\lambda_{b,\hat{\beta}\text{-proxy}} > 0$ indicates a higher MRPK for heat-tolerant firms compared to heat-averse ones under similar temperature shocks.

Heterogeneous Effect of Temperature Shocks from Firm Size. Following the approach of Bau and Matray (2023), we characterize a firm's size based on the value of its capital stock, as larger firms are typically more financially flexible in adjusting to unexpected heat shocks. For the analysis of firm size, $\hat{\beta}\text{-proxy}_{it}^{s,r}$ is defined as a continuous variable equal to Relative Size $_{it}^{s,r}$. We measure a firm's relative size using Relative Size $_{it}^{r,s} := \log K_{it}^{s,r} - \overline{\log K_{it}^{s,r}}$, which compares a firm's (log) capital stock, $\log K_{it}^{s,r}$, to the cross-sectional average of firms within the same region-sector-year, $\overline{\log K_{it}^{s,r}}$. We also standardize Relative Size $_{it}^{r,s}$ over the entire sample in the regression. This approach allows us to exploit variations across firms within each region-sector-year, aligning with the level of variations used in our reduced-form analysis, where var($mrpk$) is calculated.

Figure 6a illustrates the effect of temperature shocks on MRPK across firms of varying sizes, $\lambda_{b,\text{Relative Size}}$, for each temperature. The analysis reveals that firms of different sizes respond differently to identical weather shocks. Specifically, larger firms tend to experience a relatively higher MRPK in response to temperature extremes compared to smaller firms. For instance, an additional day with temperatures above 30°C or below -5°C, compared to a day with temperatures ranging from 10-15°C, increases the MRPK difference by around 0.1% between two firms whose sizes differ by one standard deviation. Figure 6a plots the effect of temperature shocks on MRPK across firms of varying sizes, denoted by $\lambda_{b,\text{Relative Size}}$, with the larger firm suffering less from the hot day than the smaller one. Detailed results of the estimation are presented in Table A.3. The results here validate our hypothesis that the difference in firm sizes is a source of $\hat{\beta}_i$ heterogeneity, and larger firms are more heat-tolerant.

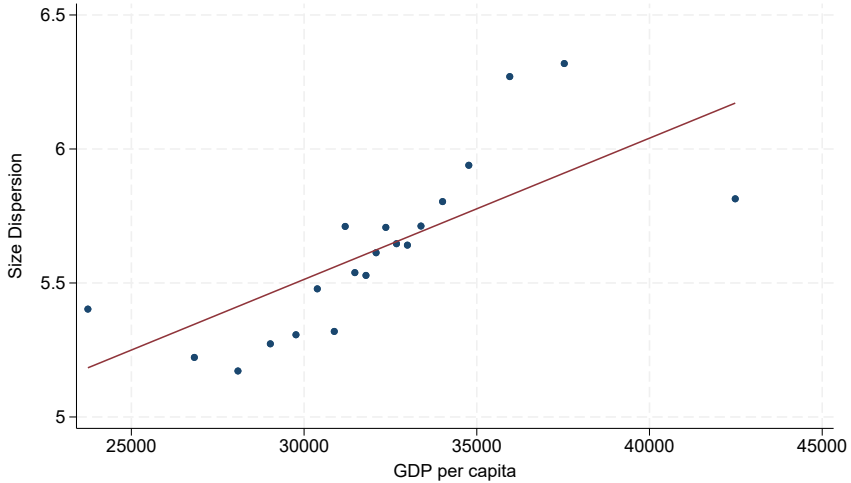
Figure 6: Effects of daily temperature shocks on log MRPK for firms of different sizes and adaptability



Notes: Graph plots the effects of daily mean temperature bins on firm-level log MRPK. Panel 6a plots the interaction terms of relative firm size and temperature bins. Each point measures the estimated effect on a large firm relative to a firm that is 1 SD smaller. We include firm and country-sector-year fixed effects. Panel 6b plots the estimated effect on firms with and without AC separately. We include firm and sector-year fixed effects (since AC data only covers the India ASI sample). Standard errors are clustered at the regional level. Shaded areas indicate a 90% confidence interval.

More interestingly, drawing back to our empirical findings on the heterogeneous impacts of extreme heat across different income levels, we find that wealthier economies suffer more from capital misallocation under extreme heat. This could be driven by the higher dispersion in firm sizes in more developed economies, as documented by Poschke (2018) and observed in our data in Figure 7.

Figure 7: Firm Size Dispersion and GDP per capita



Notes: The graph presents the bin-scatter plots illustrating the relationship between firm size dispersion (measured as the variance of log fixed assets across firms) and annual GDP per capita at the region-sector-year level.

Heterogeneous Effect of Temperature Shocks from Adaptability. Another source of heterogeneity in $\hat{\beta}_i$ could be the varying adaptability to temperature extremes among firms. We expect that firms with greater adaptation measures will be more resilient to heat shocks and thus have a higher $\hat{\beta}_i$. We measure adaptability by the installation of computerized air condi-

tioning (AC) systems, a variable collected annually in the Indian Annual Survey of Industries (ASI) since 2001. Therefore, our analysis for this part focuses on the sample from the Indian ASI.

We implement equation 29 where $\hat{\beta}\text{-proxy}_{it}^{s,r} := \text{AC}_{it}^{s,r}$ is defined as a dummy variable – it equals 1 for firms equipped with AC and 0 for those without⁴². Figure 6b shows the estimated effects on MRPK for AC-equipped firms compared to those without AC. The impact of temperature shocks on MRPK for AC-equipped firms relative to non-AC firms, $\lambda_{b,\text{AC-eq}}$, is depicted by the red line for each temperature bin b . Our findings reveal that cold temperature shocks have a negligible difference in MRPK between AC-equipped and non-AC firms. However, heat shocks significantly increase the MRPK difference for AC-equipped firms compared to non-AC firms. For example, an additional day with temperatures above 30°C, compared to a day in the 15-20°C range, leads to a relative increase of about 0.2% in MRPK between AC-equipped and non-AC firms, after controlling for firm capital stock. Detailed results are presented in Table A.4⁴³.

7 Estimating the Mechanisms of Climate-Induced Misallocation

In this section, we empirically estimate the two effects driving climate-driven misallocation: (1) the level effect due to damage volatility, and (2) the shock effect stemming from climate uncertainty, as suggested by the model in equation (27), which is reproduced below:

$$\begin{aligned}\sigma_{mfpk,(r,s),t}^2 &= \left(\frac{1}{1-\alpha_N}\right)^2 \text{Var}(\hat{a}_{nit} - \mathbb{E}_{t-1}[\hat{a}_{nit}]) \\ &= \left(\frac{1}{1-\alpha_N}\right)^2 \left[\underbrace{(T_{r,t} - T^*)^2 \sigma_{\xi,(r,s)}^2}_{\text{Damage Volatility (Level Effect)}} + \underbrace{\eta_{r,t}^T \sigma_{\beta,(r,s)}^2}_{\text{Climate Uncertainty (Shock Effect)}} + \sigma_{\varepsilon,(r,s)}^2 \right]\end{aligned}$$

We first test the level effect by empirically estimating how the level of temperature non-linearly shifts the TFP volatility and MRPK dispersion in the cross-section of firms. We also identify an optimal temperature of around 13°C, consistent with Burke, Hsiang, and Miguel (2015). Next, we provide direct evidence of the shock effect by showing climate uncertainty, measured by the mean squared forecast errors of monthly temperature, contributes to MRPK dispersion. Based on these estimates, we then quantify the relative contributions of level effect and shock effect to climate-induced misallocation.

7.1 Level Effect: Temperature and TFP Damage Volatility

Our theory suggests that MRPK dispersion is proportional to TFP volatility, which in turn is non-linearly dependent on the level of temperature $T_{r,t}$. As the temperature deviates from

42. A firm is defined as AC-equipped if it has reported the installation of AC at least once during the sample period.

43. Our baseline specification in Column 3 analyzes the within-firm variation on the effect of AC installation by including firm fixed effects δ_i and sector-year fixed effects $\theta_{s,t}$, and we include the AC indicator variable $\text{AC}_{it}^{s,r}$ and capital stock $\ln K_{it}$ as controls. However, installing air conditioning is a common adaptation strategy for firms to cope with extreme heat, but it also makes them subject to costs of adaptive investment (e.g. Somanathan et al. 2021),

the optimal level T^* , becoming either too hot or too cold, the likelihood of extreme firm-level events increases. Therefore, temperature's deviation from T^* leads to greater volatility in TFP across different firms. We now test this relationship directly in the data and try to estimate the optimal temperature T^* .

As it is hard to directly measure unexpected TFP shocks ($\hat{a}_{nit} - \mathbb{E}_{t-1}[\hat{a}_{nit}]$) due to possible mis-specifications of the law of motion and agents' information set, we adopt the approach of Asker, Collard-Wexler, and Loecker (2014), and use the variance of 'first-differenced' TFP shocks, $\text{Var}_{(r,s)t}(\hat{a}_{it} - \hat{a}_{it-1})^{44}$ to approximate⁴⁵ the TFP volatility⁴⁶ in region-sector (r, s). Inspired by Equation 21, we identify the nonlinear impact of temperature on TFP volatility from the following reduced-form specification:

$$\text{Var}_{(r,s),t}(\hat{a}_{it} - \hat{a}_{it-1}) = \alpha + \beta f(T_{r,t}) + \eta_{s,r} + \delta_{c(r),t} + \varepsilon_{s,r,t}, \quad (30)$$

where $f(T_{r,t})$ is a polynomial of annual average temperature. $\eta_{s,r}$ and $\delta_{c(r),t}$ denote region-sector and country-year fixed effects, respectively. We include region-sector-year observations with at least 15 recurrent firms in the estimation⁴⁷. The estimation results are reported in Table 1, Columns (1)-(3).

Column (1) reports the estimate of the linear effects of temperature, which is negative but not statistically significant. However, including second- and third-order terms reveals a remarkable nonlinear U-shaped pattern, aligning with our theoretical model. Column (2) shows that the quadratic temperature term is statistically significant and economically meaningful: a 1 °C increase in the annual average temperature in a location with an average of 5°C will lead to a decrease of 2.9 log points in TFP volatility; however, the same 1 °C increase in a place with an average temperature of 20°C will increase the TFP volatility by 2.5 log points. These effects are quantitatively large, especially in the context of global warming projections.⁴⁸. The cubic specification in column (3) indicates some asymmetry of the effect around the critical point T^* .

which means the investment of AC itself could change the firm's MRPK as well. Following the approach of Asker, Collard-Wexler, and Loecker (2014), we address this in our alternative specification in Column (3) by conditioning on current capital stock to make sure that we are comparing two firms making the same capital decision, but one firm has AC while the other does not. We include sector-year fixed effects in all specifications, such that λ_b and $\lambda_{b,AC}$ are identified based on the comparison of across-firm differences caused by AC installation within each sector-year.

44. Measuring firm-specific productivity shocks is challenging and sensitive to mis-specifications for the TFPR process. This is particularly true in our model, where firm-level productivity responds heterogeneously to temperature shocks. To address this, we adopt the approach of Asker, Collard-Wexler, and Loecker (2014), calculating a proxy of TFP shocks as the difference in firm-level TFP over time, represented as $\hat{a}_{it} - \hat{a}_{it-1}$. In line with the methodology of David and Venkateswaran (2019), we use the model-implied TFP in our specification: $\hat{a}_{it} = \log(P_{it}Y_{it}) - \alpha \log K_{it}$.

45. This approximation would be exact if (all components of) productivity were to follow a random walk pattern.

46. TFP can alternatively be derived as the conventional Solow residuals including labor. However, as noted in David and Venkateswaran (2019), footnote 22, TFP calculated from the Solow residual approach can no longer be directly tied to capital profitability in the presence of labor distortions, while the model-based measure of TFP remains a valid proxy for capital profitability.

47. This is to reduce measurement errors from the observations that aggregate statistics with only very small numbers of firms. The measured TFP volatility is winsorized at the top 1 percent level to avoid outliers

48. To illustrate, let us consider a simple back-of-the-envelope calculation using parameters from our model. Take, for example, a permanent increase from 16 °C to 20 °C, which aligns with an RCP 8.5 climate scenario projected for Southern Spain (World Bank Climate Change Knowledge Portal 2023). According to our model's damage uncertainty mechanism, this 4 °C increase would increase TFP Volatility by 4.24 log points. This increment translates into a 12.31 log points increase in MRPK dispersion using equation (27). Subsequently, under standard elasticity assumptions, this dispersion translates into a 7.6% loss in TFP.

Table 1: TFP Volatility and Temperature Levels

	(1) 1st Order	(2) 2nd Order	(3) 3rd Order	(4) Model-Induced
$T_{r,t}$	-0.005319 (0.004573)	-0.023121*** (0.007536)	-0.012380 (0.008537)	
$T_{r,t}^2$		0.000841*** (0.000303)	-0.000447 (0.000679)	
$T_{r,t}^3$			0.000040** (0.000018)	
$(T_{r,t}^2 + T_{r,t-1}^2)$				-0.021556*** (0.005682)
$(T_{r,t} + T_{r,t-1})$				0.000882*** (0.000216)
$(\Delta T_{r,t})^2$				-0.003604 (0.002233)
Estimated T^*		13.75 °C (3.067678)	14.64°C (2.173182)	12.22°C (2.216646)
Region-Sector FE	Yes	Yes	Yes	Yes
Country-Year FE	Yes	Yes	Yes	Yes
Observations	113,765	113,765	113,765	113,765
R^2	0.754	0.754	0.754	0.754

Notes: Standard errors in parentheses. We cluster standard errors at the region level (NUTS3 level for European countries, province level for China, and first-level administrative divisions for India).

* $p < 0.10$, ** $p < 0.05$, *** $p < 0.01$

Loosely speaking, the same 1°C increase brings more damage in hotter climates than benefits in cooler climates. The U-shaped temperature-volatility relationships from both specifications are plotted in Figure 8.

Interpreting these estimates through our model, a positive temperature shock in a colder environment will move the economy closer to the optimal temperature T^* , reducing the harmful dispersion of extreme events caused by idiosyncratic temperature sensitivity $\hat{\xi}_{it}$. In contrast, the same positive shock in a hotter climate drives the economy further away from T^* , increasing the damage volatility. This temperature-volatility relationship, as depicted in our reduced-form estimate in Figure 8, also clarifies why the same hot temperature shock in cooler climates leads to a decrease in MRPK dispersion while producing an opposite effect in hotter climates as estimated in Equation 15 and depicted in Figure 3. Next, we will identify T^* .

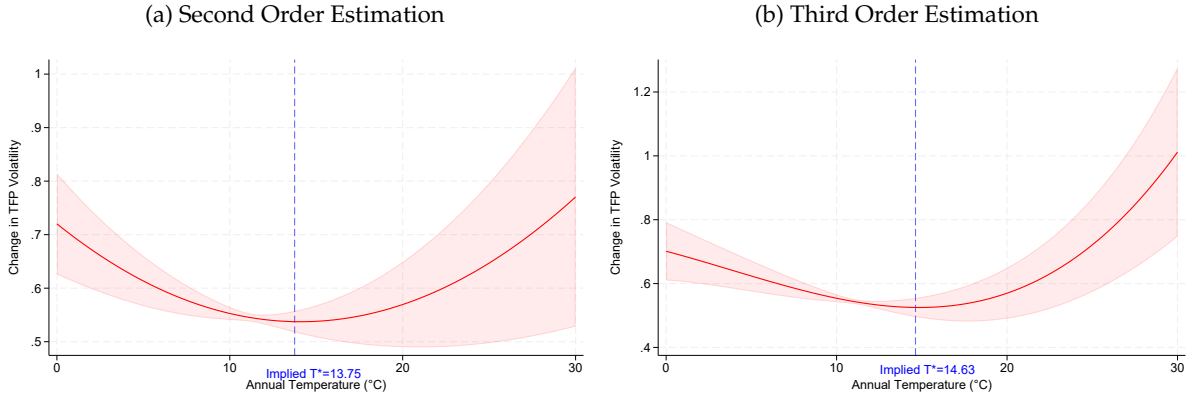
Identifying the Optimal Temperature T^* . Although easily interpretable, the reduced-form model does not account for how the lagged temperatures might affect the lagged TFP \hat{a}_{it-1} . To address this issue, we derive the exact expression for the “first-differenced” volatility:

$$\text{Var}_t(\hat{a}_{it} - \hat{a}_{it-1}) = \sigma_{\hat{\xi}}^2(T_t^2 + T_{t-1}^2) - 2\sigma_{\hat{\xi}}^2 T^*(T_t + T_{t-1}) + 2\sigma_{\hat{\xi}}^2 T^{*2} + \sigma_{\hat{\beta}}^2 (\Delta T_t)^2 + \sigma_{\Delta z}^2,$$

and estimate the model-induced specification:

$$\text{Var}_{(s,r),t}(\hat{a}_{it} - \hat{a}_{it-1}) = \alpha + \beta_1(T_{r,t}^2 + T_{r,t-1}^2) + \beta_2(T_{r,t} + T_{r,t-1}) + \gamma(\Delta T_{r,t})^2 + \eta_{s,r} + \delta_{c(r),t} + \varepsilon_{s,r,t}, \quad (31)$$

Figure 8: TFP Volatility and Annual Average Temperature



Notes: Graph plots the effects of temperature shocks on TFP volatility, based on a 3-rd order polynomial estimation derived from Equation 30. The asymmetrical pattern around the critical point $T^* = 13.19$ suggests that a 1°C in temperature increase inflicts greater damage in hotter climates than cooler ones.

where $\Delta T_{r,t}$ is the first-differenced temperature. The estimates from the model-induced regression are reported in Table 1, Column (4) are very close to those obtained from the quadratic specification in Column (2). By applying the Delta Method to the estimated coefficients, we can back out the estimate for the optimal temperature $\hat{T}^* = -\frac{\hat{\beta}_2}{2\hat{\beta}_1} = 12.22^\circ\text{C}$ (SE: 2.21°C). Similarly, the reduced-form specifications yield $\hat{T}^* = 13.75^\circ\text{C}$ and $\hat{T}^* = 14.64^\circ\text{C}$ for the quadratic and cubic specifications, respectively. These estimates align closely with those found by Burke, Hsiang, and Miguel (2015) (and recently Nath, Ramey, and Klenow (2023)), who also estimated that country-level productivity or GDP peaks at the “bliss point” 13°C. Our findings corroborate these findings by suggesting an additional mechanism: the level of temperature contributes to aggregate MRPK dispersion and TFP (output) loss as a volatility shock.

7.2 Shock Effect: Climate Uncertainty and Temperature Forecast Errors

The shock effect ties misallocation with forecast errors of temperature and climate uncertainty. In our model, even when all the firms face the same temperature forecast as common information, firms’ knowledge of their firm-specific sensitivity $\hat{\beta}_i$ would lead them to make differential investment decisions. Thus, any unexpected temperature shock, either cold or hot, would lead to dispersion in capital return. This is summarized as the climate uncertainty channel in equation 27 as MRPK dispersion increases in the squared forecast error of temperature.

We opt to utilize data directly from the monthly long-range temperature forecasts from ECMWF (Copernicus Climate Change Service and Climate Data Store 2018), instead of relying on proxies or basic statistical models to estimate forecast errors for the company’s weather predictions. Extensive research has demonstrated that accurate daily and seasonal temperature and weather forecasts can significantly impact adaptation behaviors (Shrader 2023) and mortality (Shrader, Bakkensen, and Lemoine 2023), as economic agents base their decisions on these signals. Therefore, we also assume that firms actively incorporate month-ahead weather forecasts into their learning processes and adjust investments accordingly.

As data on firm-level MRPK is reported on a yearly frequency while the long-range temperature forecast is updated every month, we need to create a yearly aggregate measure of

squared forecast errors. Let us denote the realized average temperature in the region r at month m and year t as $T_{m,r,t}$ and the month-ahead ECMWF temperature forecast as $\mathbb{E}_{m-1}T_{m,r,t}$. We construct a measure of mean squared forecast errors, $\text{MSFE}_{q,r,t}$, for each time frame q in year t , where we let $q \in \{\text{summer}, \text{winter}, \text{annual}\}$:

$$\begin{aligned}\text{MSFE}_{\text{summer},r,t} &= \frac{1}{6} \sum_{m=4}^9 (T_{m,r,t} - \mathbb{E}_{m-1}T_{m,r,t} - \widehat{\text{Bias}}_{m,r})^2, \\ \text{MSFE}_{\text{winter},r,t} &= \frac{1}{6} \sum_{m=\{1,2,3,10,11,12\}} (T_{m,r,t} - \mathbb{E}_{m-1}T_{m,r,t} - \widehat{\text{Bias}}_{m,r})^2, \\ \text{MSFE}_{\text{annual},r,t} &= \frac{1}{12} \sum_{m=1}^{12} (T_{m,r,t} - \mathbb{E}_{m-1}T_{m,r,t} - \widehat{\text{Bias}}_{m,r})^2.\end{aligned}$$

The reason behind the seasonal aggregation is that the same temperature forecast errors in warm and cold seasons might affect firms' MRPK differently. As all the firms in the sample reside in the Northern Hemisphere, we group all months between April to September as a broadly defined "summer" and the other six months as "winter". We take out the estimated forecast bias, $\widehat{\text{Bias}}_{m,r}$ from forecast error to reduce mechanical differences in temperature measurements due to the positioning of the weather stations and forecasting methods. $\widehat{\text{Bias}}_{m,r}$ is measured as the region-month fixed effect of the monthly forecast error in the past 40 years.

Equation (27) suggests a larger squared forecast error in a region-sector would lead to more capital misallocation. We directly estimate the empirical version of Equation 27 with the following regression:

$$\sigma_{mrpk,(s,r),t}^2 = \theta_q \cdot \text{MSFE}_{q,r,t} + \gamma_1 T_{rt} + \gamma_2 T_{rt}^2 + \eta_{s,r} + \delta_{c(r),t} + \varepsilon_{s,r,t}, \quad (32)$$

where θ_q measures the impact of a one-unit increase in MSFE in the time frame q on annual capital misallocation. We control for the level effect in Equation (27) by adding the linear and quadratic terms of realized annual temperature.

The estimation results are presented in Table 2. Columns (1) and (2) show that the annual MSFE (all-month average) has a positive and statistically significant effect on MRPK dispersion, even after controlling for the level effect of realized temperatures. Columns (2) and (3) display the estimates using "seasonal" MSFEs from both summer and winter. We find that an increase in the MSFE in summer is at least twice as costly as the same increase in winter, suggesting unexpected temperature shocks are more damaging in the warmer season. However, the effect of winter forecast error becomes statistically insignificant when we control for the level of realized temperature.

The estimates in Column (2) can be interpreted in the following way: a 1°C increase in the temperature forecast errors in all months would lead to a 1.6 log point increase in MRPK dispersion, compared to a perfect information counterfactual, equivalent to an approximate 0.58%⁴⁹ of annual aggregate TFP loss. Obtained from a small deviation from a perfect information state, this number should be interpreted as a lower bound of the aggregate cost of temperature

49. This is obtained by using the calibrated structural parameter, $-\frac{\tilde{\alpha}_K + \tilde{\alpha}_K^2(\sigma-1)}{2} = 0.359$.

Table 2: Temperature Forecast Errors and MRPK Dispersion

	(1)	(2)	(3)	(4)
MSFE _{annual,r,t}	0.019114*** (0.006675)	0.016249** (0.006561)		
MSFE _{summer,r,t}			0.014908** (0.007115)	0.016592** (0.007084)
MSFE _{winter,r,t}			0.008536** (0.004017)	0.006096 (0.003882)
Quadratic Temperature Control	No	Yes	No	Yes
Region-Sector FE	Yes	Yes	Yes	Yes
Country-Year FE	Yes	Yes	Yes	Yes
Observations	124,065	124,065	124,065	124,065
R ²	0.876	0.876	0.876	0.876

Notes: Standard errors in parentheses. We cluster standard errors at the region level (NUTS3 level for European countries, province level for China, and first-level administrative divisions for India)..

* $p < 0.10$, ** $p < 0.05$, *** $p < 0.01$

forecast errors. Moreover, the sample average of $\text{MSFE}_{\text{annual},r,t}$ is 1.39 in our regression, implying the average cost of temperature forecast errors is 0.81% of annual aggregate TFP across India, China, and Europe.

Our findings suggest that temperature forecast errors are costly: unexpected temperature shocks lead to dispersion in investment mistakes among firms due to their varying sensitivity to heat. In sum, the value of temperature forecasts is highlighted through a new channel in our context: accurate forecast increases the allocative efficiency of capital.

7.3 Channel Decomposition: Which Effect is More Important?

After establishing the empirical relevance of the level effect and the shock effect in the data, a natural question arises: which channel has contributed more to climate-induced misallocation? To decompose the contribution of the two effects, we ran the following model-induced regression directly following Equation 27:

$$\sigma_{mfpk,(s,r),t}^2 = \kappa_1(T_{r,t} - \hat{T}^*)^2 + \kappa_2 \hat{\eta}_{r,t}^T \hat{\eta}_{r,t} + \iota_{s,r} + \iota_{c(r),s} + \varepsilon_{s,r,t}, \quad (33)$$

where $(T_{r,t} - \hat{T}^*)^2$ is computed as the squared deviation of annual temperature from the estimated optimal temperature from Equation 30 ($\hat{T}^* = 12.22^\circ\text{C}$). $\hat{\eta}_{r,t}^T \hat{\eta}_{r,t}$, representing the squared unexpected temperature shocks in the model, is proxied by the annual mean squared forecast error, $\text{MSFE}_{\text{annual},r,t}$ in the data, or by the estimated shock from a climate-specific AR(10) process following the approach in [Nath, Ramey, and Klenow \(2023\)](#). We include region-sector fixed effect, $\iota_{s,r}$, and country-year fixed effect, $\iota_{c(r),s}$ in the regression. The coefficients κ_1 and κ_2 are closely connected to objects in the model. Through the lens of equation 27, we see that the coefficient $\kappa_1 \approx \mathbb{E}\left[\left(\frac{1}{1-\alpha_N}\right)^2 \sigma_{\xi,(s,r)}^2\right]$ governs the strength of level effect and reflects the average uncertainty of damage sensitivity across all region-sector pairs. Similarly,

$\kappa_2 \approx \mathbb{E} \left[\left(\frac{1}{1-\alpha_N} \right)^2 \sigma_{\hat{\beta},(s,r)}^2 \right]$ governs the shock effect and reflects the average degree of dispersion in persistent temperature sensitivity.

The estimated coefficients of Equation (33) are presented in Table 3⁵⁰. Under our calibration of the standard parameters⁵¹, we have $\left(\frac{1}{1-\alpha_N} \right)^2 = 1.95$. For the level effect, we estimate $\hat{\kappa}_1$ to be around 0.046 (column (1)), indicating an average degree of damage uncertainty of $\mathbb{E}[\sigma_{\xi,(s,r)}^2] \approx 0.0023$. For the shock effect, we find $\hat{\kappa}_2$ to be around 0.016 to 0.030 in columns (2) and (3), suggesting an average dispersion of persistent climate sensitivity $\sigma_{\hat{\beta}}^2$ to be around 0.008 and 0.015.

Table 3: Model-induced Regressions: Level Effects and Shock Effects

	(1)	(2)
$(T_{r,t} - \hat{T}^*)^2$	0.004663*** (0.000868)	0.004621*** (0.000865)
AR(10) Residuals $(\hat{\eta}_{r,t}^T)^2$	0.030096** (0.013394)	
Annual MSFE $(\hat{\eta}_{r,t}^T)^2$		0.016204** (0.006593)
Region-Sector FE	Yes	Yes
Country-Year FE	Yes	Yes
Observations	124,065	124,065
R^2	0.876	0.876

Notes: Standard errors in parentheses. We cluster standard errors at the region level (NUTS3 level for European countries, province level for China, and first-level administrative divisions for India)..

* $p < 0.10$, ** $p < 0.05$, *** $p < 0.01$

With these estimates, we examine which of the two effects could be more prominent across the observed realizations in an average region-sector in China, India, and European countries. We compute the average contribution of the two channels to MRPK dispersion and implied TFP loss using the estimated results of our baseline specification and the unweighted average

50. We report the mean of temperature variables in the sample, including average squared deviation from “bliss point” $\overline{(T_{r,t} - T^*)^2}$, average squared AR-estimated residuals $\overline{\eta_t^T}^2_{\text{AR}}$, average first-differenced $\overline{(\Delta T_{r,t})^2}$ and average MSFE $\overline{MSFE_{r,t}}$ in the last row of Table 3.

51. Recall we use a labor share of $\tilde{\alpha}_N = 0.65$ and $\sigma_n = 4$, both of which are standard values in the literature.

of climate variables in our regression sample:

$$\begin{aligned}\Delta \log TFP_{(s,r),t} &= -\underbrace{\frac{\tilde{\alpha}_K + \tilde{\alpha}_K^2(\sigma - 1)}{2}}_{0.359} \Delta \sigma_{mrpk,(s,r),t}^2 \\ &= -\underbrace{\frac{\tilde{\alpha}_K + \tilde{\alpha}_K^2(\sigma - 1)}{2} \frac{\hat{\sigma}_{\xi,(s,r)}^2}{(1 - \alpha_N)^2} \overline{(T_{r,t} - T^*)^2}}_{\text{Level Effect} = 3.00\%} \\ &\quad - \underbrace{\frac{\tilde{\alpha}_K + \tilde{\alpha}_K^2(\sigma - 1)}{2} \frac{\hat{\sigma}_{\beta,(s,r)}^2}{(1 - \alpha_N)^2} \overline{\eta_{r,t}^{T^*}}}_{\text{Shock Effect} = 0.81\%} \\ &= 3.81\%\end{aligned}$$

Through these back-of-envelope calculations, we find that, on average, the level effect of temperature contributes to 8.4 log points of MRPK dispersion, equivalent to a TFP loss of 3%. On the other hand, the contribution of the shock effect (proxied by annual MSFE) to MRPK dispersion is around 0.023 log points, implying a TFP loss of 0.81%. Consistent with previous results, both the level and the shock effects are quantitatively sizable. However, in our sample from 1998 to 2018, the contribution of the level effect is almost three times as large as the contribution of the shock effect. Looking ahead, these estimates suggest that the level effect of increasing global warming would play a more significant role by creating greater damage volatility in productivity losses from temperature among firms, consistent with our reduced-form projections in Section 4.4.

8 Conclusion

We provide the first causal estimates of the misallocation effect from temperature shocks using firm-level microdata from 32 countries. On average, an additional hot day with $> 30^{\circ}\text{C}$ of temperature increases MRPK dispersion by 0.31 log points and contributes to a 0.11% decline in annual aggregate TFP. Intriguingly, the detrimental impact of extreme heat on capital misallocation is more severe in regions with hotter climates and higher incomes, highlighting a significant market cost of climate change coupled with a limited capacity for adaptation. Using projected temperature and income data, we find that global warming, under the SSP3-7.0 scenario, could lead to an aggregate TFP loss of 42.7%. By writing down a firm dynamics model with heterogeneous temperature sensitivity, climate uncertainty, and damage volatility, we use model-implied regressions to explain the differential effects among regions: regions with higher deviation from optimal temperature, (around 13°C) and lower temperature fore-

cast accuracy will have larger unexpected volatility in firm-level TFP and investment mistakes. Overall, our results imply that firm-level heterogeneity matters for analyzing the aggregate effect of climate change. This paper suggests an important venue for research in understanding the impact of climate change in a distorted economy.

We conclude with a final suggestion for future research. First, the identified misallocation effect is highly heterogeneous across different geographical locations, implying a different level of TFP losses across regions and sectors globally. This will lead to shifts in comparative advantage and endogenous variations in trade patterns with deteriorating climate conditions caused by global warming. Moreover, as we only focus on the misallocation effect within a region sector as a lower-bound estimate of the climate-induced misallocation, one could also study the misallocation that arises between sectors, regions, and even countries. On the empirical side, it would be important to understand whether demand-side or supply-side factors function as the main drivers of climate-induced misallocation. We leave these questions for future research.

References

- Allcott, Hunt, Allan Collard-Wexler, and Stephen D O'Connell. 2016. "How do electricity shortages affect industry? Evidence from India." *American Economic Review*.
- Alves, Felipe, Greg Kaplan, Benjamin Moll, and Giovanni L. Violante. 2020. "A Further Look at the Propagation of Monetary Policy Shocks in HANK." *Journal of Money, Credit and Banking* 52 (S2): 521–559.
- Asker, John, Allan Collard-Wexler, and Jan De Loecker. 2014. "Dynamic Inputs and Resource (Mis)Allocation." *Journal of Political Economy* 122 (5): 1013–1063.
- Bakkensen, Laura A, and Lint Barrage. 2021. "Going Underwater? Flood Risk Belief Heterogeneity and Coastal Home Price Dynamics." *The Review of Financial Studies* 35 (8): 3666–3709.
- Baqae, David Rezza, and Emmanuel Farhi. 2019. "The Macroeconomic Impact of Microeconomic Shocks: Beyond Hulten's Theorem." *Econometrica* 87 (4): 1155–1203.
- Barrage, Lint, and William D Nordhaus. 2023. *Policies, Projections, and the Social Cost of Carbon: Results from the DICE-2023 Model*. Working Paper, Working Paper Series 31112. National Bureau of Economic Research.
- Basu, Susanto, and John G. Fernald. 2002. "Aggregate productivity and aggregate technology." *European Economic Review* 46 (6): 963–991.
- Bau, Natalie, and Adrien Matray. 2023. "Misallocation and Capital Market Integration: Evidence From India." *Econometrica* 91 (1): 67–106.
- Bilal, Adrien, and Esteban Rossi-Hansberg. 2023. *Anticipating Climate Change Across the United States*. Technical report. National Bureau of Economic Research.
- Bils, Mark, Peter J. Klenow, and Cian Ruane. 2021. "Misallocation or Mismeasurement?" *Journal of Monetary Economics* 124:S39–S56.
- Blanchard, Olivier, and Jordi Galí. 2010. "Labor Markets and Monetary Policy: A New Keynesian Model with Unemployment." *American Economic Journal: Macroeconomics* 2, no. 2 (April): 1–30.
- Bloom, Nicholas. 2009. "The impact of uncertainty shocks." *econometrica* 77 (3): 623–685.
- Brandt, Loren, Johannes Van Bieseboeck, and Yifan Zhang. 2014. "Challenges of working with the Chinese NBS firm-level data." *China Economic Review*.
- Burke, Marshall, Solomon M. Hsiang, and Edward Miguel. 2015. "Global non-linear effect of temperature on economic production." *Nature* 527 (7577): 235–239.
- Caggese, Andrea, Andrea Chiavari, Sampreet Goraya, and Carolina Villegas-Sanchez. 2023. "Climate Change, Firms, and the Aggregate Productivity." Working Paper.

- Carleton, Tamara, Amir Jina, Michael Delgado, Michael Greenstone, Trevor Houser, Solomon Hsiang, Andrew Hultgren, et al. 2022. "Valuing the Global Mortality Consequences of Climate Change Accounting for Adaptation Costs and Benefits." *The Quarterly Journal of Economics* 137 (4): 2037–2105.
- Carrillo, Paul, Dave Donaldson, Dina Pomeranz, and Monica Singhal. 2023. *Misallocation in Firm Production: A Nonparametric Analysis Using Procurement Lotteries*. Working Paper, Working Paper Series 31311. National Bureau of Economic Research.
- Casey, Gregory, Stephie Fried, and Matthew Gibson. 2022. "Understanding Climate Damages: Consumption versus Investment." Federal Reserve Bank of San Francisco Working Paper 2022-21.
- Chen, Zhang. 2022. "Economic Growth and the Rise of Large Firms."
- Christidis, Nikolaos, Dann Mitchell, and Peter A. Stott. 2023. "Rapidly increasing likelihood of exceeding 50°C in parts of the Mediterranean and the Middle East due to human influence." *npj Climate and Atmospheric Science* 6, no. 1 (May 26, 2023): 45.
- Copernicus Climate Change Service. 2021. *CMIP6 climate projections*. Copernicus Climate Change Service (C3S) Climate Data Store (CDS).
- Copernicus Climate Change Service and Climate Data Store. 2018. *Seasonal forecast daily and subdaily data on single levels*.
- Cruz, José-Luis, and Esteban Rossi-Hansberg. 2023. *The Economic Geography of Global Warming*.
- David, Joel M., and Venky Venkateswaran. 2019. "The Sources of Capital Misallocation." *American Economic Review* 109 (7): 2531–67.
- David, Joel M., and David Zeke. 2021. *Risk-Taking, Capital Allocation and Optimal Monetary Policy*. Technical report. Federal Reserve Bank of Chicago. Accessed November 27, 2023.
- Dell, Melissa, Benjamin F Jones, and Benjamin A Olken. 2012. "Temperature Shocks and Economic Growth: Evidence from the Last Half Century." *American Economic Journal: Macroeconomics* 4 (3): 66–95.
- Dellink, Rob, Jean Chateau, Elisa Lanzi, and Bertrand Magné. 2017. "Long-term economic growth projections in the Shared Socioeconomic Pathways." *Global Environmental Change*.
- Deryugina, Tatyana, and Solomon Hsiang. 2017. *The Marginal Product of Climate*. Working Paper, Working Paper Series 24072. National Bureau of Economic Research.
- Deschênes, Olivier, and Michael Greenstone. 2011. "Climate Change, Mortality, and Adaptation: Evidence from Annual Fluctuations in Weather in the US." *American Economic Journal: Applied Economics* 3 (4): 152–185.
- Dundas, Steven J., and Roger H. von Haefen. 2020. "The Effects of Weather on Recreational Fishing Demand and Adaptation: Implications for a Changing Climate." *Journal of the Association of Environmental and Resource Economists* 7 (2): 209–242.

- Flynn, Joel P., and Karthik Sastry. 2023. *Attention Cycles*.
- Gopinath, Gita, Sebnem Kalemli-Ozcan, Loukas Karabarbounis, and Carolina Villegas-Sanchez. 2017. "Capital Allocation and Productivity in South Europe." *Quarterly Journal of Economics* 132 (4).
- Gorodnichenko, Yuriy, Debora Revoltella, Jan Svejnar, and Christoph T Weiss. 2018. *Resource misallocation in European firms: The role of constraints, firm characteristics and managerial decisions*. Technical report. National Bureau of Economic Research.
- Hausfather, Zeke, Kate Marvel, Gavin A. Schmidt, John W., and Mark Zelinka. 2022. "Climate Simulations: Recognize the 'Hot Model' Problem." *Nature*.
- Hsiang, Solomon. 2016. "Climate Econometrics." *Annual Review of Resource Economics* 8 (1): 43–75.
- Hsiang, Solomon M., and Amir S Jina. 2015. "Geography, depreciation, and growth." *American Economic Review*.
- Hsieh, Chang-Tai, and Peter J. Klenow. 2009. "Misallocation and Manufacturing TFP in China and India." *Quarterly Journal of Economics* 124 (4): 1403–1448.
- Kalemli-Ozcan, Sebnem, Bent Sorensen, Carolina Villegas-Sanchez, Vadym Volosovych, and Sevcan Yesiltas. 2015. *How to Construct Nationally Representative Firm Level Data from the Orbis Global Database: New Facts and Aggregate Implications*. Working Paper, Working Paper Series 21558. National Bureau of Economic Research.
- Krusell, Per, and Anthony A. Smith Jr. 1998. "Income and Wealth Heterogeneity in the Macroeconomy." *Journal of Political Economy* 106 (5): 867–896.
- Lemoine, Derek. 2018. *Estimating the Consequences of Climate Change from Variation in Weather*. Working Paper, Working Paper Series 25008. National Bureau of Economic Research.
- Mérel, Pierre, and Matthew Gammans. 2021. "Climate Econometrics: Can the Panel Approach Account for Long-Run Adaptation?" *American Journal of Agricultural Economics* 103 (4): 1207–1238.
- Midrigan, Virgiliu, and Daniel Yi Xu. 2014. "Finance and misallocation: Evidence from plant-level data." *American economic review* 104 (2): 422–458.
- Moscona, Jacob, and Karthik A Sastry. 2023. "Does directed innovation mitigate climate damage? evidence from us agriculture." *The Quarterly Journal of Economics* 138 (2): 637–701.
- Nath, Ishan. 2023. "Climate Change, The Food Problem, and the Challenge of Adaptation through Sectoral Reallocation."
- Nath, Ishan, Valerie Ramey, and Peter Klenow. 2023. "How Much Will Global Warming Cool Global Growth?"

- Oudin Åström, Daniel, Bertil Forsberg, Kristie L. Ebi, and Joacim Rocklöv. 2013. "Attributing mortality from extreme temperatures to climate change in Stockholm, Sweden." *Nature Climate Change* 3, no. 12 (December 1, 2013): 1050–1054.
- Piao, Shilong, Philippe Ciais, Yao Huang, Zehao Shen, Shushi Peng, Junsheng Li, Liping Zhou, Hongyan Liu, Yuecun Ma, Yihui Ding, et al. 2010. "The impacts of climate change on water resources and agriculture in China." *Nature*.
- Ponticelli, Jacopo, Qiping Xu, and Stefan Zeume. 2023. *Temperature and Local Industry Concentration*. Technical report w31533. National Bureau of Economic Research.
- Poschke, Markus. 2018. "The Firm Size Distribution across Countries and Skill-Biased Change in Entrepreneurial Technology." *American Economic Journal: Macroeconomics* 10 (3): 1–41.
- Restuccia, Diego, and Richard Rogerson. 2008. "Policy distortions and aggregate productivity with heterogeneous establishments." *Review of Economic dynamics* 11 (4): 707–720.
- Rudik, I., G. Lyn, W. Tan, and A. Ortiz-Bobea. 2021. *The Economic Effects of Climate Change in Dynamic Spatial Equilibrium*.
- Sabater, Joaquin Muñoz. 2019. *ERA5-Land monthly averaged data from 1950 to present*. Copernicus Climate Change Service (C3S) Climate Data Store (CDS).
- Schlenker, Wolfram, and Charles A. Taylor. 2021. "Market expectations of a warming climate." *Journal of Financial Economics*.
- Shiogama, Hideo, Shinichiro Fujimori, Tomoko Hasegawa, Michiya Hayashi, Yukiko Hirabayashi, Tomoo Ogura, Toshichika Iizumi, Kiyoshi Takahashi, and Toshihiko Takemura. 2023. "Important Distinctiveness of SSP3–7.0 for Use in Impact Assessments." *Nature Climate Change*.
- Shrader, Jeffrey. 2023. "Improving climate damage estimates by accounting for adaptation." Available at SSRN 3212073.
- Shrader, Jeffrey, Laura Bakkensen, and Derek Lemoine. 2023. "Fatal Errors: The Mortality Value of Accurate Weather Forecasts." National Bureau of Economic Research Working Paper.
- Somanathan, E., Rohini Somanathan, Anant Sudarshan, and Meenu Tewari. 2021. "The Impact of Temperature on Productivity and Labor Supply: Evidence from Indian Manufacturing" [in en]. *Journal of Political Economy* 129 (6). Accessed November 27, 2023.
- Sraer, David, and David Thesmar. 2023. "How to Use Natural Experiments to Estimate Misallocation." *American Economic Review* 113 (4): 906–38.
- Wang, Tingting, and Fubao Sun. 2022. "Global gridded GDP data set consistent with the shared socioeconomic pathways." *Scientific Data*.
- Wenz, Leonie, Robert Devon Carr, Noah Kögel, Maximilian Kotz, and Matthias Kalkuhl. 2023. "DOSE – Global data set of reported sub-national economic output." *Scientific Data* 10 (1): 425.

World Bank Climate Change Knowledge Portal. 2023.

Zhang, Peng, Olivier Deschenes, Kyle C Meng, and Junjie Zhang. 2018. "Temperature effects on productivity and factor reallocation: Evidence from a half million Chinese manufacturing plants." *Journal of Environmental Economics and Management* 88:1–17.

Zivin, Joshua Graff, and Matthew Neidell. 2014. "Temperature and the Allocation of Time: Implications for Climate Change." *Journal of Labor Economics* 32 (1): 1–26.

A Tables

Table A.1: Descriptive Table of Dataset by Country

Dataset	Country	Coverage	Number of Regions	Number of Firm-Year Obs
NBS China Industrial	China	1998-2007	325	2069100
India ASI	India	1998-2017	267	473646
	Austria	2004-2018	34	185029
	Belgium	1998-2018	44	781322
	Bulgaria	1998-2018	28	1439871
	Switzerland	2003-2018	3	1701
	Cyprus	2005-2018	1	17356
	Czech Republic	1998-2018	14	1425901
	Germany	1998-2018	346	765981
	Denmark	1999-2018	11	392015
	Estonia	1998-2018	5	791340
	Greece	1998-2018	44	342636
	Spain	1998-2018	52	12210663
	Finland	1998-2018	19	1909080
	France	1998-2018	96	15151185
	Croatia	1998-2018	21	1202515
BvD Orbis	Hungary	2004-2018	20	3095326
	Ireland	2000-2018	8	115344
	Italy	1998-2018	107	12083926
	Lithuania	1998-2018	10	129442
	Luxembourg	1998-2018	1	74287
	Latvia	2010-2018	6	533640
	Malta	2000-2018	1	21249
	Netherlands	1998-2018	36	201182
	Norway	1998-2018	12	2462277
	Poland	1998-2018	73	1207428
	Portugal	1998-2018	24	3882515
	Romania	1998-2018	42	4636047
	Sweden	1998-2018	21	3934403
	Slovenia	1998-2018	12	744495
	Slovakia	1998-2018	8	1008353
	United Kingdom	1998-2018	178	3537701

Table A.2: Effects of daily mean temperature bins on MRPK dispersion and TFP loss

	(1) σ_{mrpk}^2	(2) σ_{mrpk}^2	(3) σ_{mrpk}^2	(4) σ_{mrpk}^2	(5) Implied TFP Loss
< -5°C	0.0026*** (0.0010)	0.0025*** (0.0009)	0.0028*** (0.0009)	0.0012 (0.0023)	0.0935*** (0.0342)
-5 ~ 0°C	0.0015** (0.0006)	0.0013** (0.0006)	0.0016*** (0.0006)	0.0006 (0.0013)	0.0526** (0.0212)
0 ~ 5°C	0.0004 (0.0004)	0.0002 (0.0004)	0.0005 (0.0004)	-0.0019** (0.0009)	0.0131 (0.0146)
10 ~ 15°C	0.0009** (0.0004)	0.0008** (0.0004)	0.0008** (0.0004)	0.0036*** (0.0010)	0.0308** (0.0137)
15 ~ 20°C	0.0013** (0.0005)	0.0012** (0.0005)	0.0014*** (0.0005)	0.0045*** (0.0013)	0.0471** (0.0190)
20 ~ 25°C	0.0015** (0.0007)	0.0015** (0.0007)	0.0015** (0.0007)	0.0080*** (0.0020)	0.0546** (0.0259)
25 ~ 30°C	0.0028*** (0.0009)	0.0027*** (0.0009)	0.0027*** (0.0009)	0.0095*** (0.0021)	0.1008*** (0.0331)
> 30°C	0.0031*** (0.0011)	0.0030*** (0.0011)	0.0030*** (0.0011)	0.0090*** (0.0021)	0.1112*** (0.0401)
Controls	No	No	Yes	No	No
Region-Sector FE	Yes	Yes	Yes	Yes	Yes
Country-Year FE	Yes	No	Yes	Yes	Yes
Country-Sector-Year FE	No	Yes	No	No	No
1995 VA Weighted	No	No	No	Yes	No
Observations	124,065	123,518	124,065	123,847	124,065
R ²	0.876	0.903	0.878	0.897	0.876

Notes: Standard errors in parentheses. We cluster standard errors at the region level (NUTS3 level for European countries, province level for China, and first-level administrative divisions for India). Dependent variables in Columns 1 to 5 are the variance of log MRPK. Columns 1 to 5 show results from estimating equation 14 with controls in Column 3 weighted OLS regression in Column 4. Countries included are China, India, and 32 European countries.

* $p < 0.10$, ** $p < 0.05$, *** $p < 0.01$

Table A.3: Relative Firm Size and Firm MRPK

	(1)	(2)
< -5°C	0.00056** (0.00027)	0.00046* (0.00027)
-5 ~ 0°C	0.00019 (0.00016)	0.00012 (0.00015)
0 ~ 5°C	0.00015 (0.00013)	0.00010 (0.00013)
5 ~ 10°C	0.00005 (0.00014)	0.00001 (0.00013)
15 ~ 20°C	0.00004 (0.00011)	0.00002 (0.00011)
20 ~ 25°C	-0.00016 (0.00016)	-0.00024 (0.00016)
25 ~ 30°C	-0.00019 (0.00024)	-0.00028 (0.00024)
> 30°C	-0.00119*** (0.00045)	-0.00133*** (0.00044)
< -5°C × Relative Size		0.00089*** (0.00019)
-5 ~ 0°C × Relative Size		0.00077*** (0.00024)
0 ~ 5°C × Relative Size		0.00062*** (0.00022)
5 ~ 10°C × Relative Size		0.00041 (0.00027)
15 ~ 20°C × Relative Size		0.00021*** (0.00008)
20 ~ 25°C × Relative Size		0.00092*** (0.00017)
25 ~ 30°C × Relative Size		0.00098*** (0.00031)
> 30°C × Relative Size		0.00105** (0.00049)
Control: Relative Size	Yes	Yes
Firm FE	Yes	Yes
Country-Sector-Year FE	Yes	Yes
Observations	73350226	73350226
R ²	0.880	0.880

Notes: Standard errors in parentheses. We cluster standard errors at the region level (NUTS3 level for European countries, province level for China, and first-level administrative divisions for India). The dependent variables are the log MRPK. These results are obtained by estimating Equation 29. Column 2 presents results that interact with relative firm size, $\text{Relative Size}_{it}^{r,s} := \log K_{it}^{s,r} - \bar{\log K_{it}^{s,r}}$, which is standardized over the entire sample.

* $p < 0.10$, ** $p < 0.05$, *** $p < 0.01$

Table A.4: AC Installation and Firm MRPK

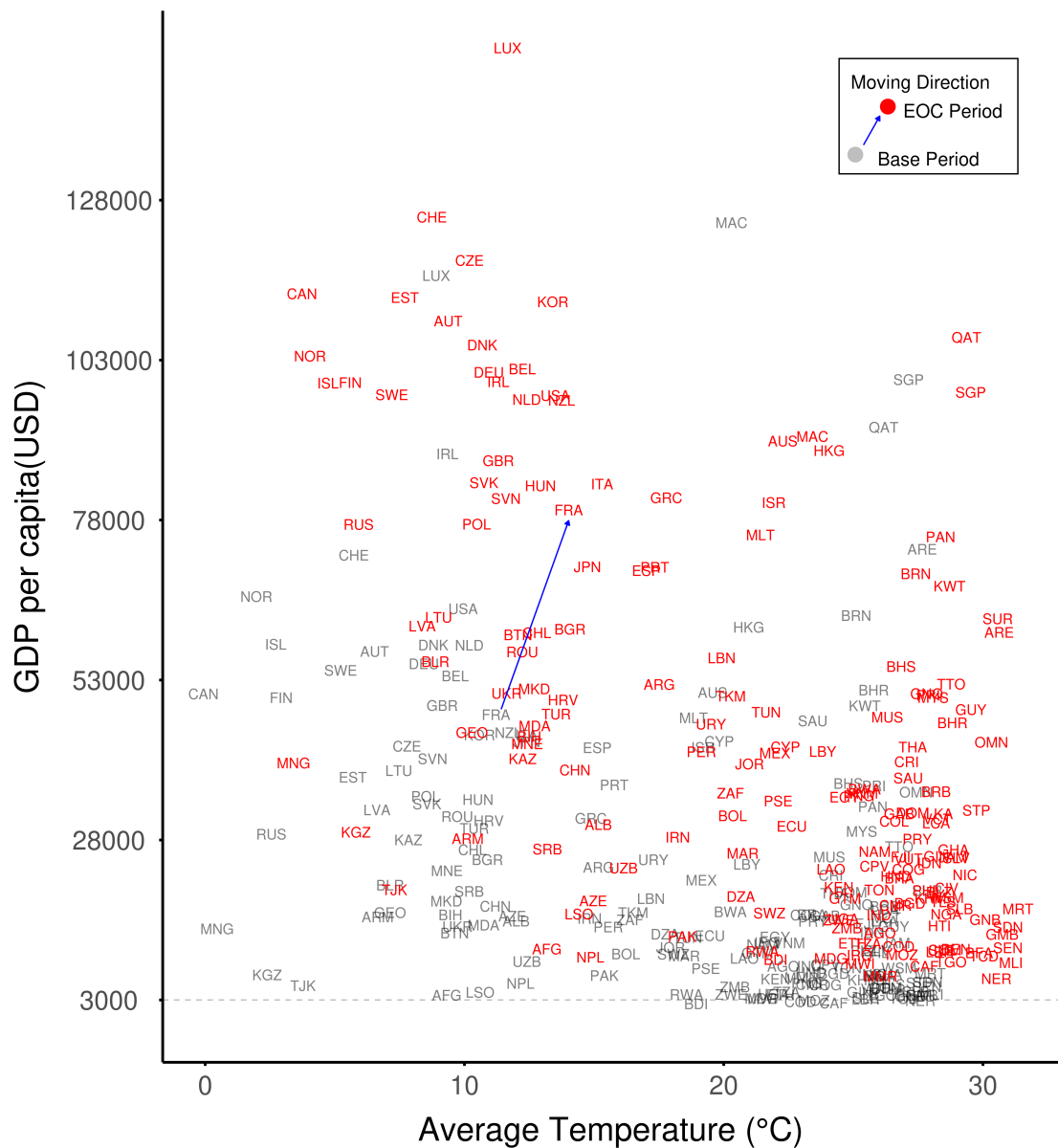
	(1)	(2)	(3)	(4)
< 10°C	0.00156 (0.00105)	0.00124 (0.00101)	0.00083 (0.00268)	0.00178 (0.00202)
10 ~ 15°C	0.00032 (0.00051)	0.00075 (0.00051)	-0.00064 (0.00085)	0.00131* (0.00075)
20 ~ 25°C	-0.00037 (0.00027)	-0.00015 (0.00024)	-0.00226*** (0.00080)	-0.00175*** (0.00061)
25 ~ 30°C	-0.00060* (0.00031)	-0.00035 (0.00028)	-0.00286*** (0.00083)	-0.00245*** (0.00065)
> 30°C	-0.00068* (0.00040)	-0.00044 (0.00035)	-0.00249** (0.00099)	-0.00224*** (0.00075)
< 10°C × AC Installation			0.00089 (0.00305)	-0.00051 (0.00243)
10 ~ 15°C × AC Installation			0.00110 (0.00095)	-0.00062 (0.00085)
15 ~ 20°C × AC Installation			0.00218*** (0.00081)	0.00185*** (0.00062)
20 ~ 25°C × AC Installation			0.00259*** (0.00087)	0.00240*** (0.00068)
25 ~ 30°C × AC Installation			0.00208** (0.00102)	0.00206*** (0.00077)
Control: $\ln K$	No	Yes	No	Yes
Firm FE	Yes	Yes	Yes	Yes
Sector-Year FE	Yes	Yes	Yes	Yes
Observations	532,425	532,425	532,425	532,425
R^2	0.748	0.815	0.748	0.815

Notes: Standard errors in parentheses. We cluster standard errors at the districts level. The dependent variables are the log MRPK. These results are obtained by estimating Equation 29. Column 1 and 3 present results that do not include control variables $\log K$.

* $p < 0.10$, ** $p < 0.05$, *** $p < 0.01$

B Figures

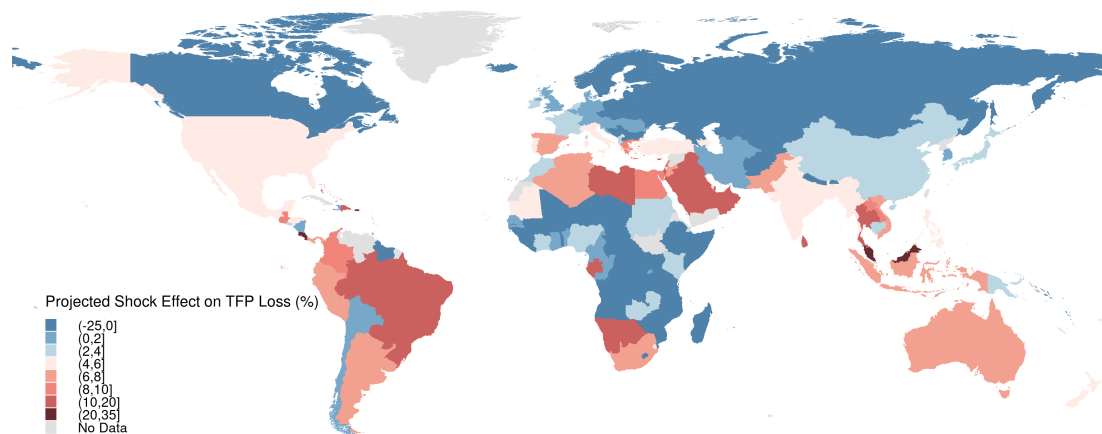
Figure B.1: Joint Evolution of Income and Average Temperature from 2019 to End of Century (under SSP3-7.0)



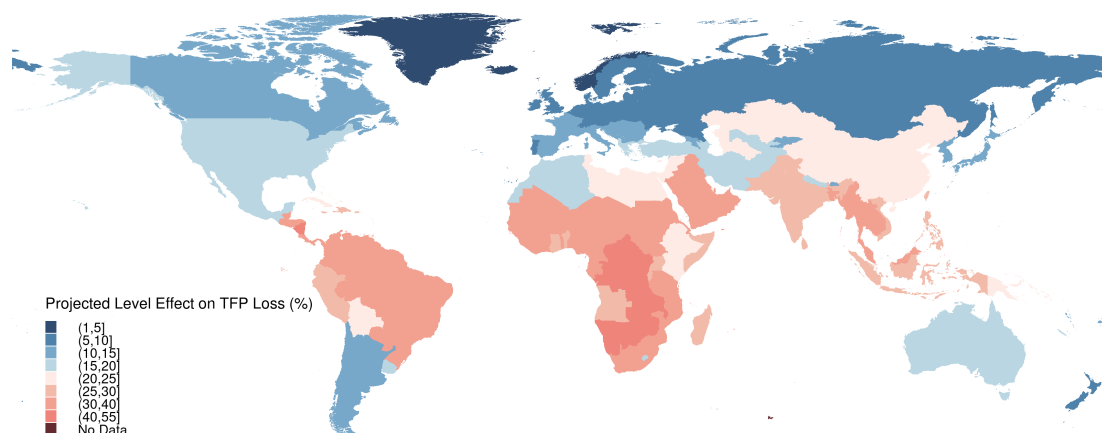
Notes: Grey texts represent the baseline period of the year 2019 and the red texts represent the End-of-the-Century (2081 - 2100). End-of-century projection comes from SSP3-7.0 projection. The graph shows the joint evolution of income per capita and average temperature for each country.

Figure B.2: Three Effects Contribution to Projected TFP Loss (SSP3-7.0)

(a) Shock Effects Projection



(b) Level Effects Projection



(c) Income Effects Projection

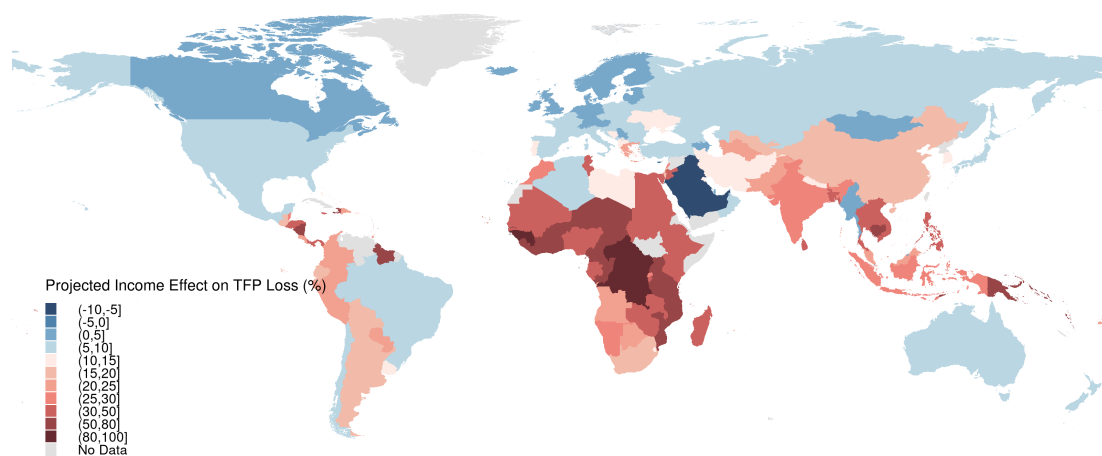


Figure B.3: Global TFP Loss Projection By Current Income Levels from Other Scenarios (Part 1)



Figure B.4: Global TFP Loss Projection By Current Income Levels from Other Scenarios (Part 2)



C Derivations of the Accounting Framework

We start by writing down the maximization problem:

$$\begin{aligned} \max_{P_{nit}, K_{nit}, L_{nit}} & (1 - \tau_{nit}^Y) P_{nit} \underbrace{A_{nit} K_{nit}^{\alpha_{Kn}} L_{nit}^{\alpha_{Ln}}}_{Y_{nit}} - (1 + \tau_{nit}^K) R_{nt} K_{nit} \\ & - (1 + \tau_{nit}^L) W_{nt} L_{nit} \\ \text{subject to : } & Y_{nit} = B_{nit} Y_{nt} \left[\frac{P_{nit}}{P_{nt}} \right]^{-\sigma_n}. \end{aligned} \quad (34)$$

The first order conditions associated with 4 gives us

$$MRPF_{nit} = \alpha_{F_n} \frac{\sigma_n - 1}{\sigma_n} \frac{P_{nit} Y_{nit}}{F_{nit}} = \frac{1 + \tau_{ni}^F(\tilde{T}_{rt}, \cdot)}{1 - \tau_{ni}^Y(\tilde{T}_{rt}, \cdot)} P_{nt}^F,$$

which is equation 5.

Plugging in Y_{nit} into the optimal CES demand, we get

$$\begin{aligned} P_{nit} &= \left(\frac{Y_{nit}}{Y_{nt} B_{nit}} \right)^{-\frac{1}{\sigma_n}} P_{nt} = B_{nit}^{\frac{1}{\sigma_n}} \left(\frac{A_{nit} K_{nit}^{\alpha_{Kn}} L_{nit}^{\alpha_{Ln}}}{Y_{nt}} \right)^{-\frac{1}{\sigma_n}} P_{nt} \\ &= B_{nit}^{\frac{1}{\sigma_n}} \left(\frac{A_{nit} (\frac{L_{nit}}{K_{nit}})^{\alpha_{Ln}} K_{nit}}{Y_{nt}} \right)^{-\frac{1}{\sigma_n}} P_{nt} \\ &= B_{nit}^{\frac{1}{\sigma_n}} \left(\frac{A_{nit} (\frac{K_{nit}}{L_{nit}})^{\alpha_{Kn}} L_{nit}}{Y_{nt}} \right)^{-\frac{1}{\sigma_n}} P_{nt} \end{aligned} \quad (35)$$

After some algebra, we arrive at:

$$\begin{aligned} F_{nit} &= \frac{B_{nit} A_{nit}^{\sigma_n - 1} (1 - \tau_{nit}^Y)^{\sigma_n}}{(1 + \tau_{nit}^F)(1 + \tau_{nit}^K)^{\alpha_{Kn}(\sigma_n - 1)} (1 + \tau_{nit}^L)^{\alpha_{Ln}(\sigma_n - 1)}} \\ &\cdot \left(\frac{\sigma_n - 1}{\sigma_n} \right)^{\sigma_n} \left(\frac{P_{nt}^F}{\alpha_{F_n}} \right)^{-1} \left(\frac{R_{nt}}{\alpha_{Kn}} \right)^{\alpha_{Kn}(1 - \sigma_n)} \left(\frac{W_{nt}}{\alpha_{Ln}} \right)^{\alpha_{Ln}(1 - \sigma_n)} P_{nt}^{\sigma_n} Y_{nt}, \end{aligned} \quad (36)$$

where $F \in \{K, L\}$.

Then we can write:

$$\begin{aligned} Y_{nit} &= A_{nit} K_{nit}^{\alpha_{Kn}} L_{nit}^{\alpha_{Ln}} = \frac{B_{nit} A_{nit}^{\sigma_n} (1 - \tau_{nit}^Y)^{\sigma_n}}{(1 + \tau_{nit}^{Ks})^{\alpha_{Kn}\sigma_n} (1 + \tau_{nit}^{Ls})^{\alpha_{Ln}\sigma_n}} \\ &\cdot \left(\frac{\sigma_n - 1}{\sigma_n} \right)^{\sigma_n} \left(\frac{\alpha_{Kn}}{R_{nt}} \right)^{\alpha_{Kn}\sigma_n} \left(\frac{\alpha_{Ln}}{W_{nt}} \right)^{\alpha_{Ln}\sigma_n} P_{nt}^{\sigma_n} Y_{nt} \end{aligned} \quad (37)$$

Using expressions for K_{si} and L_{si} , we can rewrite the total factor demand F_{nt} as,

$$F_{nt} = \int_0^{J_n} F_{nit} di = \left(\frac{\sigma_n - 1}{\sigma_n} \right)^{\sigma_n} \left(\frac{P_{nt}^F}{\alpha_{F_n}} \right)^{-1} \left(\frac{R_{nt}}{\alpha_{Kn}} \right)^{\alpha_{Kn}(1-\sigma_n)} \left(\frac{W_{nt}}{\alpha_{Ln}} \right)^{\alpha_{Ln}(1-\sigma_n)} P_{nt}^{\sigma_n} Y_{nt} \\ \cdot \int_0^{J_n} \frac{B_{nit} A_{nit}^{\sigma_n-1} (1 - \tau_{nit}^Y)^{\sigma_n}}{(1 + \tau_{nit}^K)^{\alpha_{Kn}(\sigma_n-1)+1} (1 + \tau_{nit}^L)^{\alpha_{Ln}(\sigma_n-1)}} di, \quad (38)$$

where $F \in \{K, L\}$.

C.1 Proof of Proposition 1.

The optimal factor input for firm i in the distorted economy, $F_{nit}, F \in \{K, L\}$.

$$F_{nit} = \frac{B_{nit} A_{nit}^{\sigma_n-1} (1 - \tau_{nit}^Y)^{\sigma_n}}{(1 + \tau_{nit}^F) (1 + \tau_{nit}^K)^{\alpha_{Kn}(\sigma_n-1)} (1 + \tau_{nit}^L)^{\alpha_{Ln}(\sigma_n-1)}} \\ \cdot \left(\frac{\sigma_n - 1}{\sigma_n} \right)^{\sigma_n} \left(\frac{P_{nt}^F}{\alpha_{F_n}} \right)^{-1} \left(\frac{R_{nt}}{\alpha_{Kn}} \right)^{\alpha_{Kn}(1-\sigma_n)} \left(\frac{W_{nt}}{\alpha_{Ln}} \right)^{\alpha_{Ln}(1-\sigma_n)} P_{nt}^{\sigma_n} Y_{nt} \quad (39)$$

We can then write the share of factor allocation for the firm i in the distorted economy as:

$$\frac{F_{nit}}{F_{nt}} = \frac{F_{nit}}{\int_0^{J_n} F_{nit} di} = \frac{B_{nit} A_{nit}^{\sigma_n-1} (1 - \tau_{nit}^Y)_n^\sigma}{(1 + \tau_{nit}^K)^{\alpha_{Kn}(\sigma_n-1)+1} (1 + \tau_{nit}^L)^{\alpha_{Ln}(\sigma_n-1)}} \\ \cdot \left(\frac{\sigma_n - 1}{\sigma_n} \right)^{\sigma_n} \left(\frac{P_{nt}^F}{\alpha_{F_n}} \right)^{-1} \left(\frac{R_{nt}}{\alpha_{Kn}} \right)^{\alpha_{Kn}(1-\sigma_n)} \left(\frac{W_{nt}}{\alpha_{Ln}} \right)^{\alpha_{Ln}(1-\sigma_n)} P_{nt}^{\sigma_n} Y_{nt} \\ \cdot \frac{1}{\int_0^{J_n} \frac{B_{nit} A_{nit}^{\sigma_n-1} (1 - \tau_{nit}^Y)_n^\sigma}{(1 + \tau_{nit}^K)^{\alpha_{Kn}(\sigma_n-1)+1} (1 + \tau_{nit}^L)^{\alpha_{Ln}(\sigma_n-1)}} di} \\ \cdot \frac{1}{\left(\frac{\sigma_n - 1}{\sigma_n} \right)^{\sigma_n} \left(\frac{P_{nt}^F}{\alpha_{F_n}} \right)^{-1} \left(\frac{R_{nt}}{\alpha_{Kn}} \right)^{\alpha_{Kn}(1-\sigma_n)} \left(\frac{W_{nt}}{\alpha_{Ln}} \right)^{\alpha_{Ln}(1-\sigma_n)} P_{nt}^{\sigma_n} Y_{nt}} \quad (40)$$

The efficient input $F_{nit}^* F \in \{K, L\}$, when all distortions go to zero, can be written as:

$$F_{nit}^* = B_{nit} A_{nit}^{\sigma_n-1} \cdot \left(\frac{\sigma_n - 1}{\sigma_n} \right)^{\sigma_n} \left(\frac{P_{nt}^* F}{\alpha_{F_n}} \right)^{-1} \left(\frac{R_{nt}^*}{\alpha_{Kn}} \right)^{\alpha_{Kn}(1-\sigma_n)} \left(\frac{W_{nt}^*}{\alpha_{Ln}} \right)^{\alpha_{Ln}(1-\sigma_n)} P_{nt}^{*\sigma_n} Y_{nt} \quad (41)$$

Similarly, in an efficient economy we have:

$$\frac{F_{nit}^*}{F_{nt}} = \frac{F_{nit}^*}{\int_0^{J_n} F_{nit}^* di} \\ = B_{nit} A_{nit}^{\sigma_n-1} \cdot \left(\frac{\sigma_n - 1}{\sigma_n} \right)^{\sigma_n} \left(\frac{P_{nt}^* F}{\alpha_{F_n}} \right)^{-1} \left(\frac{R_{nt}^*}{\alpha_{Kn}} \right)^{\alpha_{Kn}(1-\sigma_n)} \left(\frac{W_{nt}^*}{\alpha_{Ln}} \right)^{\alpha_{Ln}(1-\sigma_n)} P_{nt}^{*\sigma_n} Y_{nt} \\ \cdot \frac{1}{\left(\frac{\sigma_n - 1}{\sigma_n} \right)^{\sigma_n} \left(\frac{P_{nt}^* F}{\alpha_{F_n}} \right)^{-1} \left(\frac{R_{nt}^*}{\alpha_{Kn}} \right)^{\alpha_{Kn}(1-\sigma_n)} \left(\frac{W_{nt}^*}{\alpha_{Ln}} \right)^{\alpha_{Ln}(1-\sigma_n)} P_{nt}^{*\sigma_n} Y_{nt} \int_0^{J_n} B_{nit} A_{nit}^{\sigma_n-1} di} \quad (42)$$

Next, we compute the ratio:

$$\frac{F_{nit}/F_{nt}}{F_{nit}^*/F_{nt}} = \frac{(1 - \tau_{nit}^Y)^{\sigma_n}}{(1 + \tau_{nit}^F)(1 + \tau_{nit}^K)^{\alpha_{Kn}(\sigma_n-1)}(1 + \tau_{nit}^L)^{\alpha_{Ln}(\sigma_n-1)}} \cdot \frac{\int_0^{J_n} B_{nit} A_{nit}^{\sigma_n-1} di}{\int_0^{J_n} \frac{B_{nit} A_{nit}^{\sigma_n-1} (1 - \tau_{nit}^Y)_n^\sigma}{(1 + \tau_{nit}^K)^{\alpha_{Kn}(\sigma_n-1)} (1 + \tau_{nit}^L)^{\alpha_{Ln}(\sigma_n-1)}} di} \quad (43)$$

The integral is a constant independent of firm i , by defining

$$C_{Fnt} := \frac{\int_0^{J_n} B_{nit} A_{nit}^{\sigma_n-1} di}{\int_0^{J_n} \frac{B_{nit} A_{nit}^{\sigma_n-1} (1 - \tau_{nit}^Y)_n^\sigma}{(1 + \tau_{nit}^K)^{\alpha_{Kn}(\sigma_n-1)} (1 + \tau_{nit}^L)^{\alpha_{Ln}(\sigma_n-1)}} di},$$

we therefore simplify the expression further:

$$\frac{F_{nit}/F_{nt}}{F_{nit}^*/F_{nt}} = \frac{(1 - \tau_{nit}^Y)^{\sigma_n}}{(1 + \tau_{nit}^F)(1 + \tau_{nit}^K)^{\alpha_{Kn}(\sigma_n-1)}(1 + \tau_{nit}^L)^{\alpha_{Ln}(\sigma_n-1)}} \cdot C_{Fnt}. \quad (44)$$

Taking logs, we yield the expression:

$$\log\left(\frac{F_{nit}}{F_{nit}^*}\right) - \log\left(\frac{F_{nt}}{F_{nt}^*}\right) = -\log(1 + \tau_{nit}^F) + \sigma_n \log(1 - \tau_{nit}^Y) - (\sigma_n - 1) \sum_{F'=\{K,L\}} \alpha_{F'_n} \log(1 + \tau_{ni}^{F'}) + \log(C_{Fnt}) \quad (45)$$

which can be simplified into

$$\log\left(\frac{F_{nit}}{F_{nit}^*}\right) = -\log(1 + \tau_{nit}^F) + \sigma_n \log(1 - \tau_{nit}^Y) - (\sigma_n - 1) \sum_{F'=\{K,L\}} \alpha_{F'_n} \log(1 + \tau_{ni}^{F'}) + \log(C_{Fnt}), \quad (46)$$

where $\log\left(\frac{F_{nt}}{F_{nt}^*}\right) = 0$ and the above is Equation 6 in the text.

C.2 Proof of Proposition 2

Plug expression of F_{nt} into $\text{TFP}_{nt} := \frac{Y_{nt}}{K_{nt}^{\alpha_{Kn}} L_{nt}^{\alpha_{Ln}}}$, we get:

$$\begin{aligned}
\text{TFP}_{nt} &= \frac{Y_{nt}}{P_{nt}^{\sigma_n} Y_{nt}} \\
&\cdot \frac{1}{\left(\frac{\sigma_n - 1}{\sigma_n} \right)^{\sigma_n} \left(\frac{R_{nt}}{\alpha_{Kn}} \right)^{-\alpha_{Kn}} \left(\frac{W_{nt}}{\alpha_{Ln}} \right)^{-\alpha_{Ln}} \left(\frac{R_{nt}}{\alpha_{Kn}} \right)^{\alpha_{Kn}(1-\sigma_n)} \left(\frac{W_{nt}}{\alpha_{Ln}} \right)^{\alpha_{Ln}(1-\sigma_n)}} \\
&\cdot \frac{1}{\left(\int_0^{J_n} \frac{B_{nit} A_{nit}^{\sigma_n-1} (1-\tau_{nit}^Y)_n^\sigma}{(1+\tau_{nit}^K)^{\alpha_{Kn}(\sigma_n-1)+1} (1+\tau_{nit}^L)^{\alpha_{Ln}(\sigma_n-1)}} di \right)^{\alpha_{Kn}}} \\
&\cdot \frac{1}{\left(\int_0^{J_n} \frac{B_{nit} A_{nit}^{\sigma_n-1} (1-\tau_{nit}^Y)_n^\sigma}{(1+\tau_{nit}^K)^{\alpha_{Kn}(\sigma_n-1)} (1+\tau_{nit}^L)^{\alpha_{Ln}(\sigma_n-1)+1}} di \right)^{\alpha_{Ln}}} \\
&= \left\{ \frac{1}{P_{nt}} \frac{\sigma_n}{\sigma_n - 1} \left(\frac{R_{nt}}{\alpha_{Kn}} \right)^{\alpha_{Kn}} \left(\frac{W_{nt}}{\alpha_{Ln}} \right)^{\alpha_{Ln}} \right\}^{\sigma_n} \\
&\cdot \frac{1}{\left(\int_0^{J_n} \frac{B_{nit} A_{nit}^{\sigma_n-1} (1-\tau_{nit}^Y)_n^\sigma}{(1+\tau_{nit}^K)^{\alpha_{Kn}(\sigma_n-1)+1} (1+\tau_{nit}^L)^{\alpha_{Ln}(\sigma_n-1)}} di \right)^{\alpha_{Kn}}} \\
&\cdot \frac{1}{\left(\int_0^{J_n} \frac{B_{nit} A_{nit}^{\sigma_n-1} (1-\tau_{nit}^Y)_n^\sigma}{(1+\tau_{nit}^K)^{\alpha_{Kn}(\sigma_n-1)} (1+\tau_{nit}^L)^{\alpha_{Ln}(\sigma_n-1)+1}} di \right)^{\alpha_{Ln}}} \tag{47}
\end{aligned}$$

Finally, using the CES aggregator and expressions for Y_{nit} , we can obtain Y_{nt} :

$$\begin{aligned}
Y_{nt} &= \left[\int_0^{J_n} Y_{nit}^{\frac{\sigma_n - 1}{\sigma_n}} di \right]^{\frac{\sigma_n}{\sigma_n - 1}} = \left(\frac{\sigma_n - 1}{\sigma_n} \right)^{\sigma_n} \left(\frac{\alpha_{Kn}}{R_{nt}} \right)^{\alpha_{Kn}\sigma_n} \left(\frac{\alpha_{Ln}}{W_{nt}} \right)^{\alpha_{Ln}\sigma_n} P_{nt}^{\sigma_n} Y_{nt} \\
&\cdot \left[\int_0^{J_n} \left(\frac{B_{nit} A_{nit}^{\sigma_n} (1 - \tau_{nit}^Y)^{\sigma_n}}{(1 + \tau_{nit}^K)^{\alpha_{Kn}\sigma_n} (1 + \tau_{nit}^L)^{\alpha_{Ln}\sigma_n}} \right)^{\frac{\sigma_n - 1}{\sigma_n}} di \right]^{\frac{\sigma_n}{\sigma_n - 1}} \tag{48}
\end{aligned}$$

Cancelling out Y_{nt} on both side, we can solve for the inverse for the region-sector price index as:

$$\begin{aligned}
\frac{1}{P_{nt}} &= \left(\frac{\sigma_n - 1}{\sigma_n} \right) \left(\frac{\alpha_{Kn}}{R_{nt}} \right)^{\alpha_{Kn}} \left(\frac{\alpha_{Ln}}{W_{nt}} \right)^{\alpha_{Ln}} \\
&\cdot \left[\int_0^{J_n} \left(\frac{B_{nit}^{\frac{1}{\sigma_n}} A_{nit} (1 - \tau_{nit}^Y)}{(1 + \tau_{nit}^K)^{\alpha_{Kn}} (1 + \tau_{nit}^L)^{\alpha_{Ln}}} \right)^{\sigma_n - 1} di \right]^{\frac{1}{\sigma_n - 1}} \tag{49}
\end{aligned}$$

Pluggin in $\frac{1}{P_{nt}}$ back into equation 47, we get:

$$\begin{aligned} \text{TFP}_{nt} &= \left[\int_0^{J_n} \left(\frac{B_{nit}^{\frac{1}{\sigma_n}} A_{nit} (1 - \tau_{nit}^Y)}{(1 + \tau_{nit}^K)^{\alpha_{Kn}} (1 + \tau_{nit}^L)^{\alpha_{Ln}}} \right)^{\sigma_n-1} \right]^{\frac{\sigma_n}{\sigma_n-1}} \\ &\cdot \frac{1}{\left(\int_0^{J_n} \frac{B_{nit} A_{nit}^{\sigma_n-1} (1 - \tau_{nit}^Y)_n^\sigma}{(1 + \tau_{nit}^K)^{\alpha_{Kn}(\sigma_n-1)+1} (1 + \tau_{nit}^L)^{\alpha_{Ln}(\sigma_n-1)}} di \right)^{\alpha_{Kn}}} \\ &\cdot \frac{1}{\left(\int_0^{J_n} \frac{B_{nit} A_{nit}^{\sigma_n-1} (1 - \tau_{nit}^Y)_n^\sigma}{(1 + \tau_{nit}^K)^{\alpha_{Kn}(\sigma_n-1)} (1 + \tau_{nit}^L)^{\alpha_{Ln}(\sigma_n-1)+1}} di \right)^{\alpha_{Ln}}} \end{aligned} \quad (50)$$

Taking log to both sides, we get:

$$\begin{aligned} \log \text{TFP}_{nt} &= \frac{\sigma_n}{\sigma_n - 1} \log \int_0^{J_n} \left(\frac{B_{nit}^{\frac{1}{\sigma_n}} A_{nit} (1 - \tau_{nit}^Y)}{(1 + \tau_{nit}^K)^{\alpha_{Kn}} (1 + \tau_{nit}^L)^{\alpha_{Ln}}} \right)^{\sigma_n-1} di \\ &- \alpha_{Kn} \log \int_0^{J_n} \frac{B_{nit} A_{nit}^{\sigma_n-1} (1 - \tau_{nit}^Y)_n^\sigma}{(1 + \tau_{nit}^K)^{\alpha_{Kn}(\sigma_n-1)+1} (1 + \tau_{nit}^L)^{\alpha_{Ln}(\sigma_n-1)}} di \\ &- \alpha_{Ln} \log \int_0^{J_n} \frac{B_{nit} A_{nit}^{\sigma_n-1} (1 - \tau_{nit}^Y)_n^\sigma}{(1 + \tau_{nit}^K)^{\alpha_{Kn}(\sigma_n-1)} (1 + \tau_{nit}^L)^{\alpha_{Ln}(\sigma_n-1)+1}} di \end{aligned} \quad (51)$$

Under the assumption that B_{nit} , A_{nit} , $1 + \tau_{nit}^K$ and $1 + \tau_{nit}^L$ follow a joint log-normal distribution, and all firm-level fundamentals $\{B_{nit}, A_{nit}, \tau_{nit}^Y, \tau_{nit}^F\}$ to be firm-specific and smooth functions of $(\tilde{\mathbf{T}}_{rt}, \tilde{\mathbf{X}}_{nt}, \tilde{\mathbf{Z}}_{nit})$:

$$\begin{aligned} \log \text{TFP}_n(\tilde{\mathbf{T}}_{rt}, \cdot) &= \underbrace{\frac{1}{\sigma_n - 1} \log \mathbb{E}_i \left[B_{ni}(\tilde{\mathbf{T}}_{rt}, \cdot) \left(A_{ni}(\tilde{\mathbf{T}}_{rt}, \cdot) \right)^{\sigma_n-1} \right]}_{\text{Technology}(\log \text{TFP}_n^E)} - \underbrace{\frac{\sigma_n}{2} \text{var}_{\log(1 - \tau_{ni}^Y)}(\tilde{\mathbf{T}}_{rt}, \cdot)}_{\text{Output Wedge Dispersion}} \\ &- \underbrace{\sum_{F \in \{K, L\}} \frac{\alpha_{Fn} + \alpha_{Fn}^2 (\sigma_n - 1)}{2} \text{var}_{\log(1 + \tau_{ni}^F)}(\tilde{\mathbf{T}}_{rt}, \cdot)}_{\text{Factor Wedge Dispersion}} \\ &+ \underbrace{\sigma_n \sum_{F \in \{K, L\}} \alpha_{Fn} \text{cov}_{\log(1 - \tau_{ni}^Y), \log(1 + \tau_{ni}^F)}(\tilde{\mathbf{T}}_{rt}, \cdot)}_{\text{Output-Factor Mixed Distortion}} \\ &- \underbrace{(\sigma_n - 1) \alpha_{Kn} \alpha_{Ln} \text{cov}_{\log(1 + \tau_{ni}^K), \log(1 + \tau_{ni}^L)}(\tilde{\mathbf{T}}_{rt}, \cdot)}_{\text{Factor Mixed Distortion}} \end{aligned} \quad (52)$$

which is the Equation 10 in the text.

D Additional Empirical Results

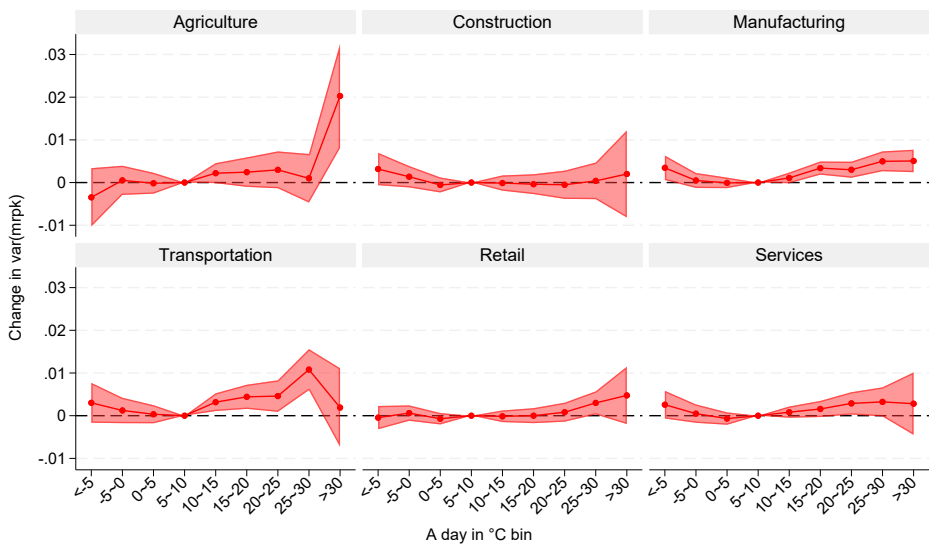
D.1 Heterogeneous Effect Across Sectors

We further investigate how temperature might also pose differential effects on different sectors by estimating the specification in equation 14 for each sector's MRPK dispersion.

Figure D.1 presents the estimation for the six most common sectors in our sample. Consistent with the findings in Rudik et al. (2021) and Cruz and Rossi-Hansberg (2023), our study also identifies the agricultural sector as particularly susceptible to heat. We find that an additional day with temperatures exceeding 30°C impacts the dispersion of MRPK in agriculture by 2 log points, translating to 0.3% annual TFP loss. This heightened sensitivity might be primarily due to the heterogeneity of crops' sensitivity to weather and climate conditions. Extreme heat can adversely impact different crop yields and sales differentially, thus influencing firm productivity and MRPK dispersion within the sector.

The manufacturing sector is particularly susceptible to temperature, where extreme cold and hot conditions lead to increased MRPK dispersion (Zhang et al. 2018). This sensitivity in manufacturing might be attributed to the impact of extreme temperatures on production processes and worker productivity. Regarding the retail and service sectors, the U-shaped pattern in response to temperature variations is still observed and quantitatively important, although the results are less statistically significant. Interestingly, when using spatial variations in trade patterns to identify the productivity damage functions, Rudik et al. (2021) also find that the effect of heat on productivity loss is most prominent in agriculture sectors, followed by manufacturing sectors, and found a null effect in services, which is consistent with our findings on misallocation across sectors.

Figure D.1: Climate-induced Misallocation Across Major Sectors



Notes: The graphs plot the estimated effect of exposure to daily mean temperatures on MRPK dispersion by estimating Equation 14 for six sectors, respectively. The graphs include 90% confidence intervals, and standard errors are clustered at the regional level.

E Firm Dynamics Model

E.1 Lemma 1 TFP volatility

The difference between TFP volatility and expected TFP volatility is:

$$\hat{a}_{it} - \mathbb{E}_{t-1}[\hat{a}_{it}] = (T_t - T^*)\hat{\xi}_{it} + \hat{\eta}_t^T \hat{\beta}_i + \hat{\varepsilon}_{it} + c \left((T_t - T^*)^2 - \mathbb{E}_{t-1}[(T_t - T^*)^2] \right) \quad (53)$$

After some algebra, we achieve:

$$\begin{aligned} \hat{a}_{it} - \mathbb{E}_{t-1}[\hat{a}_{it}] &= (T_t - T^*)\hat{\xi}_{it} + \hat{\eta}_t^T \hat{\beta}_i + \hat{\varepsilon}_{it} \\ &\quad - c(\eta_t^T)^2 - c\sigma_\eta^2 + 2c(T_t - T^*)\eta_t^T \end{aligned} \quad (54)$$

TFP Volatility, $\text{Var}(\hat{a}_{it} - \mathbb{E}_{t-1}[\hat{a}_{it}])$, therefore can be written as:

$$\text{Var}(\hat{a}_{it} - \mathbb{E}_{t-1}[\hat{a}_{it}]) = (T_t - T^*)^2 \sigma_{\hat{\xi}}^2 + \eta_t^T \sigma_{\hat{\beta}}^2 + \sigma_{\hat{\varepsilon}}^2, \quad (55)$$

which is equation 55 in the paper.

E.2 Solution

The static input choice solves

$$\max_{N_{it}} \exp \left(\hat{\beta}_{it} (T_t - T^*) \right) \hat{Z}_{it} K_{it}^{\alpha_K} N_{it}^{\alpha_N} - W_t N_{it},$$

with the associated first order condition:

$$\begin{aligned} P_{it} Y_{it} &= \hat{A}_{it} K_{it}^{\alpha_K} N_{it}^{\alpha_N} \\ &= e^{\hat{\beta}_{it}(T_t - T^*) + \hat{z}_{it}} K_{it}^{\alpha_K} N_{it}^{\alpha_N} \end{aligned} \quad (56)$$

where $\alpha_F = (1 - \frac{1}{\sigma})\tilde{\alpha}_F$, $\forall F \in \{K, N\}$ and $\hat{A}_{it} = B_{it}^{\frac{1}{\sigma}} (\tilde{A}_{it})^{(1-\frac{1}{\sigma})}$ is the revenue-based productivity (TFPR).

Substituting for the wage with $W_t = \bar{W} \exp(\chi(T_t - T^*))$ and rearranging gives profits

$$\Pi_{it} = G A_{it} K_{it}^\alpha := G \exp(\beta_{it}(T_t - T^*) + z_{it}) K_{it}^\alpha, \quad (57)$$

where $G := \bar{W}^{-\frac{\alpha_N}{1-\alpha_N}} \alpha_N^{\frac{\alpha_N}{1-\alpha_N}} (1 - \alpha_N)$, $z_{it} = \frac{1}{1-\alpha_N} \hat{z}_{it}$, and $\alpha = \frac{\alpha_K}{1-\alpha_N}$, which is equation 22 in the text.

The firm's dynamic capital investment problem then takes the form:

$$\begin{aligned} V(T_t, Z_{it}, K_{it}) &= \max_{K_{it+1}} G \exp(\beta_{it}(T_t - T^*) + z_{it}) K_{it}^\alpha - K_{it+1} + (1 - \delta) K_{it} \\ &\quad + \frac{1}{1+r} \mathbb{E}_t [V(T_{t+1}, Z_{it+1}, K_{it+1})], \end{aligned}$$

Policy function. The first order and envelope conditions associated with (E.2) give the Euler equation:

$$1 = \underbrace{\frac{1}{1+r}}_{\text{Discount Factor}} \left(\underbrace{\alpha G K_{it+1}^{\alpha-1} \mathbb{E}_t [\exp(z_{it+1} + \beta_{it+1}(T_{t+1} - T^*))]}_{\text{Expected Value of Marginal Profits of Capital}} + \underbrace{(1-\delta)}_{\text{Value of Undepreciated Capital}} \right). \quad (58)$$

Compute the expectation and rearrange Euler to get:

$$\begin{aligned} K_{it+1}^{1-\alpha} &= \frac{\alpha G}{r+\delta} \mathbb{E}_t [\exp(z_{it+1} + \beta_{it+1}(T_{t+1} - T^*))] = \frac{\alpha G}{r+\delta} \mathbb{E}_t [\exp(a_{it+1})] \\ &= \frac{\alpha G}{r+\delta} \exp \left(\mathbb{E}_t (a_{it+1}) + \text{Var}_t (a_{it+1}) \right) \end{aligned} \quad (59)$$

After taking logs on both sides, we get the policy function in linearized form:

$$k_{it+1} = \frac{1}{1-\alpha} \left(\mathbb{E}_t [a_{it+1}] + \text{Var} [a_{it+1}] \right) + k_0$$

where $k_0 = \frac{1}{1-\alpha} \left(\log \left[\frac{\alpha G}{r+\delta} \right] \right)$.

We ignore the high-order risk-adjusted terms and rewrite policy function in linearized form as:

$$\begin{aligned} k_{it+1} &\approx \frac{1}{1-\alpha} \mathbb{E}_t [a_{it+1}] \\ &= \frac{1}{1-\alpha} \left(\frac{1}{1-\alpha_N} \mathbb{E}_t [\hat{a}_{it+1}] - \frac{\alpha_N}{1-\alpha_N} \mathbb{E}_t [w_{t+1} - \bar{w}] \right) + k_0 \\ &= \frac{1}{1-\alpha} \left(\frac{1}{1-\alpha_N} (\mathbb{E}_t [\hat{z}_{it+1}] + \mathbb{E}_t [\hat{\beta}_{it+1}(T_{t+1} - T^*)]) - \frac{\alpha_N \chi}{1-\alpha_N} \mathbb{E}_t [T_{t+1} - T^*] \right) + k_0, \end{aligned} \quad (60)$$

which is expression 24 in the text. Plugging in the values in expectations, we finally achieve the policy function for capital:

$$k_{it+1} = \frac{1}{1-\alpha} \left(\rho_z z_{it} + \beta_i (\rho_T T_t + (1-\rho_T) \bar{T} - T^*) + \frac{c}{1-\alpha_N} \left[(\rho_T T_t + (1-\rho_T) \bar{T} - T^*)^2 + \sigma_\eta^2 \right] \right) + k_0 \quad (61)$$

E.3 MRPK Dispersion

We know mrpk can be written as:

$$mrpk_{it} = a_{it} + (\alpha - 1)k_{it} + \log(\alpha_K \bar{G})^{52} \quad (62)$$

Plugging in our policy function we get:

$$\begin{aligned}
mrpk_{it} &= (a_{it} - \mathbb{E}_{it-1}[a_{it}]) + \log(r + \delta) \\
&= \frac{1}{1 - \alpha_N} \left\{ (\hat{a}_{it} - \mathbb{E}_{it-1}[\hat{a}_{it}]) - \chi \alpha_N (T_t - \mathbb{E}_{t-1}[T_t]) \right\} + \log(r + \delta) \\
&= \frac{1}{1 - \alpha_N} \left(\underbrace{\hat{\beta}_i \eta_t^T}_{\text{Unexpected T Shock on Productivity}} + \underbrace{\hat{\xi}_{it}(T_t - T^*)}_{\text{Unexpected Damage Sensitivity}} - c(\eta_t^T)^2 - c\sigma_\eta^2 + 2c(T_t - T^*)\eta_t^T - \underbrace{\chi \alpha_N \eta_t^T}_{\text{Unexpected T Shock on Wage}} + \hat{\varepsilon}_{it} \right) + \log(r + \delta)
\end{aligned} \tag{63}$$

After variance calculation we obtain:

$$\begin{aligned}
\sigma_{mrpk,(r,s),t}^2 &= \left(\frac{1}{1 - \alpha_N} \right)^2 \text{Var}(\hat{a}_{nit} - \mathbb{E}_{t-1}[\hat{a}_{nit}]) \\
&= \left(\frac{1}{1 - \alpha_N} \right)^2 \left[\underbrace{(T_{r,t} - T^*)^2 \sigma_{\xi,(r,s)}^2}_{\text{Damage Uncertainty Channel}} + \underbrace{\eta_{r,t}^T \sigma_{\beta,(r,s)}^2}_{\text{Climate Uncertainty Channel}} + \sigma_{\varepsilon,(r,s)}^2 \right]
\end{aligned} \tag{64}$$

E.4 Aggregation

We first obtain optimaltiy condition for labor from the production function:

$$\begin{aligned}
P_{it} Y_{it} &= \hat{A}_{it} K_{it}^{\alpha_K} N_{it}^{\alpha_N} \\
&= e^{\hat{\beta}_{it}(T_t - T^*) + \hat{z}_{it}} K_{it}^{\alpha_K} N_{it}^{\alpha_N}
\end{aligned} \tag{65}$$

where $\alpha_F = (1 - \frac{1}{\sigma})\tilde{\alpha}_F$, $\forall F \in \{K, N\}$ and $\hat{A}_{it} = B_{it}^{\frac{1}{\sigma}} (\tilde{A}_{it})^{(1-\frac{1}{\sigma})}$ is the revenue-based productivity (TFPR).

Firm's optimality condition for labor is:

$$N_{it} = \left(\frac{\alpha_N e^{\hat{\beta}_{it}(T_t - T^*) + \hat{z}_{it}} K_{it}^{\alpha_K}}{W_t} \right)^{\frac{1}{1 - \alpha_N}}$$

We plug in

$$W_t = \bar{W} \exp(\chi(T_t - T^*)),$$

and obtain the following:

$$N_{it} = \left(\frac{\alpha_N}{\bar{W}} e^{(\hat{\beta}_{it} - \chi)(T_t - T^*) + \hat{z}_{it}} K_{it}^{\alpha_K} \right)^{\frac{1}{1 - \alpha_N}}$$

Labor market clearing implies

$$\begin{aligned}
N_t &= \int N_{it} di = \int \left(\frac{\alpha_N}{\bar{W}} e^{(\hat{\beta}_{it} - \chi)(T_t - T^*) + \hat{z}_{it}} K_{it}^{\alpha_K} \right)^{\frac{1}{1 - \alpha_N}} di \\
&= \left(\frac{\alpha_N}{\bar{W}} \right)^{\frac{1}{1 - \alpha_N}} e^{\frac{-\chi}{1 - \alpha_N}(T_t - T^*)} \int e^{\frac{1}{1 - \alpha_N} \hat{\beta}_{it}(T_t - T^*) + \hat{z}_{it}} K_{it}^\theta di,
\end{aligned}$$

where $z_{it} = \frac{\hat{z}_{it}}{1-\alpha_N}$, $\theta = \frac{\alpha_K}{1-\alpha_N}$.

so that

$$\left(\frac{\alpha_N}{W}\right)^{\frac{\alpha_N}{1-\alpha_N}} e^{\frac{-\chi\alpha_N}{1-\alpha_N}(T_t-T^*)} = \left(\frac{N_t}{\int e^{\frac{1}{1-\alpha_N}\hat{\beta}_{it}(T_t-T^*)+z_{it}} K_{it}^\theta di}\right)^{\alpha_N}$$

Plug in labor optimality condition into revenue function

$$\begin{aligned} P_{it} Y_{it} &= e^{\hat{\beta}_{it}(T_t-T^*)+\hat{z}_{it}} K_{it}^{\alpha_K} N_{it}^{\alpha_N} \\ &= e^{\hat{\beta}_{it}(T_t-T^*)+\hat{z}_{it}} K_{it}^{\alpha_K} \cdot \left(\frac{\alpha_N}{W} e^{(\hat{\beta}_{it}-\chi)(T_t-T^*)+\hat{z}_{it}} K_{it}^{\alpha_K}\right)^{\frac{\alpha_N}{1-\alpha_N}} \\ &= \frac{e^{\frac{1}{1-\alpha_N}\hat{\beta}_{it}(T_t-T^*)+z_{it}} K_{it}^\theta N_t^{\alpha_N}}{\int \left(e^{\frac{1}{1-\alpha_N}\hat{\beta}_{it}(T_t-T^*)+z_{it}} K_{it}^\theta di\right)^{\alpha_N}} \end{aligned}$$

By definition,

$$MRPK_{it} = \frac{\theta e^{\frac{1}{1-\alpha_N}\hat{\beta}_{it}(T_t-T^*)+z_{it}} K_{it}^{\theta-1} N_t^{\alpha_N}}{\int \left(e^{\frac{1}{1-\alpha_N}\hat{\beta}_{it}(T_t-T^*)+z_{it}} K_{it}^\theta di\right)^{\alpha_N}}$$

Rearrange to get K_{it}

$$K_{it} = \left(\frac{\theta e^{\frac{1}{1-\alpha_N}\hat{\beta}_{it}(T_t-T^*)+z_{it}}}{MRPK_{it}}\right)^{\frac{1}{1-\theta}} \cdot \left(\frac{N_t}{\int e^{\frac{1}{1-\alpha_N}\hat{\beta}_{it}(T_t-T^*)+z_{it}} K_{it}^\theta di}\right)^{\frac{\alpha_N}{1-\theta}}$$

Capital Market clearing gives

$$K_t = \int K_{it} di = \theta^{\frac{1}{1-\theta}} \left(\frac{N_t}{\int e^{\frac{1}{1-\alpha_N}\hat{\beta}_{it}(T_t-T^*)+z_{it}} K_{it}^\theta di}\right)^{\frac{\alpha_N}{1-\theta}} \cdot \int e^{\frac{1}{1-\alpha_N}\frac{1}{1-\theta}\hat{\beta}_{it}(T_t-T^*)+\frac{z_{it}}{1-\theta}} MRPK_{it}^{-\frac{1}{1-\theta}} di$$

Rearranging terms gives

$$\theta^{\frac{1}{1-\theta}} \left(\frac{N_t}{\int e^{\frac{1}{1-\alpha_N}\hat{\beta}_{it}(T_t-T^*)+z_{it}} K_{it}^\theta di}\right)^{\frac{\alpha_N}{1-\theta}} = \frac{K_t}{\int e^{\frac{1}{1-\alpha_N}\frac{1}{1-\theta}\hat{\beta}_{it}(T_t-T^*)+\frac{z_{it}}{1-\theta}} MRPK_{it}^{-\frac{1}{1-\theta}} di}$$

Use $MRPK_{it}$ to represent N_t and rewrite the equation above to get:

$$K_{it}^\theta = \left(\frac{e^{\frac{1}{1-\alpha_N}\frac{1}{1-\theta}\hat{\beta}_{it}(T_t-T^*)+\frac{z_{it}}{1-\theta}} MRPK_{it}^{-\frac{1}{1-\theta}}}{\int e^{\frac{1}{1-\alpha_N}\frac{1}{1-\theta}\hat{\beta}_{it}(T_t-T^*)+\frac{z_{it}}{1-\theta}} MRPK_{it}^{-\frac{1}{1-\theta}} di} K_t\right)^\theta$$

And now substitute this back into the expression for $P_{it} Y_{it}$:

$$P_{it}Y_{it} = \frac{e^{\frac{1}{1-\alpha_N} \frac{1}{1-\theta} \hat{\beta}_{it}(T_t - T^*) + \frac{z_{it}}{1-\theta}} MRPK_{it}^{-\frac{\theta}{1-\theta}}}{\left(\int e^{\frac{1}{1-\alpha_N} \frac{1}{1-\theta} \hat{\beta}_{it}(T_t - T^*) + \frac{z_{it}}{1-\theta}} MRPK_{it}^{-\frac{1}{1-\theta}} di \right)^\theta} K_t^{\alpha_K} N_t^{\alpha_N}$$

Note that $P_{it}Y_{it} = B_{it}^{\frac{1}{\sigma}} Y_{it}^{\frac{\sigma-1}{\sigma}}$

Aggregate output is then:

$$\begin{aligned} Y_t &= \left(\int B_{it}^{\frac{1}{\sigma}} Y_{it}^{\frac{\sigma-1}{\sigma}} di \right)^{\frac{\sigma}{\sigma-1}} = \left(\int P_{it}Y_{it} di \right)^{\frac{\sigma}{\sigma-1}} \\ &= \left[\frac{\int e^{\frac{1}{1-\alpha_N} \frac{1}{1-\theta} \hat{\beta}_{it}(T_t - T^*) + \frac{z_{it}}{1-\theta}} MRPK_{it}^{-\frac{\theta}{1-\theta}} di}{\left(\int e^{\frac{1}{1-\alpha_N} \frac{1}{1-\theta} \hat{\beta}_{it}(T_t - T^*) + \frac{z_{it}}{1-\theta}} MRPK_{it}^{-\frac{1}{1-\theta}} di \right)^\theta} \right]^{(1-\alpha_N)\frac{\sigma}{\sigma-1}} K_t^{\alpha_K \frac{\sigma}{\sigma-1}} N_t^{\alpha_N \frac{\sigma}{\sigma-1}}, \\ &= \tilde{A}_t^{\frac{\sigma}{\sigma-1}} K_t^{\alpha_K} N_t^{\alpha_N} \end{aligned}$$

$$\text{where we define } \tilde{A}_t := \left[\frac{\int e^{\frac{1}{1-\alpha_N} \frac{1}{1-\theta} \hat{\beta}_{it}(T_t - T^*) + \frac{z_{it}}{1-\theta}} MRPK_{it}^{-\frac{\theta}{1-\theta}} di}{\left(\int e^{\frac{1}{1-\alpha_N} \frac{1}{1-\theta} \hat{\beta}_{it}(T_t - T^*) + \frac{z_{it}}{1-\theta}} MRPK_{it}^{-\frac{1}{1-\theta}} di \right)^\theta} \right]^{(1-\alpha_N)}.$$

To simplify exposition, we further define $\dot{A}_{it} = e^{\frac{1}{1-\alpha_N} \hat{\beta}_{it}(T_t - T^*) + z_{it}}$, and rewrite

$$\tilde{A}_t := \left[\frac{\int \dot{A}_{it}^{1-\theta} MRPK_{it}^{-\frac{\theta}{1-\theta}} di}{\left(\int \dot{A}_{it}^{1-\theta} MRPK_{it}^{-\frac{1}{1-\theta}} di \right)^\theta} \right]^{(1-\alpha_N)},$$

or in logs,

$$\tilde{a}_t = (1 - \alpha_N) \left[\log \left(\int \dot{A}_{it}^{1-\theta} MRPK_{it}^{-\frac{\theta}{1-\theta}} di \right) - \theta \log \left(\int \dot{A}_{it}^{1-\theta} MRPK_{it}^{-\frac{1}{1-\theta}} di \right) \right]$$

The first term inside brackets is equal to

$$\frac{1}{1-\theta} \bar{\dot{a}}_{it} - \frac{\theta}{1-\theta} \overline{mRPk_{it}} + \frac{1}{2} \left(\frac{1}{1-\theta} \right)^2 \sigma_{\dot{a},t}^2 + \frac{1}{2} \left(\frac{\theta}{1-\theta} \right)^2 \sigma_{mRPk,t}^2 - \frac{\theta}{(1-\theta)^2} \sigma_{mRPk,\dot{a},t},$$

where $\dot{a}_t = \log \dot{A}_t = \frac{1}{1-\alpha_N} \hat{\beta}_{it}(T_t - T^*) + z_{it}$ and $mRPk_{it} = \log(MRPK_{it})$

and the second,

$$\frac{\theta}{1-\theta} \bar{\dot{a}}_{it} - \frac{\theta}{1-\theta} \overline{mRPk_{it}} + \frac{1}{2} \theta \left(\frac{1}{1-\theta} \right)^2 \sigma_{\dot{a},t}^2 + \frac{1}{2} \theta \left(\frac{1}{1-\theta} \right)^2 \sigma_{mRPk,t}^2 - \frac{\theta}{(1-\theta)^2} \sigma_{mRPk,\dot{a},t}$$

Combining,

$$\tilde{a}_t = (1 - \alpha_N) \left[\bar{\tilde{a}}_t + \frac{1}{2} \frac{1}{1-\theta} \sigma_{\tilde{a},t}^2 - \frac{1}{2} \frac{\theta}{1-\theta} \sigma_{mfpk,t}^2 \right]$$

and

$$\begin{aligned} y_t &= \frac{\sigma}{\sigma-1} \tilde{a}_t + \tilde{\alpha}_K k_t + \tilde{\alpha}_N n_t \\ &= \frac{\sigma}{\sigma-1} (1 - \alpha_N) \left[\bar{\tilde{a}}_t + \frac{1}{2} \frac{1}{1-\theta} \sigma_{\tilde{a},t}^2 - \frac{1}{2} \frac{\theta}{1-\theta} \sigma_{mfpk,t}^2 \right] + \tilde{\alpha}_K k_t + \tilde{\alpha}_N n_t \\ &:= a_t + \tilde{\alpha}_K k_t + \tilde{\alpha}_N n_t, \end{aligned}$$

where the total factor productivity is defined as:

$$\begin{aligned} a_t &= \frac{\sigma}{\sigma-1} (1 - \alpha_N) \left[\bar{\tilde{a}}_t + \frac{1}{2} \frac{1}{1-\alpha} \sigma_{\tilde{a},t}^2 - \frac{1}{2} \frac{\alpha}{1-\alpha} \sigma_{mfpk,t}^2 \right] \\ &= \frac{\sigma}{\sigma-1} \bar{\tilde{a}}_t + \frac{1}{2} \frac{\sigma}{\sigma-1} \frac{1}{(1-\alpha)(1-\alpha_N)} \sigma_{\tilde{a},t}^2 \\ &\quad - \frac{1}{2} \frac{\sigma}{\sigma-1} \frac{\alpha_K}{1-\alpha} \sigma_{mfpk,t}^2 \end{aligned}$$

Plugging in the definition for $\bar{\tilde{a}}_t$ and $\sigma_{\tilde{a},t}^2$, we can write the TFP as:

$$\begin{aligned} a_{nt} &= \frac{\sigma}{\sigma-1} \left[\bar{\hat{\beta}}_i (T_t - T^*) + c (T_t - T^*)^2 \right] \\ &\quad + \frac{\sigma}{2} \frac{\sigma}{\sigma-1} \left[(\sigma_{\hat{\beta}}^2 + \sigma_{\hat{\xi}}^2) (T_t - T^*)^2 + \frac{\sigma_{\hat{\varepsilon}}^2}{1 - \rho_z^2} \right] \\ &\quad - \frac{\tilde{\alpha}_K + \tilde{\alpha}_K^2(\sigma-1)}{2} \left(\frac{1}{1-\alpha_N} \right)^2 \left[(T_t - T^*)^2 \sigma_{\hat{\xi}}^2 + \eta_t^T \sigma_{\hat{\beta}}^2 + \sigma_{\hat{\varepsilon}}^2 \right] \end{aligned} \tag{66}$$

Under the parametrization that $c = -\frac{\sigma}{2} \left(\sigma_{\hat{\beta}}^2 + \sigma_{\hat{\xi}}^2 \right)$, we will have:

$$\begin{aligned} a_t &= a_t^* - \text{Misallocation Loss}_t \\ &= \frac{\sigma}{\sigma-1} \left[\bar{\hat{\beta}}_i (T_t - T^*) \right] + \frac{\sigma}{2} \frac{\sigma}{\sigma-1} \left[\frac{\sigma_{\hat{\varepsilon}}^2}{1 - \rho_z^2} \right] \\ &\quad - \frac{\tilde{\alpha}_K + \tilde{\alpha}_K^2(\sigma-1)}{2} \left(\frac{1}{1-\alpha_N} \right)^2 \left[(T_t - T^*)^2 \sigma_{\hat{\xi}}^2 + \eta_t^T \sigma_{\hat{\beta}}^2 + \sigma_{\hat{\varepsilon}}^2 \right] \end{aligned} \tag{67}$$